BUDI PRAYOGO SUNARIYANTO - 4617649

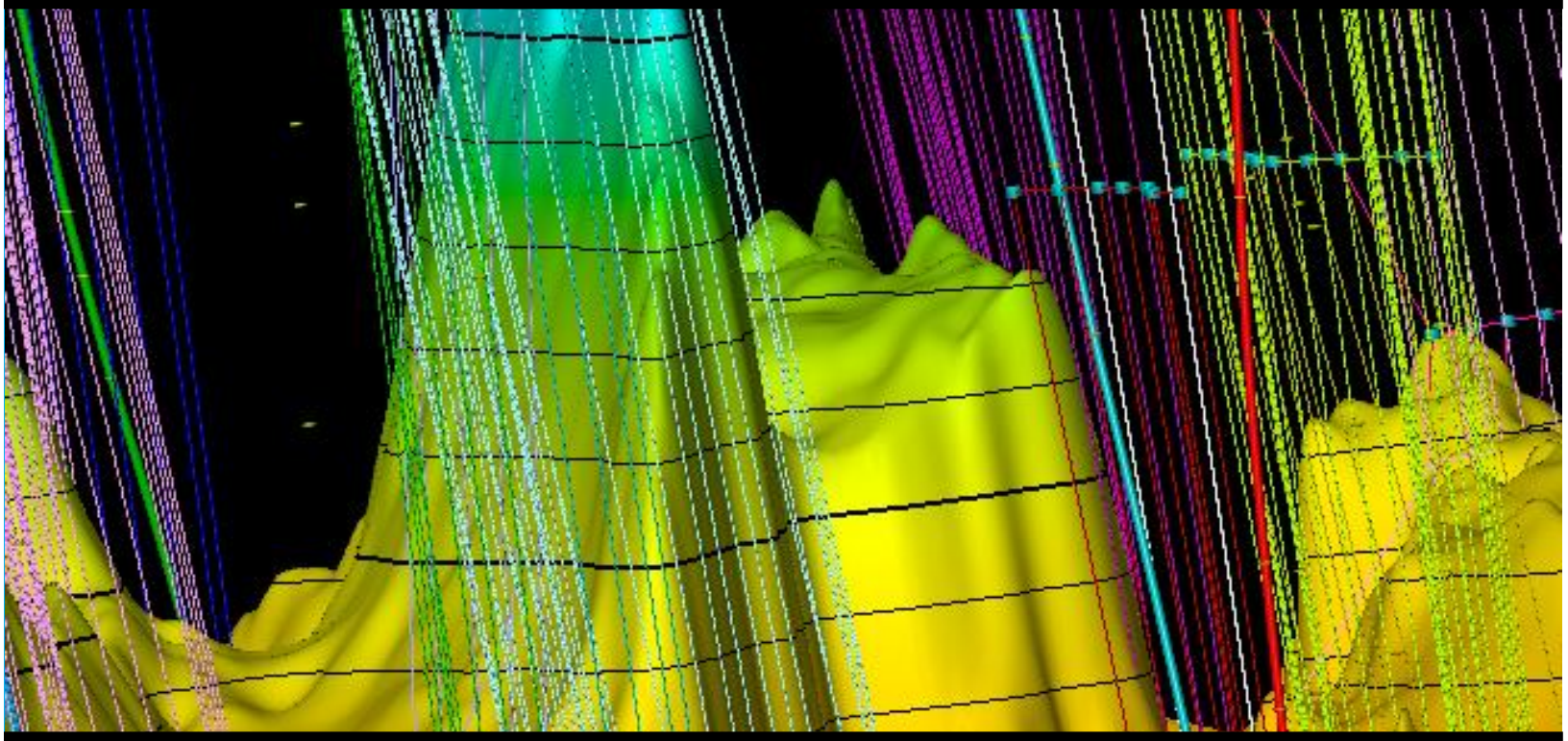

Geothermal Aquifer Architecture Model of Alblasserdam Member in Drechtsteden, the Netherlands

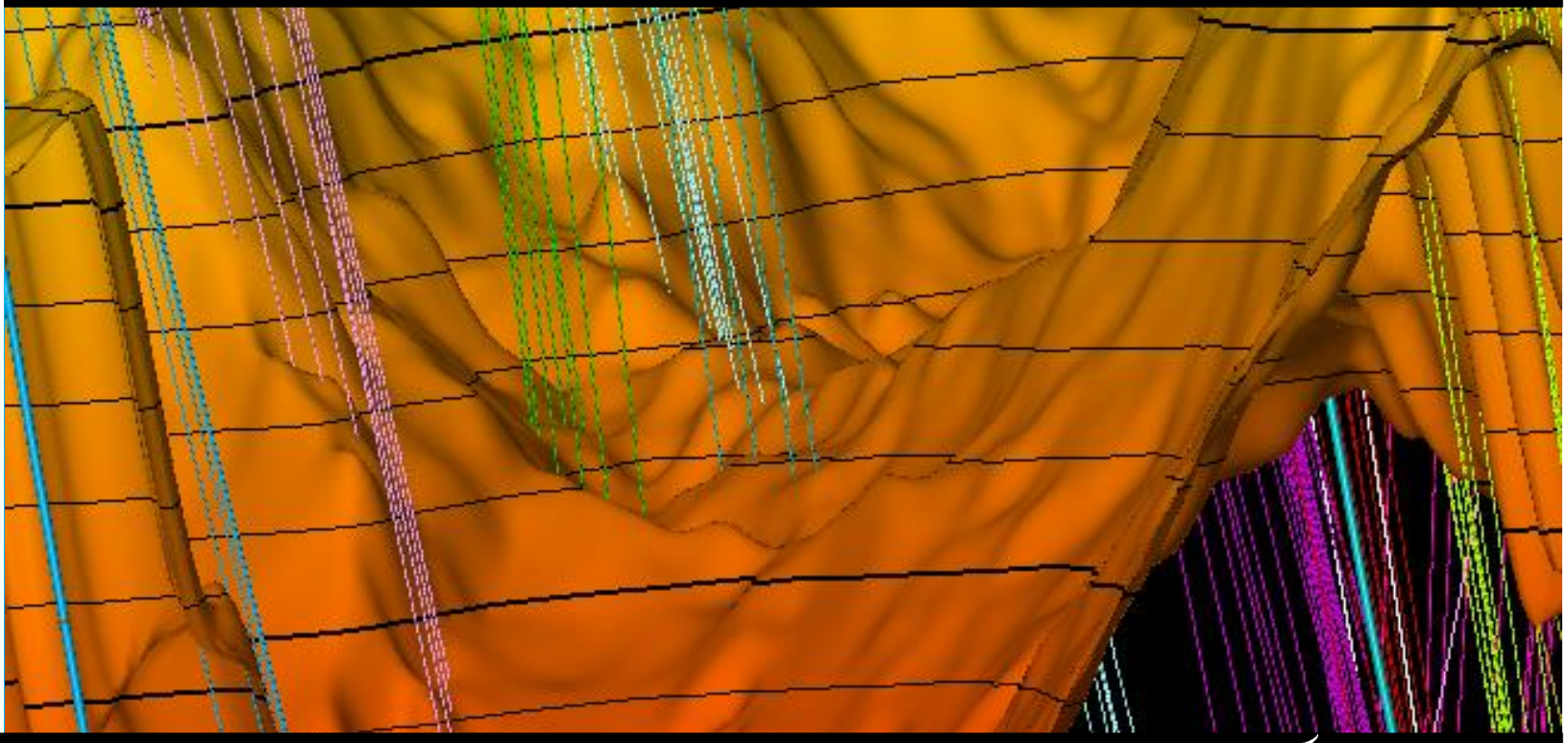

TU Delft

Geothermal Aquifer Architecture Model of Alblasserdam Member in Drechtsteden, the Netherlands

By

Budi Prayogo Sunariyanto

in partial fulfilment of the requirements for the degree of

Master of Science

in Applied Earth Sciences

at the Delft University of Technology,

To be defended publicly on Thursday September 27, 2018 at 12.30

Student number	: 4617649	
Project duration	: November 17th, 2017 – September 27th, 2018	
Supervisor	: Dr. M. E. Donselaar	TU Delft, Chairman
	Charlotte de Wijkerslooth	HVC
	Gerhard Diephuis	TU Delft
	Axel Sanden	Veegeo Energy
Thesis Committee	: Dr. M. E. Donselaar	TU Delft, Chairman
	Prof. dr. W. Rossen	TU Delft
	Drs. J. C. Blom	TU Delft
	Charlotte de Wijkerslooth	HVC
	Gerhard Diephuis	TU Delft
	Axel Sanden	Veegeo Energy

An electronic version of this thesis is available at http://repository.tudelft.nl/

TU Delft Delft University of Technology

HVC

www.hvcgroep.nl

Acknowledgements

Praise to God Almighty for all His blessing and protection.

With the completion of this master thesis which also means that my studies at TU Delft are over. Though the following master thesis is an individual work, I could never have reached the heights without the help, support, guidance, blessing, and efforts of many people.

First, I would like to express my sincere gratitude to my university supervisor, Dr. M. E. Donselaar for his guidance and patience during the process of this master thesis. My external supervisors, Charlotte de Wijkerslooth (HVC groep), Gerhard Diephuis and Axel Sanden (Veegeo Energy) who give all of the support, data, very useful tips and ideas to solve every problem during my thesis work.

Also, I would like to thank the Indonesian Endowment Fund for Education (LPDP) for giving me the opportunity to study in TU Delft, by providing me full financial support during the two-years master program.

I would like to dedicate this achievement to my beloved parents, my sister and my brother for their unconditional support at any time.

Last, I would like to thank all my classmates in Petroleum Engineering and Geosciences and all Indonesian student in the Netherlands for their friendship and warmness.

Budi Prayogo Sunariyanto

Delft, *20 September 2018*

Abstract

The decrease in the production of hydrocarbons in combination with a growing urgency to reduce carbon emissions drives a rapid study and application of geothermal energy in the Netherlands. The produced heat from the low enthalpy geothermal energy can be used for heating up the buildings and greenhouses. A doublet system is used in the geothermal scheme, which consists of one production well and one injection well. The reinjection is done to maintain the reservoir pressure and reduce pressure decline due to production, earthquake and subsidence prevention, and environmental safety. Thus, it is crucial to model the aquifer distributions appropriately as the injection and production well should be placed at the communicated sand bodies.

In this study, the architecture of the Alblasserdam Member in the Drechtsteden, West Netherlands Basin is modelled. An investigation of the paleo flow and the distribution of sand prone succession within the Alblasserdam Member is done by integrating seismic interpretation, reservoir sedimentology, and petrophysical evaluation. The data used consist of seismic data, well log dataset and core data from the acquired hydrocarbon exploration data. The Alblasserdam Member was deposited during the Late Jurassic to Early Cretaceous when the high tectonic activities occurred in the West Netherlands Basin and followed by series of inversion impulses made this member bounded by various members at the bottom and the top. The seismic response of the Alblasserdam Member shows a high thickness and depth variations. The sediments of the Alblasserdam Member are highly accumulated in the central part of the study area, bounded by two major faults striking SE-NW.

Several sections of well correlation are made based on cycles of changing accommodation to sediment supply ratio (A/S cycles). The correlation is supported with seismic interpretation, allow to map the distribution of sand-rich interval of the Alblasserdam Member in the Drechtsteden. Two potential aquifer intervals are found. A southwestward shifting of the main fluvial system is observed from the thickness trend of the shallower aquifer intervals. A petrophysical evaluation is made to analyze the properties of the potential aquifer that encompass net to gross thickness (N/G), average porosity, and average permeability. The deeper potential aquifer has a higher clean sand N/G, but lower average permeability, that might be caused by the compaction, and mineral precipitation after the inversion period, especially in the highly inverted area. In the end, a recommendation to place a pair of production and injection wells are proposed based on the high accumulation of sand-rich intervals, sufficient depth to produce heat >70^{o}C and absences of the fault. The wells are placed toward SE-NW trend which is parallel to the distribution of the main fluvial distribution and the orientation of the faults, with production well placed at the deeper level.

Table of Contents

List of Tables

List of Figures

1. Introduction

The application of geothermal energy in the Netherlands has been rapidly growing since 2008. The decrease in the production of hydrocarbons in combination with a growing urgency to reduce carbon emissions drive the need to further develop renewable heat sources. Producing heat from the subsurface through low enthalpy geothermal system provides a solution for a sustainable green alternative energy source. In European countries, notably the Netherlands, the produced heat from the low enthalpy geothermal energy can be used for heating up the buildings and greenhouses.

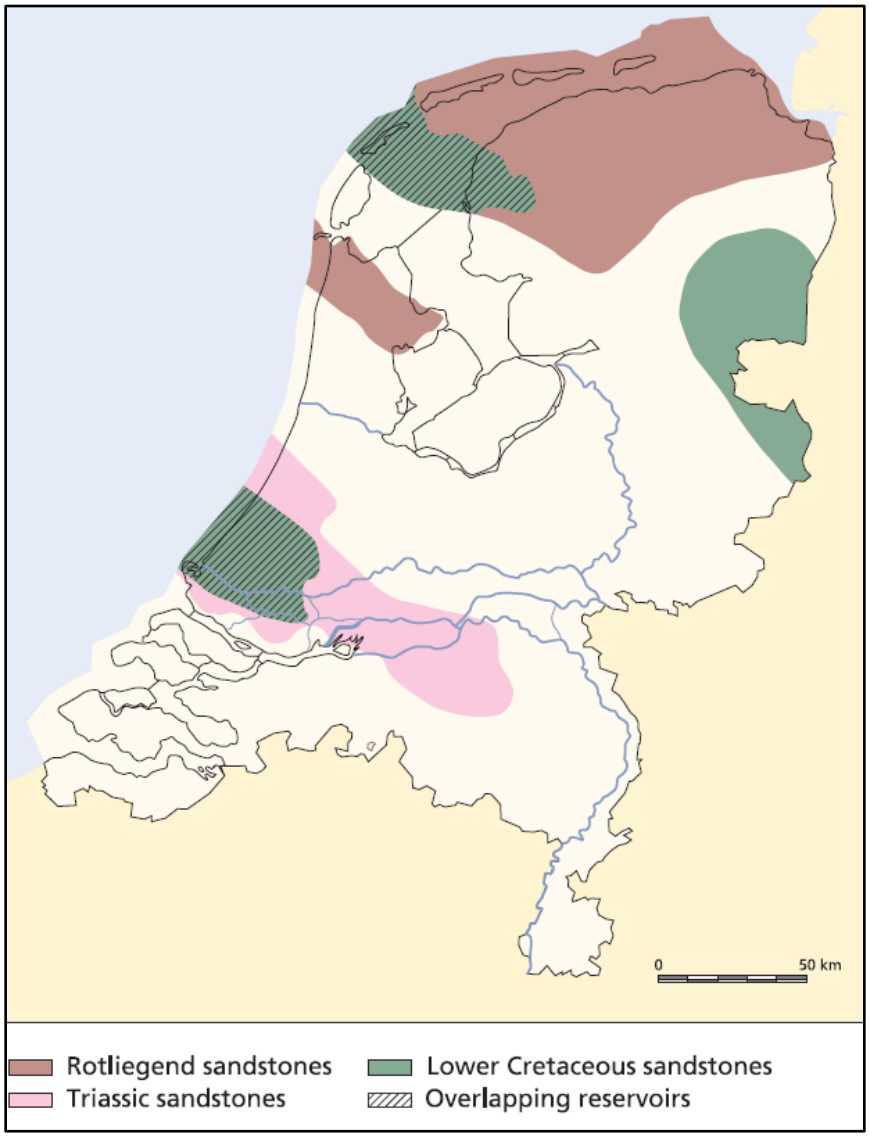

Figure 1 Distribution of potential geothermal aquifers in the Netherlands (Lokhorst & Wong, 2007)

The average thermal gradient and surface temperature in the Netherlands is 31.3 ^{o}C/km and 10.1 ^{o}C respectively (Bonté, Van Wees, & Verweij, 2012). Toegepast Natuurwetenschappelijk Onderzoek (TNO) requirement for minimum production temperature for greenhouses and houses heating is equal to 45 ^{o}C and 65 ^{o}C respectively with minimum production depth at -1200 m for the greenhouses and -2000 m for the houses. Lokhorst and Wong (2007) proposed four potential aquifers that suitable for low enthalpy geothermal energy extraction in the Netherlands to meet a general heat requirement for greenhouses and warming up the building. There are in Permian, Lower Triassic, Lower Cretaceous and Tertiary sands with distribution as depicted in Figure 1. This study will discuss the reservoir architecture of the Lower Cretaceous sandstones in the West Netherlands Basin (WNB).

Due to legislation in the Netherlands, the acquired data from the oil and gas exploration can be used to investigate potential aquifers for geothermal energy. Also, the technical approach for geothermal exploration is similar to oil and gas technology.

1.1 Research Overview

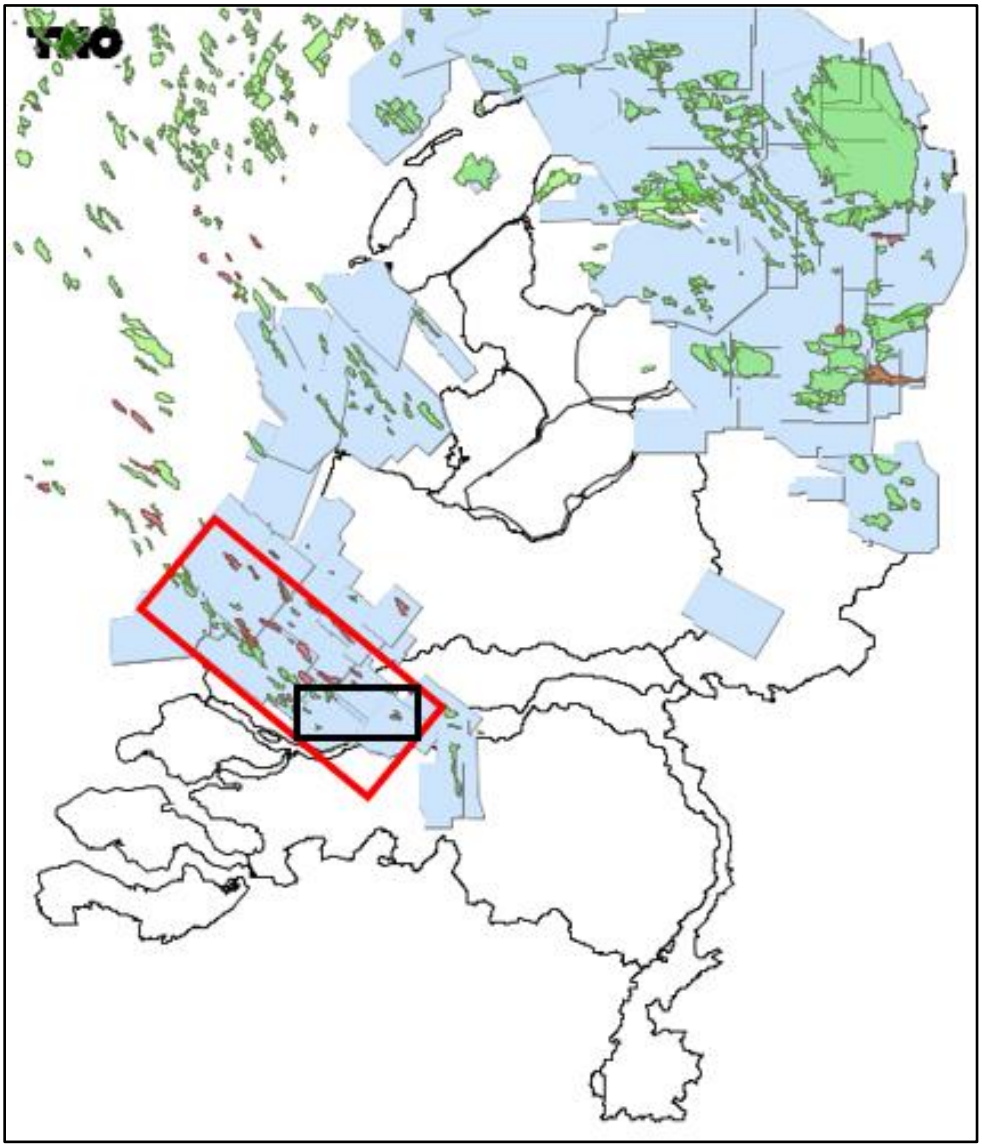

Figure 2 Map shown: distribution of 3D seismic data (light blue polygon) and hydrocarbon fields in the Netherlands; The red and black square indicates the location of the West Netherlands Basin and the Drechtsteden area respectively.

The WNB is located in the Southwest of the Netherlands and is known as a mature oil and gas province in the Netherlands. Figure 2 is produced from ThermoGIS TNO software, illustrates the distributions of 3D seismic data and hydrocarbon fields in the Netherlands. Seismic, well logs and core data from oil and gas exploration in the WNB are available for geothermal study. A group of municipalities called Drechtsteden located in the south-easternmost of the WNB will be the focus of the study area in this study as illustrated in Figure 3. The produced heat will be used to supply heat demand in the study area by connecting to the heat networks.

Studies of the Nieuwerkerk Formation (SLDN) as the potential geothermal aquifer had been done in the central to the northern part of the WNB. Boogaert and Kouwe (1993), Den Hartog Jager (1996), Devault and Jeremiah (2002), Herngreen and Wong (2007), and de Jager (2007) described the facies unit and tectonostratigraphy in the WNB. Donselaar et al. (2015), Willems et al. (2017), and Vondrak (2017) studied chronostratigraphy of Delft Sandstone of the SLDN in the WNB. The Delft Sandstone is the primary target of geothermal projects in the Netherlands where most of doublets and exploration licenses are targeting this layer (Willems, Vondrak, Munsterman, Donselaar, & Mijnlieff, 2017).

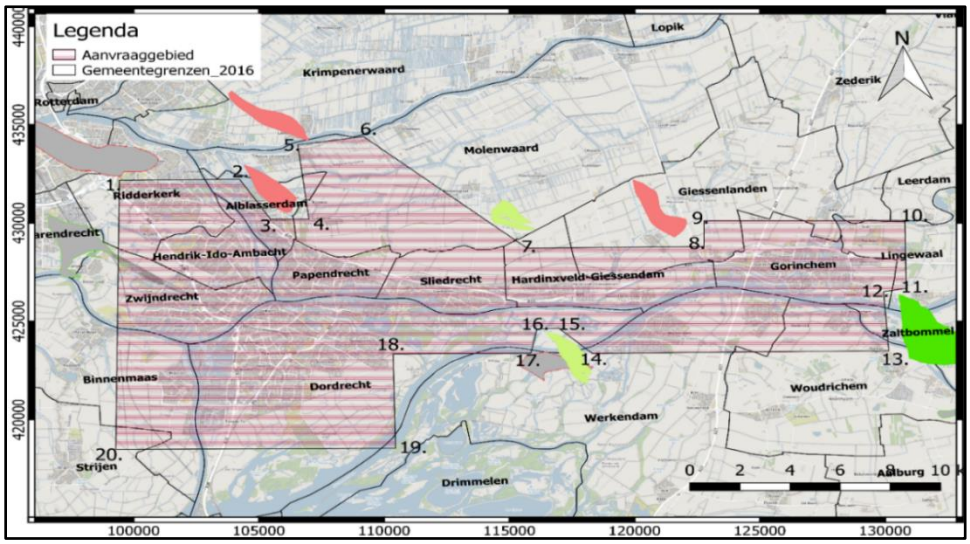

Figure 3 Map of the Drechtsteden area as the focus of the study area

However, the southern part of the WNB remains a question to be discussed. The older fluvial deposits of the SLDN, the Alblasserdam Member, which are highly accumulated in this area with both sedimentary and tectonics complexities, contain the possible potential of aquifers for geothermal energy.

This study aims to model the architecture of the Alblasserdam Member as the low enthalpy geothermal aquifer. Focus topics of this study are to investigate the paleo flow and the distribution of sand prone succession within the Alblasserdam Member and petrophysical evaluation to produce a porosity and permeability profile of the Alblasserdam Member. In the end, a recommendation to place a pair of production and injection wells will be proposed.

The Alblasserdam Member is predominantly composed of continental sediments and has a significant tectonic depositional overprint (Devault & Jeremiah, 2002). Sedimentary processes in

the fluvial system and tectonic activity during and after sedimentation, interpretation of the Alblasserdam Member would face high uncertainties. The uncertainties encompass the distribution, thickness variations, and continuity of the sand prone succession within the Alblasserdam Member.

Besides the structural differences of a hydrocarbon and geothermal reservoir, a geothermal well is different from a hydrocarbon well. In the geothermal scheme, a doublet system is used, which consist of one production well and one injection well. The reinjection is done to maintain the reservoir pressure and reduce pressure decline due to production, earthquake and subsidence prevention, and environmental safety since the produced water has a higher salinity compare to the surface fresh water. Thus, it is crucial to model the aquifer distributions appropriately as the injection and production well should be placed at the communicated sand bodies.

To reduce the uncertainties of the model and find the best area to place the doublet, integration of literature study, seismic interpretation, reservoir sedimentology, well logs analysis and core description from the available 3D seismic, well logs and core data from acquired oil and gas exploration data will be done in this study.

1.2 Outline of the Report

The report consists of five chapters. The first chapter discusses the introduction, research overview, and the outline of the report. The second chapter consists of regional geology of the WNB including the structural setting of the WNB and the stratigraphy of the Alblasserdam Member. The available dataset and methodologies will be discussed in Chapter 3. In Chapter 4, the result of seismic interpretation, reservoir sedimentology, and petrophysical evaluation are presented. A further discussion to obtain the best area to place the doublet are presented in Chapter 5. The final chapter consists of the conclusion of this study and recommendation for further research.

2. Regional Geology

2.1 West Netherlands Basin

The Drechtsteden area is located at the southernmost of the WNB, near the fringe with the Roer Valley Graben (RVG) (Figure 4). The WNB situated in the Southwest of the Netherlands with a trend toward NW-SE, bordering with the RVG at the Southeast and the Broad Fourteens Basin at the Northwest. From Northeast to Southwest, the WNB is located in between the Zandvoort Ridge and the London Brabant Massif.

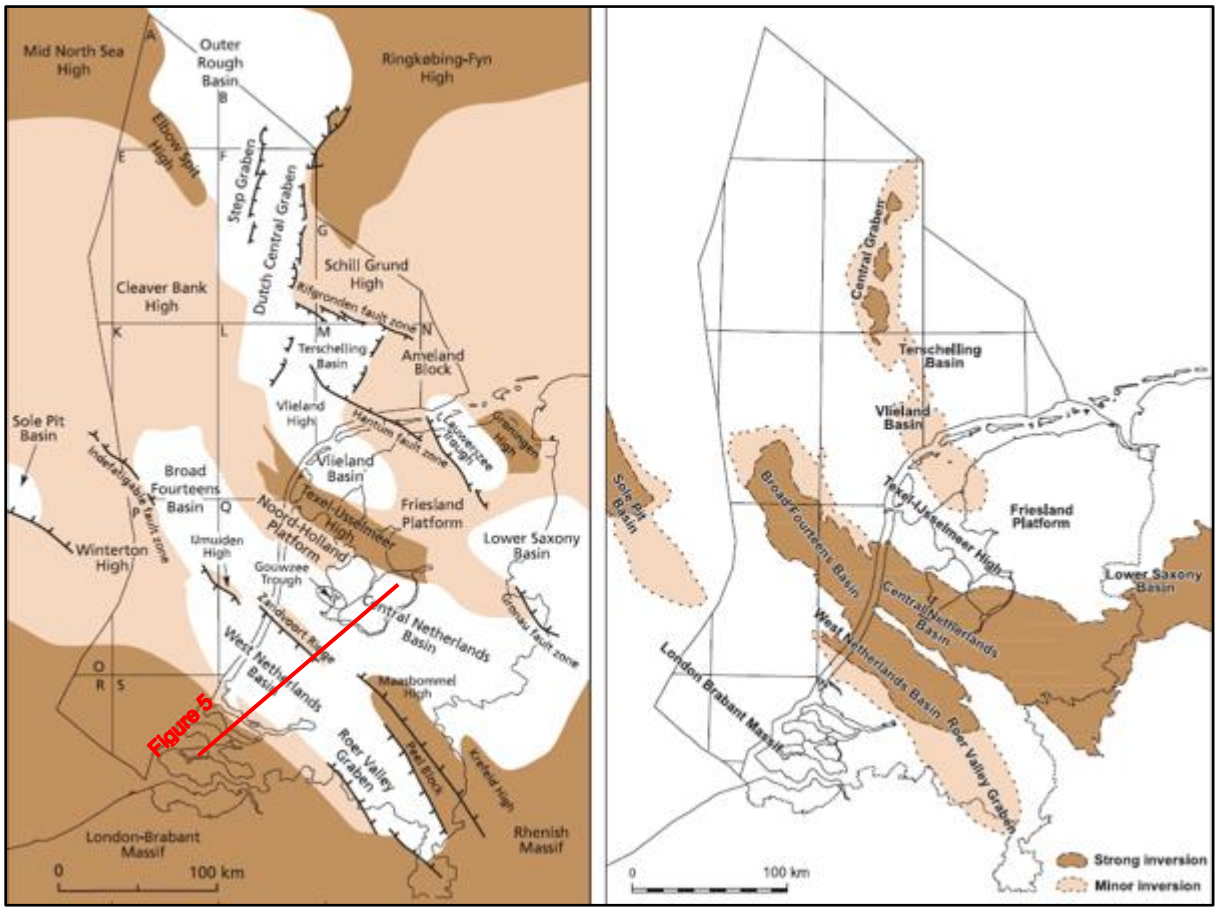

Figure 4 Map of Late Jurassic to Early Cretaceous structural elements in the Netherlands (left) and Inverted basins in the Netherlands (right) (de Jager, 2003).

Tectonic evolution during the Triassic until the Early Tertiary primarily controlled the structural geometry of the WNB. During the Triassic until Late Jurassic, regional rifting occurred in the Netherlands that associated with the Pangea break-up. The former single extensive Southern Permian Basin split into several fault-bounded basins and highs. The difference in subsidence and existence of the old structure, three primary rift system can be recognized during the late

Middle and Late Jurassic as depicted in Figure 4. There are the N-S oriented, the E-W oriented and the NW-SE rift systems (Wong, 2007). The WNB is part of the NW-SE rift system and characterized by a titled half-graben structure (Figure 5).

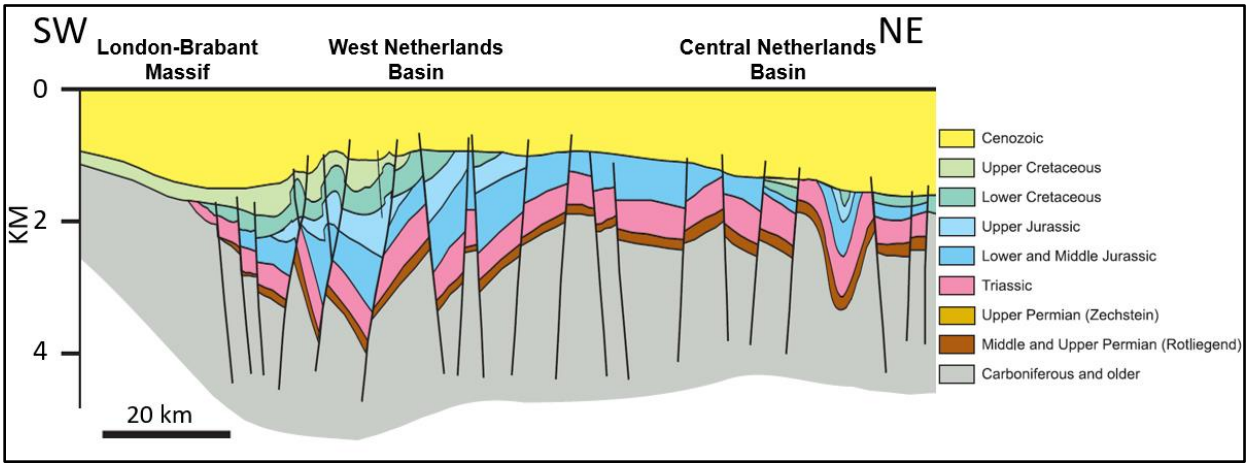

Figure 5 SW-NE cross section of London-Brabant Massif, West Netherlands Basin and Central Netherlands Basin (de Jager, 2007)

The convergence of Africa-Arabia and Eurasia that took place during the Late Cretaceous and Early Tertiary created series of inversion pulses that changed the geometry of the WNB. De Jager (2003) described the inversion was occurred simultaneously and defined them into four pulses. There are Subhercynian, Laramide, Pyrenean, and Savian. The Laramide pulse is the most robust inversion in the WNB that occurred during Paleocene that eroded over deeper formation reaching the Jurassic sediments. Furthermore, the change from extensional to compressional stress regime in the WNB reactivated the pre-existing normal faults from rifting period into reverse faults and forming a prominent ridge of flower structures (Racero-Baena & Drake, 1996), (de Jager, 2007).

Racero-Baena and Drake (1996) divided the stratigraphy in the WNB into four sequences: i) a pre-rift clastic sequence from the Permian to the Early – Mid Jurassic, ii) a syn-rift sequence of Late Jurassic to Early Cretaceous age, ii) a post-rift sequence of Early to Late Cretaceous age, and iv) a syn- and post-inversion sequence of Late Cretaceous-Tertiary to Quaternary age.

2.2 Alblasserdam Member

The target layer for this study is the Alblasserdam Member (SLDNA), a fluvial strata deposited under the syn-rift sequence of the Late Jurassic to the Early Cretaceous. The SLDNA is the Lower Member of the SLDN. The SLDN is a sand-shale stratification sediment as part of mainly continental Schieland Group that deposited in the coastal-plain environments and reached a thickness of more than 1 km (Devault & Jeremiah, 2002) .

The boundary between the Lower and Upper Member of the SLDN formed as the transition of syn-rift to early post-rift period as illustrated in Figure 6. The SLDNA is characterized as fluvial sediment with high thickness variations and low lateral extensive as the consequence of the fault-bounded structure and difference in basin subsidence rate. The Upper Member of the SLDN, the Rodenrijs Claystone (SLDNR), deposited during the post-rift period and characterized as widely homogeneous thick stepped on the SLDNA as marine transgression sediments (Jeremiah, 2000), (Devault & Jeremiah, 2002) (Donselaar, Groenenberg, & Gilding, 2015).

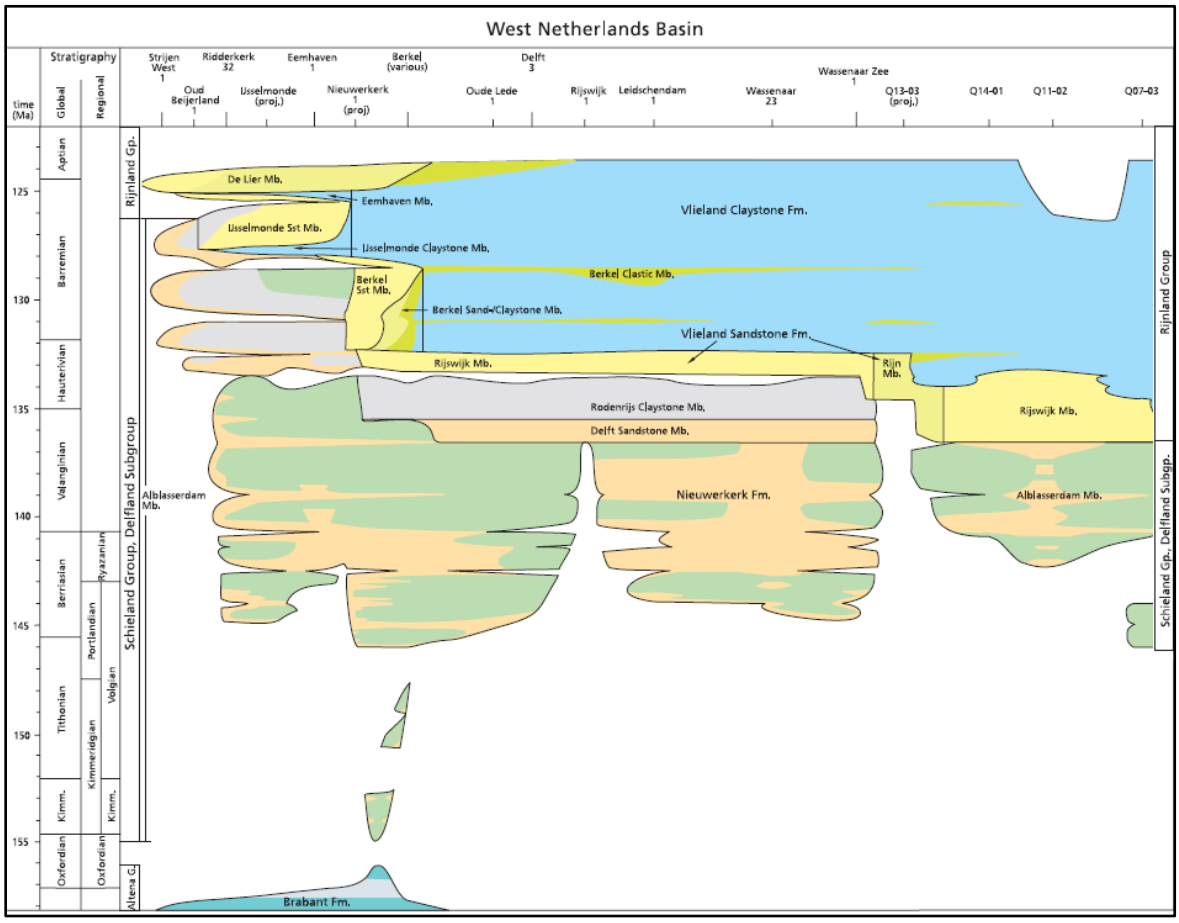

Figure 6 Stratigraphic schemes of the Cretaceous sediments in the WNB (Herngreen & Wong, 2007)

The present-day deposits of the SLDNA have high variation in thickness, depth, and continuity. The SLDNA was deposited during the Late Jurassic to Early Cretaceous when the high tectonic activities occurred in the WNB and followed by series of inversion impulses made this member bounded by various members at the bottom and the top. In this study, four horizons are interpreted in the seismic data, from the bottom to the top there are the Base Schieland Group (SLD), Base Rijnland Group (KN), Base Chalk Group (CK), and Base North Sea Supergroup (NSG).

The sediments of the SLDNA were deposited after the Mid Kimmerian uplift and unconformably overlie the highly eroded sediments of Altena Group which were originally deposited during pre-rift to early syn-rift period and interpreted as the SLD in this study (Wong, 2007). The top of the SLDNA is bounded by the Rodenrijs Claystone Member, Rijnland Group, and North Sea Supergroup. In the WNB, the SLDNA initially covered by the SLDNR and the Rijnland Group sediments. Due to the inversion period during the Late Cretaceous until Early Tertiary, the top of the SLDNA is overlain by the Tertiary post-inversion sediments (North Sea Supergroup) in the highly inverted area.

3. Research Methodology and Available Dataset

In order to evaluate the suitability of the Alblasserdam Member in the Drechtsteden area for low enthalpy geothermal energy production, the reservoir architecture will be modelled by utilizing the existing acquired oil and gas exploration dataset is done in this study. A realistic reservoir architecture model can be obtained by reducing the uncertainties of the model parameters by applying an integration of literature study, seismic interpretation, reservoir sedimentology, and petrophysical evaluation.

3.1 Research Methodology

Figure 7 illustrates the workflow of employed methodologies used in this study. The first step is gathering information from the literature to gain an initial insight into the regional geology, key sedimentary processes, and tectonic history of the study area.

Figure 7 Workflow of reservoir architecture modelling

The next step is performing a seismic interpretation to obtain an insight of the basin geometries. The seismic interpretation includes the well to seismic integration, horizon interpretation, and fault interpretation using Petrel 2014 software. Four primary horizons and faults corresponding to the Alblasserdam Member are interpreted. In this process, integration between the responses of seismic acoustic and the well logs is done to reduce uncertainty in picking the supposed horizon. The geometry of the basin provides insight into the regional geological setting of the basin, such as the inverted half-graben structures of the WNB related to the rifting and inversion periods that occurred during the Triassic until the Early Tertiary. Furthermore, analyzing the trend of the formations within the basin, such as the continuity, unconformity, faults, layer thickening and thinning of such formation, will give an idea of sedimentology and tectonic histories of a formation.

The following step is to correlate the result from seismic interpretation with the well logs responses and core descriptions to obtain the characteristics of the aquifer through reservoir sedimentology and petrophysical evaluation. This step aims to predict the distribution and continuity of the sand bodies of the Alblasserdam Member. The estimated porosity and permeability profiles are obtained by a petrophysical evaluation from the well logs data and core plug measurement data.

Finally, the result from the seismic interpretation, reservoir sedimentology, and petrophysics evaluation are combined to obtain the model of the reservoir architecture of the Alblasserdam Member in the Drechtsteden and to estimate its suitability as a low enthalpy geothermal aquifer. In the end, the area with sufficient depth, thickness, continuity, porosity, and permeability is proposed as the area of the doublet placement.

3.2 Available Dataset

3.2.1 Seismic Data

The seismic data used in this study is 3D PSDM seismic data that had been reprocessed by NAM from several old 3D seismic dataset covering the WNB. Seismic interpretations are performed in the depth domain using Petrel 2014 software and displayed in European polarity convention, a hard kick is represented as a trough, negative number, and coloured red in the seismic section. The seismic dataset is in depth-domain. Thus, the seismic cross-section gives an excellent approximation of the actual subsurface image. Table 1 gives the detail information of the reprocessed 3D PSDM seismic data.

Table 1 Parameter of the seismic data

Coordinate System	Rijksdriehoekstelsel New (RD New) - Netherlands
Number of Inlines	3754
Number of Crosslines	1724
Inline length	34461.79 m
Inline interval Trace spacing	20 by 20 m
Crossline length	75060.6 m
Inline rotation from the north	38.59
Inline range	1429 – 5182
Interpreted Inline range	3400-5182
Crossline range	2267 – 3990
Area of the study area	35.64 x 34.46 km
Depth	0 – 6000 m

The seismic interpretations are performed within inline 3400 until 5182 and crossline 2267 until 3990 with an area of the study area around 1200 km^2 as illustrated by a red-dashed square in Figure 8. However, empty seismic traces are found in some areas within the reprocessed 3D PSDM seismic data cube as these areas are outside the original data coverage. The blue polygon in Figure 8 illustrates the actual area of the seismic interpretation that equal to the coverage of four old 3D seismic data, L3NAM1986-A, L3NAM1988-H, L3NAM19880-J, and L3NAM1991-B.

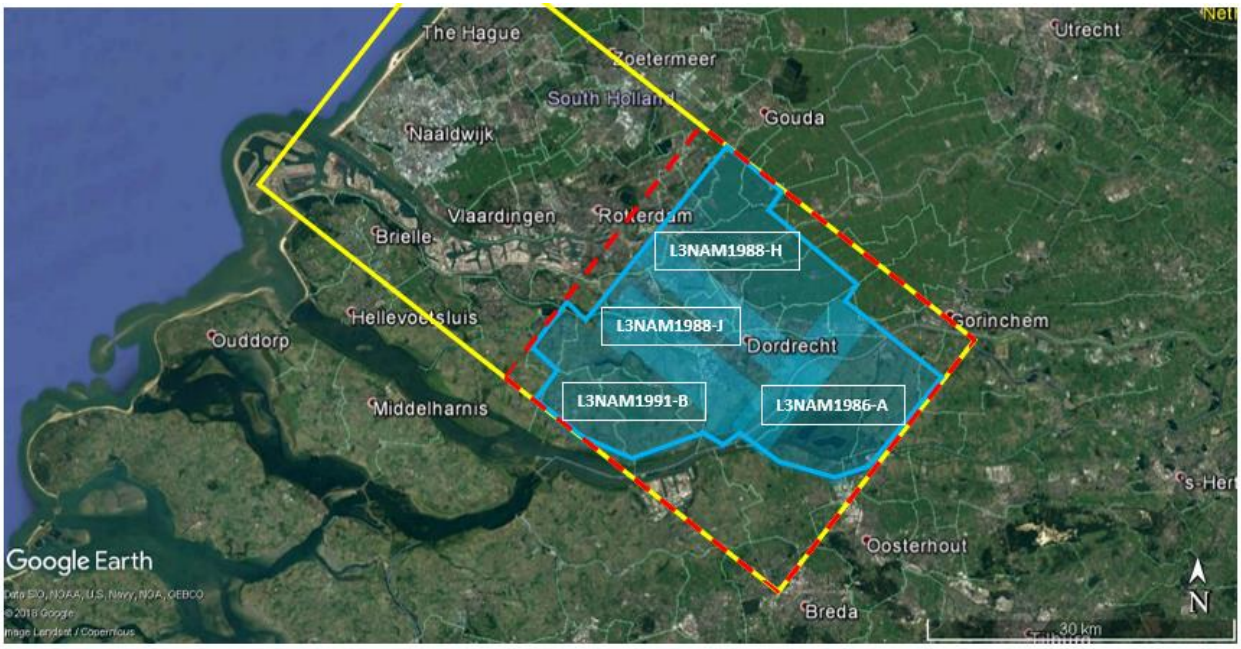

Figure 8 Map of seismic data coverage. Light blue polygons are the original 3D seismic data in time domain. Yellow square is the full area of NAM reprocessed 3D PSDM seismic data in the depth domain. Red-dashed square is the used seismic covering the study area. (Source: Google Earth and TNO database)

3.2.2 Well Data

The well logs data are accessed from the Netherlands open source website, www.nlog.nl. The available wells were drilled for hydrocarbon exploration and production purposes with target formation that differs for each well. A preconditioning data is done to sort the wells that penetrate the Alblasserdam Member by creating a database of 172 available wells within the seismic coverage. The well is classified based on the depth penetration, the availability of core data, and well logs data such as gamma ray, density, sonic, and neutron porosity logs. Table 2 provides the resume of wells used in this study. The distributions of the wells with their uses are presented in Figure 9 and Figure 10.

Table 2 Resume of the available wells and their uses

Total available wells in the study area	172
Wells with depth penetrating the Alblasserdam Member	61
Wells with well logs data of the Alblasserdam Member	19
Wells with complete well logs data (GR, DT, RHOB, NPHI) of the Alblasserdam Member	15
Wells with cores of the Alblasserdam Member	11
Wells for petrophysical evaluation	7

Furthermore, pathways of the wells are varying from nearly vertical to deviated. The well deviation is an important input parameter of the well as it could lead to misinterpretation. In the deviated well, the depth of a layer is measured higher than the true vertical depth. Thus, the measured depth should be corrected with the well deviation to obtain the true vertical depth.

Another possible misinterpretation occurs when the well penetrating a fault. In a vertical well, a missing layer reading of a stratigraphic column indicates that the well is possibly penetrating a normal fault. Also, a doubled layer reading of a stratigraphic column indicates that the well is penetrating a reverse fault. On the other hand, in the deviated well, a doubled layer reading of a stratigraphic column is interpreted as a normal fault and a missing layer reading of a stratigraphic column as a reverse fault penetrated by the well.

All wells are equipped with lithostratigraphic interpretation by Boogaret & Kouwe, (1993) and Munsterman et al. (2012). The lithostratigraphic interpretation is used as a guide to creating a lithology well marker for the four main horizons, the SLD, the KN, the CK, and the NSG. A lithology well marker is an important tool for well correlation and well to seismic integration.

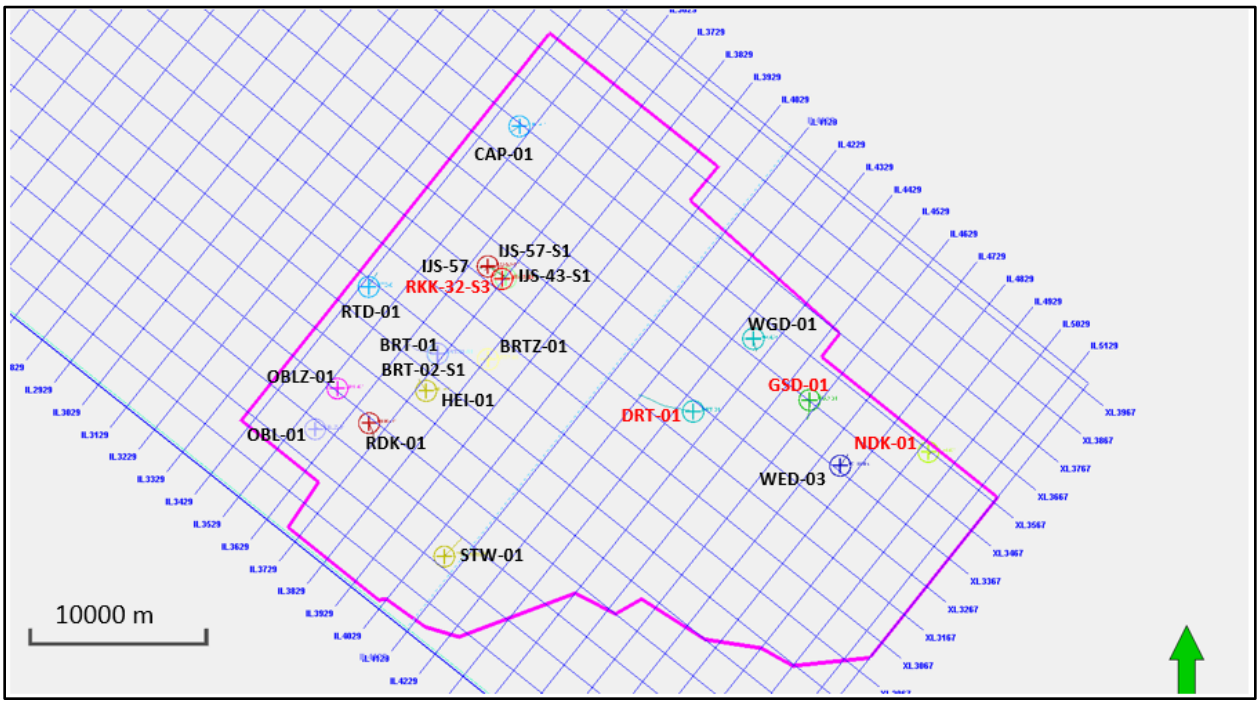

Figure 9 Distribution map of wells with well logs data penetrating the Alblasserdam Member. Wells with black labels have a complete gamma-ray, sonic, density and neutron log responses.

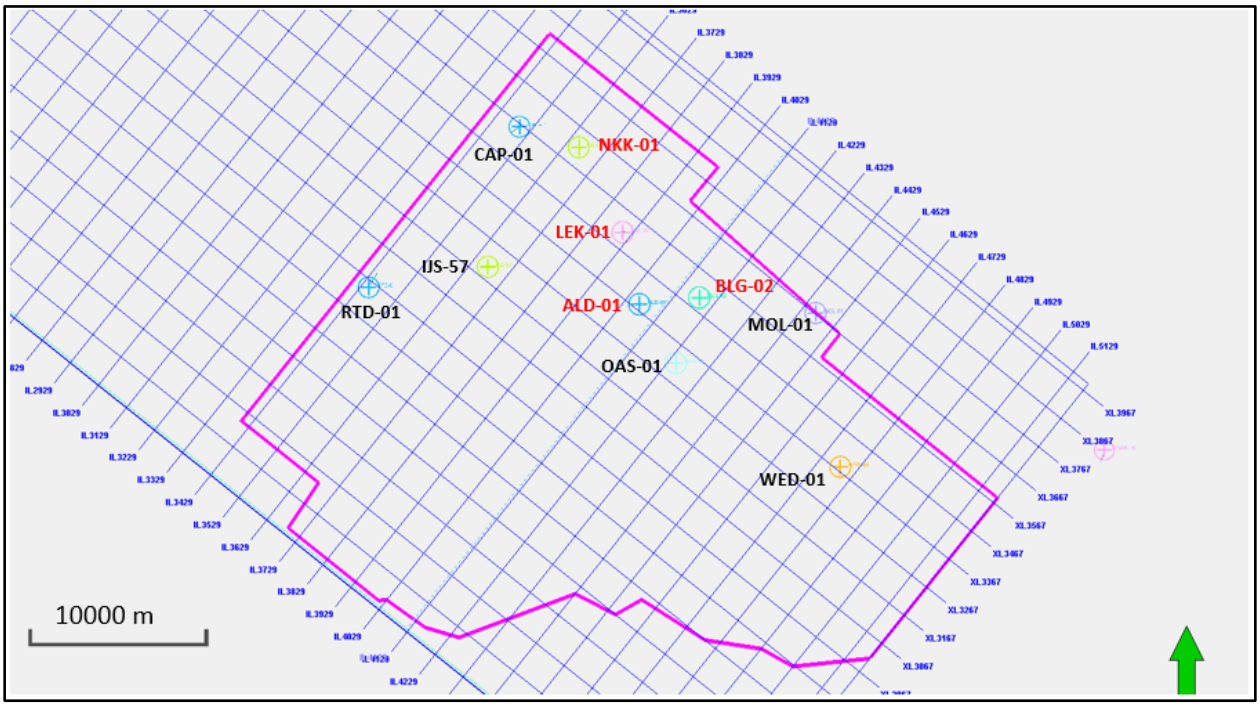

Figure 10 Distribution map of wells with core data penetrating the Alblasserdam Member. Core descriptions are taken from wells with a red label.

3.2.3 Core Data

Core descriptions were performed to study the lithofacies characteristics of the reservoir on centimetre scale, such as grain size trends, sedimentary structures, and diagenetic features that provide an idea of facies and environmental development of the reservoir.

The cores are provided by NAM, and the core descriptions were conducted in NAM Corestore, Assen. In this study, cores from four wells (Figure 10) penetrating the Alblasserdam Member are described with a scale of 1:50 and the total length of 46.9 m. The cores are slabbed and preserved as a set of fragments with lengths between 3 – 12 cm.

4. Results

4.1 Seismic Interpretation

The seismic interpretation is performed in-depth domain using Petrel 2014 software. In general, the seismic interpretation is done by initially performing well to seismic integration by investigating the acoustic character of the horizons from density and sonic logs. The seismic acoustic character of each horizon is used as guide and lithology marker in horizon interpretation, to reduce the uncertainties and inconsistencies during interpretation. The horizons interpretation is performed simultaneously with fault interpretation to obtain a result that is in accordance with the geological background. Figure 11 illustrates the workflow of the seismic interpretation steps. A detailed process of each step is discussed the following subchapters.

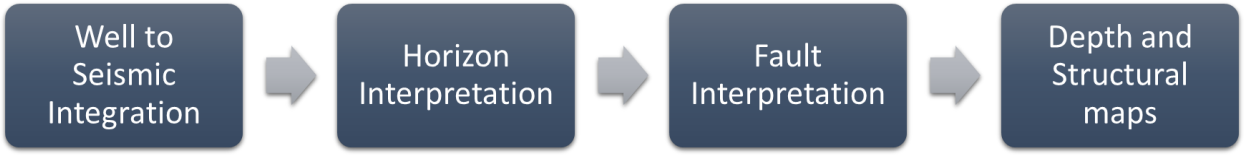

Figure 11 Workflow of Seismic Interpretation

4.1.1 Well to Seismic Integration

The first step in seismic interpretation is well to seismic integration. Well to seismic integration is done by importing the lithology well marker of the four horizons, the NSG, the CK, the KN and the SLD, from lithostratigraphy interpretation by Boogaert and Kouwe (1993) and updated by Munsterman et al. (2012) contained in the extracted well dataset. The lithostratigraphy interpretation is in measured depth. By inputting the deviation of the well, the lithostratigraphy interpretation can be displayed in the true vertical depth within the same panel as the seismic section.

Initially, an investigation of the seismic acoustic character of each horizon is derived from the sonic and density log responses to improve the confidence in horizons interpretation. In conjunction with analyzing the gamma-ray log response, a well log analysis of the NSG, CK, KN and SLD horizons is discussed in the following paragraph and presented in Figure 12.

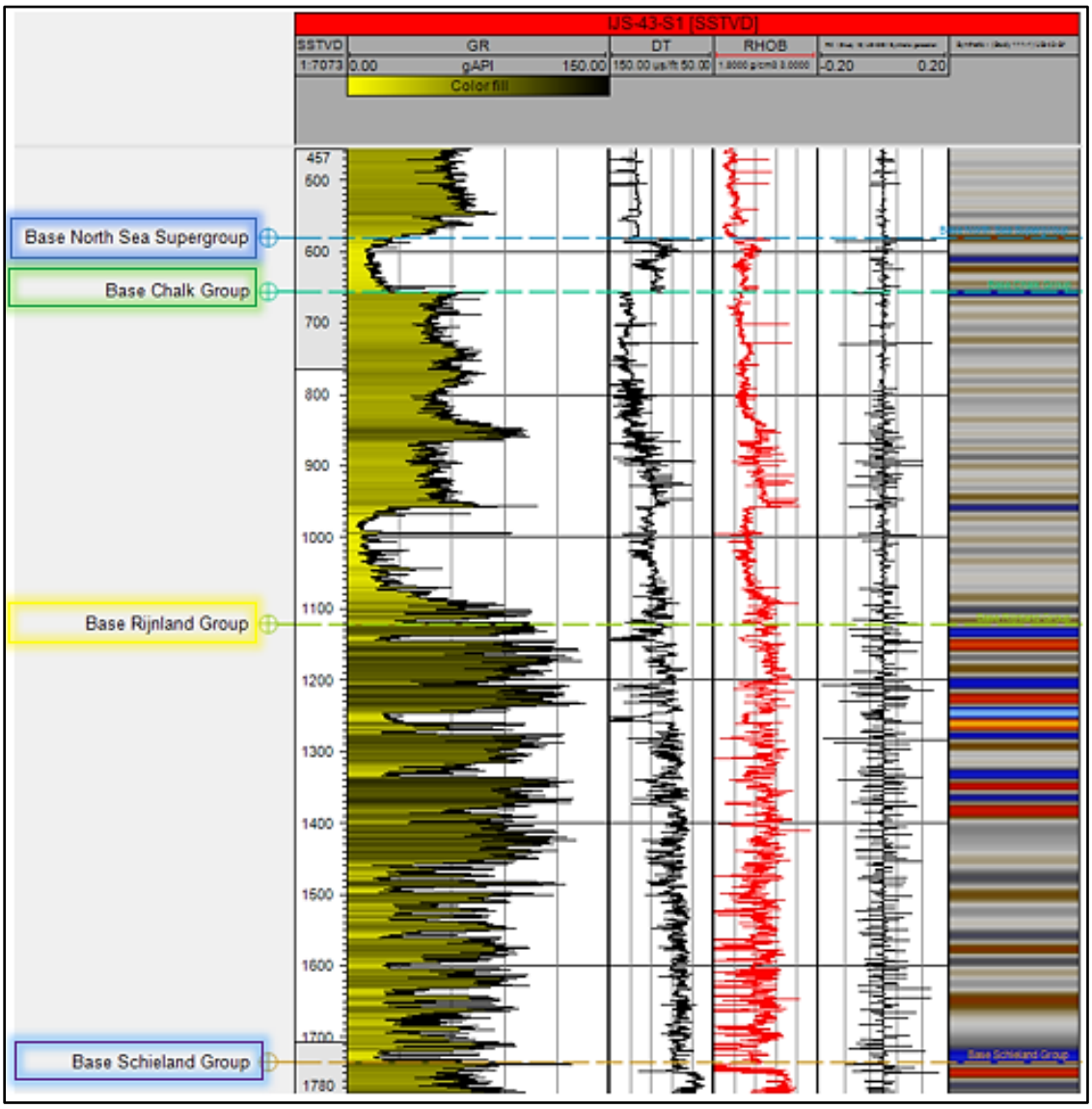

Figure 12 Seismic acoustic character and log responses of the NSG, CK, KN and SLD horizons in well IJS-43-S1

- *Base North Sea Supergroup (NSG)*

The NSG horizon is formed by the transition between the of the Landen Formation sediments of the Lower North Sea Group (NL) and the CK (Figure 12). The CK is absent in the southeast part of the study area, and the NSG sediments directly overlain the SLD sediments and can be observed in seismic acoustic character from well WED-03, GSD-01 and WGD-01. This horizon characterized by a strong hard kick as the gamma-ray log response is gradually decreased, significantly increased in the density log, and significantly decreased in the sonic log.

- *Base Chalk Group (CK)*

  A significant increase in gamma-ray log responses with a sharp boundary characterized the CK horizon. The density log response shows a sharply decreased, on the other hand, the sonic log shows a sharply increased, resulting in a significant negative contrast impedance as illustrated in Figure 12.

- *Base Rijnland Group (KN)*

  The KN horizon is a boundary between the Schieland Group and the Rijnland Group that formed by the transition between the Rodenrijs Claystone Member of the SLDN Formation with Vlieland Sandstone Formation or Vlieland Claystone Formation. The log responses show a decrease in gamma-ray where the Vlieland Claystone Formation overlies the Rodenrijs Claystone Member. On the other hand, a decrease in gamma-ray when the Vlieland Sandstone Formation overlies the Rodenrijs Claystone. As illustrated in Figure 12, the density log responses show a slight decrease while the sonic log is increased resulting in a negative reflection coefficient.

- *Base Schieland Group (SLD)*

  The boundary between the Alblasserdam Member and the Brabant Formation formed the SLD horizon. Characterized by an increase in the gamma-ray log and density log, and decrease in the sonic log, resulting in a positive contrast impedance and shows as a hard kick in the seismic section. However, the Brabant Formation is absent at the southwestern part of the study area. Thus, the Alblasserdam Member lies on the deeper Formation of the Altena Group, the Aalburg Formation. From wells BRT-01 and BRTZ-01 (Appendix A), the boundary between the Alblasserdam Member and the Aalburg Formation, the logs responses show as a sharp increase in the gamma-ray log. Increased in the sonic log while the density log is decreased resulting in a negative reflection coefficient.

The well to seismic integration of the NSG and the CK horizons has good coherencies. On the other hand, some discrepancies are found at some places in the KN, and the SLD horizons with deviation vary between 5 - 20 m. These deviations possibly caused by the limitation of the velocity model used for time to depth conversion during reprocessing data, especially when facing an area with high structural complexities as found in the WNB. Figure 13 illustrates the result of well to seismic integration across a composite line crossing well NKK-01, IJS-43-S1, BRT-01, and RDK-01.

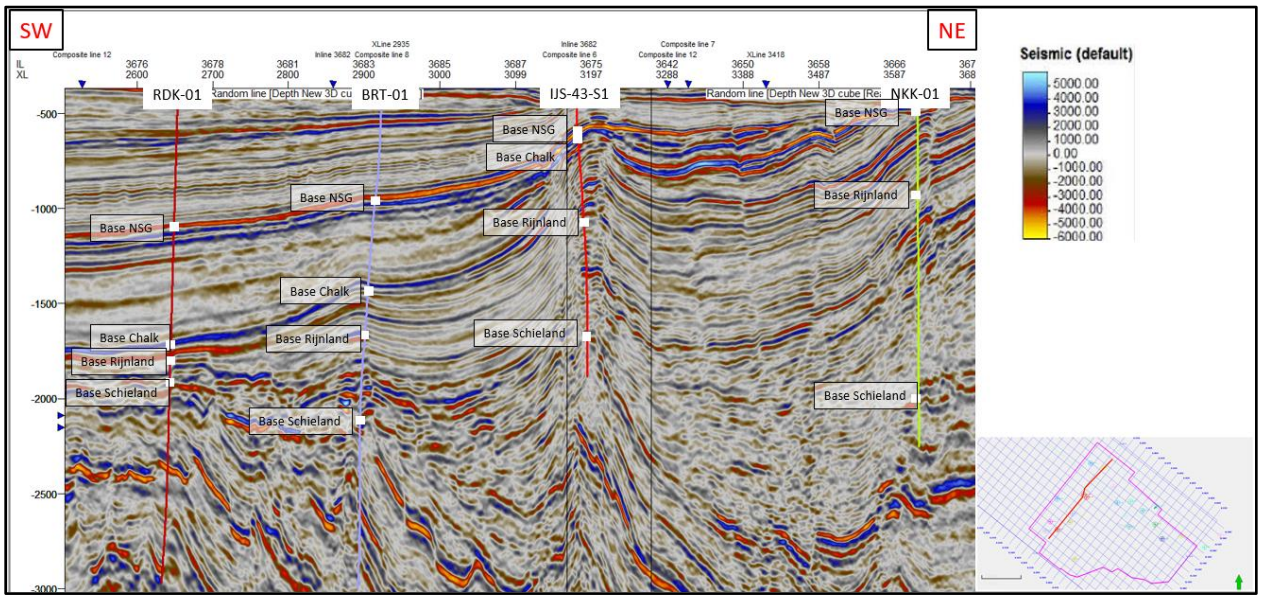

Figure 13 Well to seismic integration cross-section of a composite line

4.1.2 Horizons Interpretation

The four horizons show moderate to excellent reflections in the seismic section. Table 3 presents the resume of the seismic acoustic character and the seismic quality in the seismic section of the four horizons.

Table 3 Resume of the seismic acoustic character of the NSG, the CK, the KN, and the SLD

Lithology	Horizon	Seismic Acoustic Character	Seismic Quality
Base North Sea Supergroup	NSG	Strong hard kick	Excellent
Base Chalk Group	CK	Strong soft kick	Excellent
Base Rijnland Group	KN	Soft kick	Moderate
Base Schieland Group	SLD	Hard kick where Brabant Formation (NE) is present and Soft kick where absent (SW)	Moderate to Good

First, the horizon interpretation is performed in several composite lines intersecting the wells in the Drechtsteden to give an initial reference point. This process is important to reduce an error in picking the supposed horizon, especially for the KN and SLD horizons.

The primary structural trends in the WNB are toward NW-SE and parallel to the seismic crossline. Thus, the horizons and faults interpretations are performed in the seismic inline section every 8th increments. For an area with high structural complexities, the interpretations are performed with 4th or 2nd increments. The horizon interpretations are done by manual picking and finished with the guided auto-tracking to create a surface map as illustrated in Figure 14.

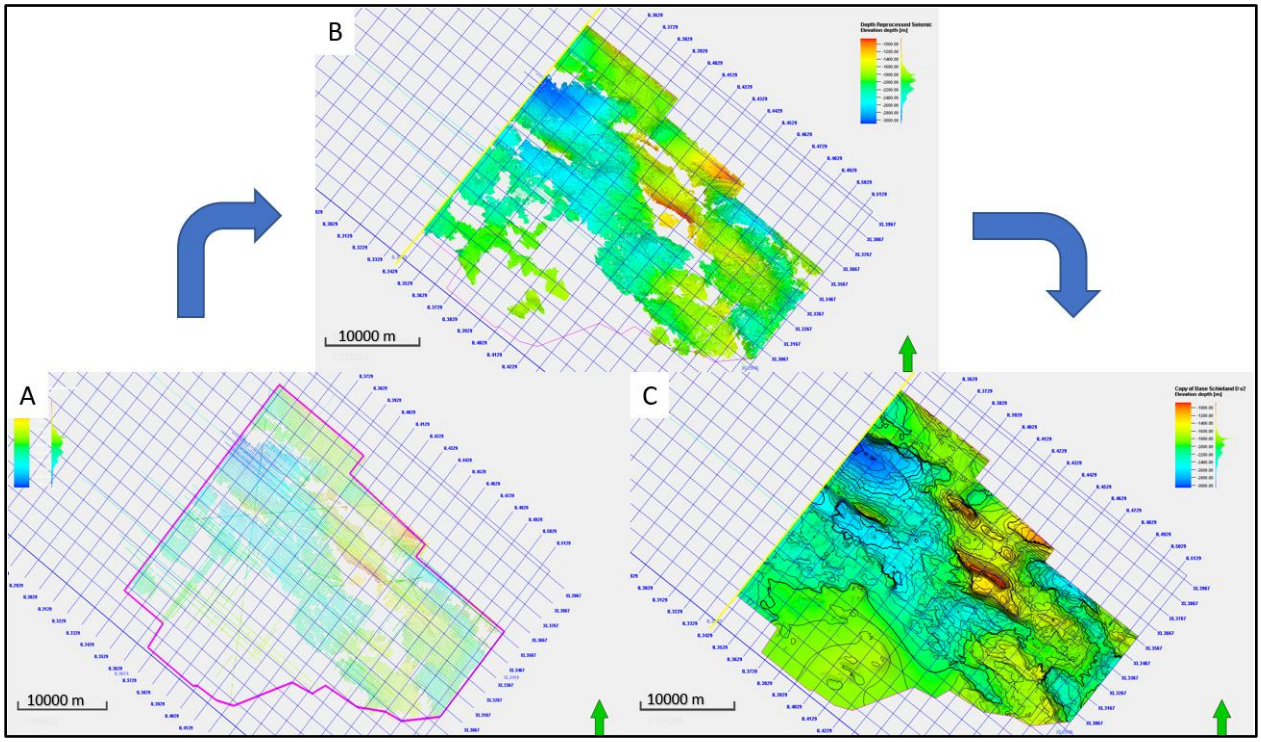

Figure 14 Steps in horizons interpretation at Base Schieland Group A) Result of 2D interpretation across inline and crossline; B) Result from 3D guided auto-tracking; C) Surface Map

4.1.3 Faults Interpretation

Intense tectonic activity has occurred in the WNB, especially between the Triassic and the Early Tertiary at the time of the Pangea break-up and followed by the Alpine Collision. These two big tectonic activities have resulted in numerous faults that can be observed in the seismic section. The faults have a varying trend, penetration, length, displacement, dip, and tectonic regime.

An Ant-tracking volume attribute is utilized to map the propagation of the faults. The ant tracking volume attribute is sliced at a depth of -1504, -2000 and -2504 m to observe the faults within the Alblasserdam Member that lies at a depth between ~-1000 to ~-3000 m.

Figure 15, Figure 16, and Figure 17 show the faults distribution across the study area. At -1504 m depth, the faults are concentrated in the NE part only. Tracking such a trend of a single fault propagation from the ant tracking volume attribute is difficult as the faults have a short lateral continuity. Nevertheless, the faults are forming a major NW-SE striking trend.

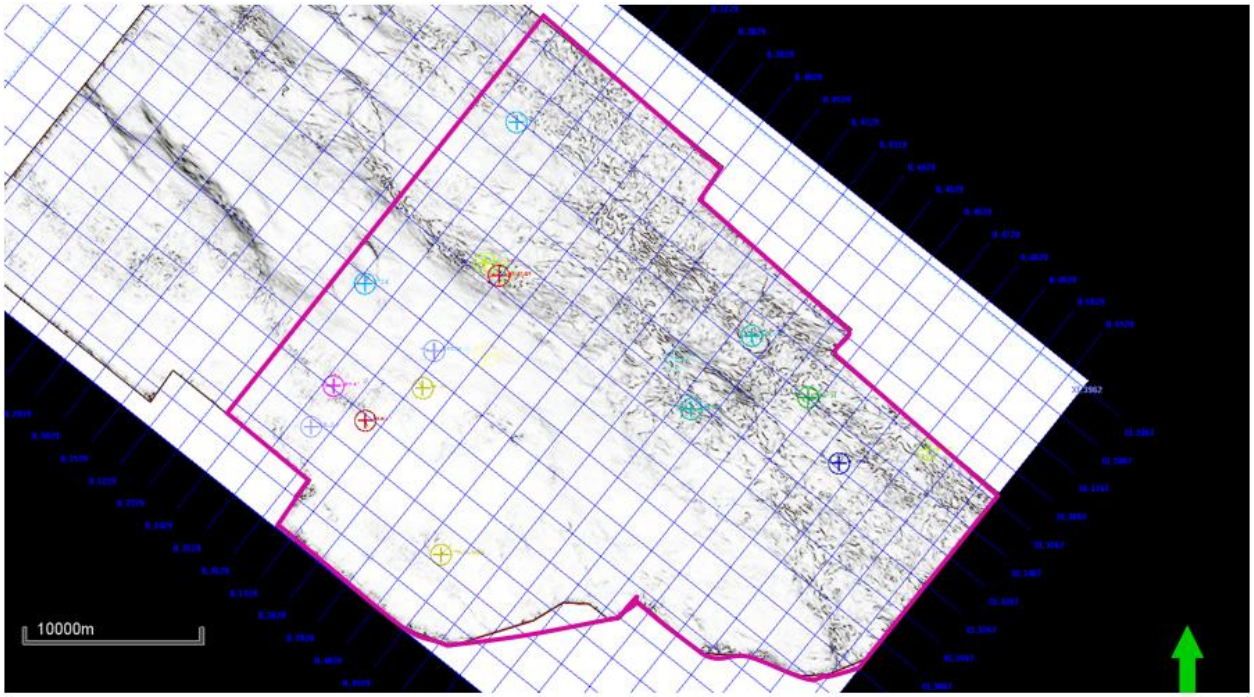

Figure 15 Ant-tracking volume attribute map as depth -1504 m

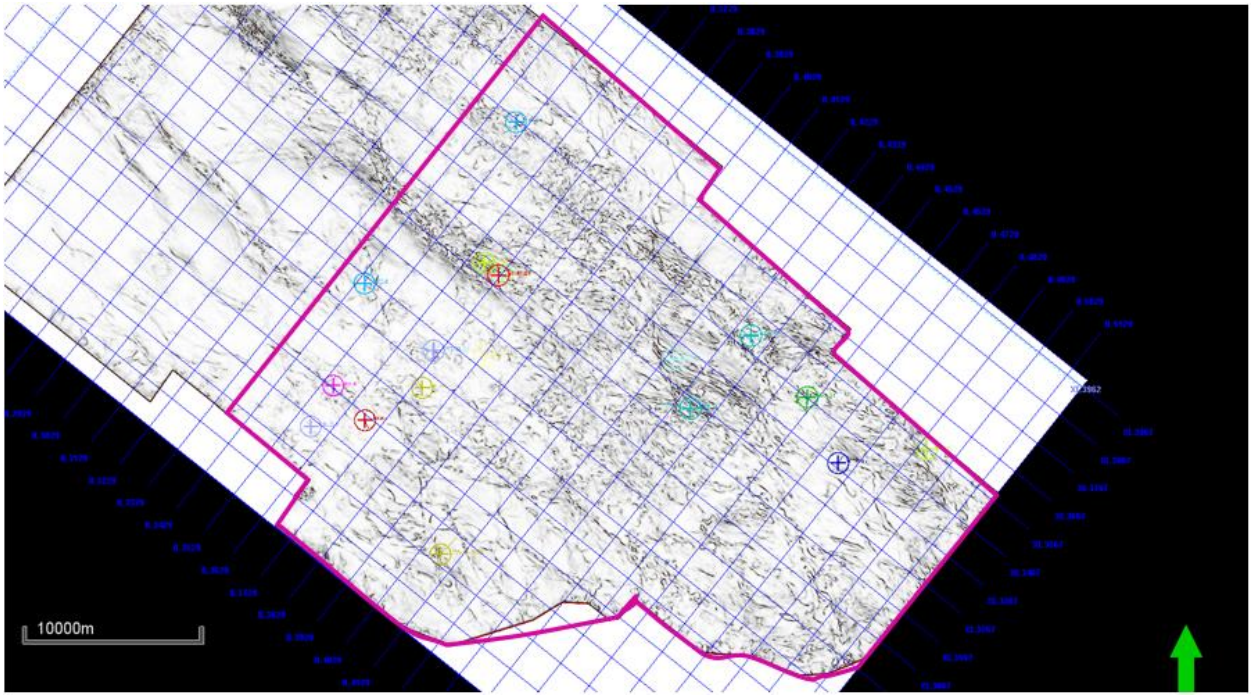

Figure 16 Ant-tracking volume attribute map at depth -2000 m

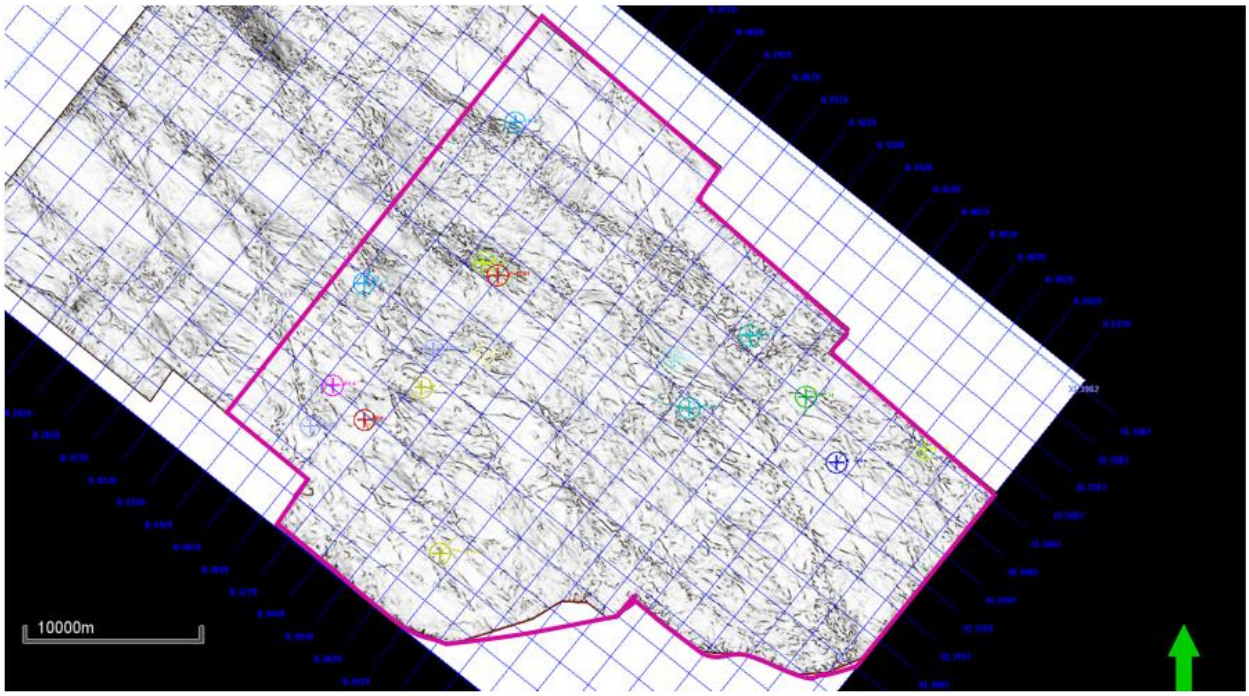

Figure 17 Ant-tracking volume attribute map at depth -2504 m

The penetrations of the faults indicate the time of the fault being developed. In this study, based on the timing of the fault's development, the faults are classified into three different group as described below:

Old Faults Group

This group consists of faults that were formed during the rifting period. The faults are characterized as normal faults that forming the base of the SLDNA (Figure 18) and densely distributed all over the study area (Figure 16 and Figure 17). The faults propagate through the Triassic until the Late Jurassic sediments with displacements that varying from about 50 m to about 200 m lengths. Some of the faults were active during the deposition of the SLDNA, causing the SLDA to have a different thickness.

New Faults Group

This group of faults was developed during the late Cretaceous and the Early Tertiary that corresponds to the Alpine collision. The faults are reverse faults with displacement varying from 25 to 110 m and propagate through the Late Jurassic - Early Cretaceous to the Early Tertiary sediments (Figure 18). Unlike the distribution of the old fault group, this group of faults is concentrated in the NE part of the study area (Figure 15).

Reactivated Faults Group

This group consists of faults that already formed during the rifting period in the Triassic – Late Jurassic and being reactivated during the inversion period in Late Cretaceous. The faults characterized as a normal fault with high displacement at the bottom and a reverse fault with less displacement at the top (Figure 18). The fault penetrations vary from the Triassic to the Early Cretaceous at the SW part and from the Triassic up to the Early Tertiary sediments at the NE part which corresponded to the occurrence and the magnitude of the inversion pulses. The fault reactivation occurred at a slightly different angle than the older fault that already exists. Thus, the reactivated faults forming a listric fault as illustrated in Figure 18.

Furthermore, based on the displacement of the faults, the faults are classified into major and minor faults group. The major faults group is a group of faults with a significant displacement, up to 1 km length, that divide and bound the Schieland Group into several main bodies. On the other hand, the minor faults group is a group of faults with minor displacement in between the major faults but still give an impact to the continuity of the layer. Figure 19 and Figure 20 illustrate the distribution of the major and the minor faults.

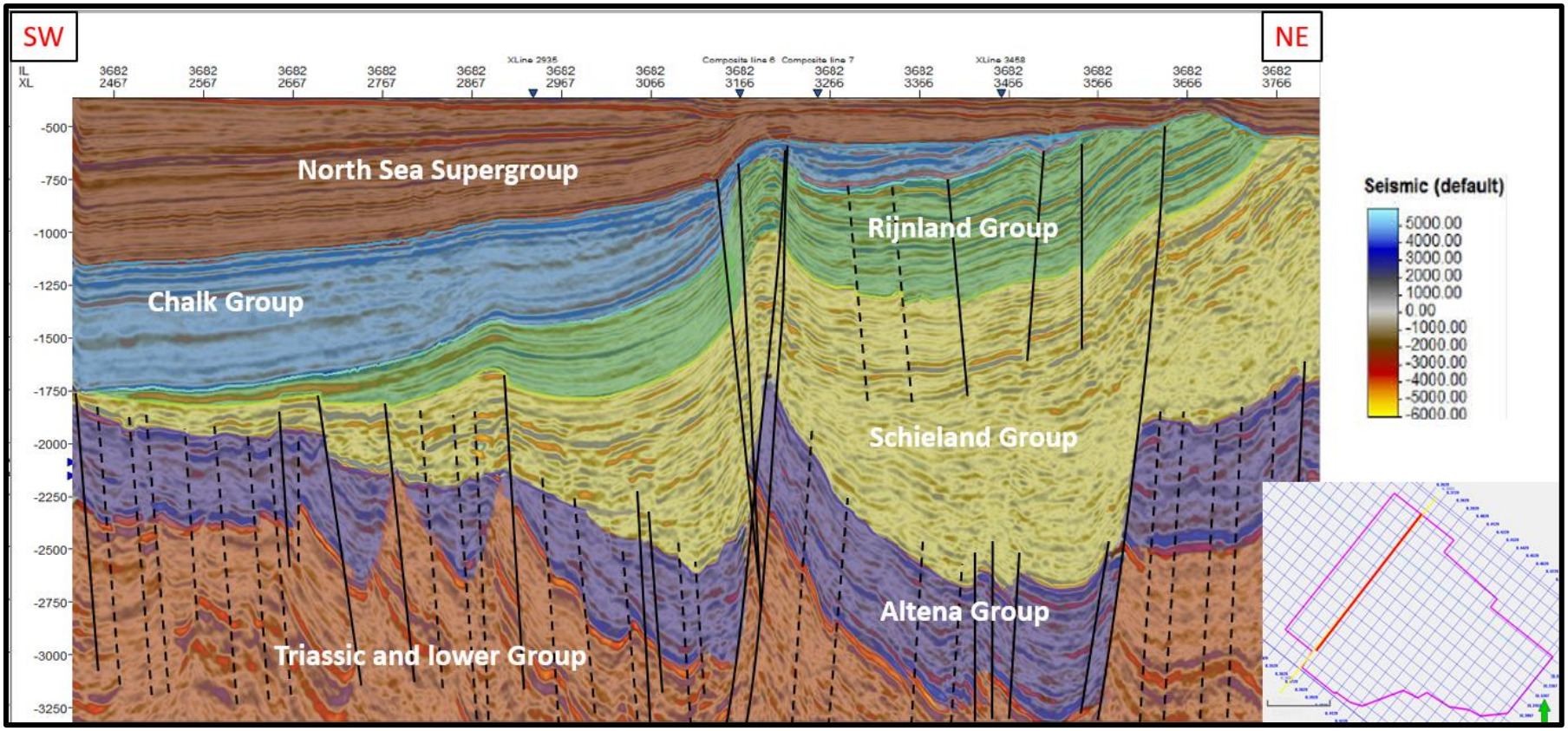

Figure 18 Horizons and Faults Interpretations shown in seismic cross section at inline 3682

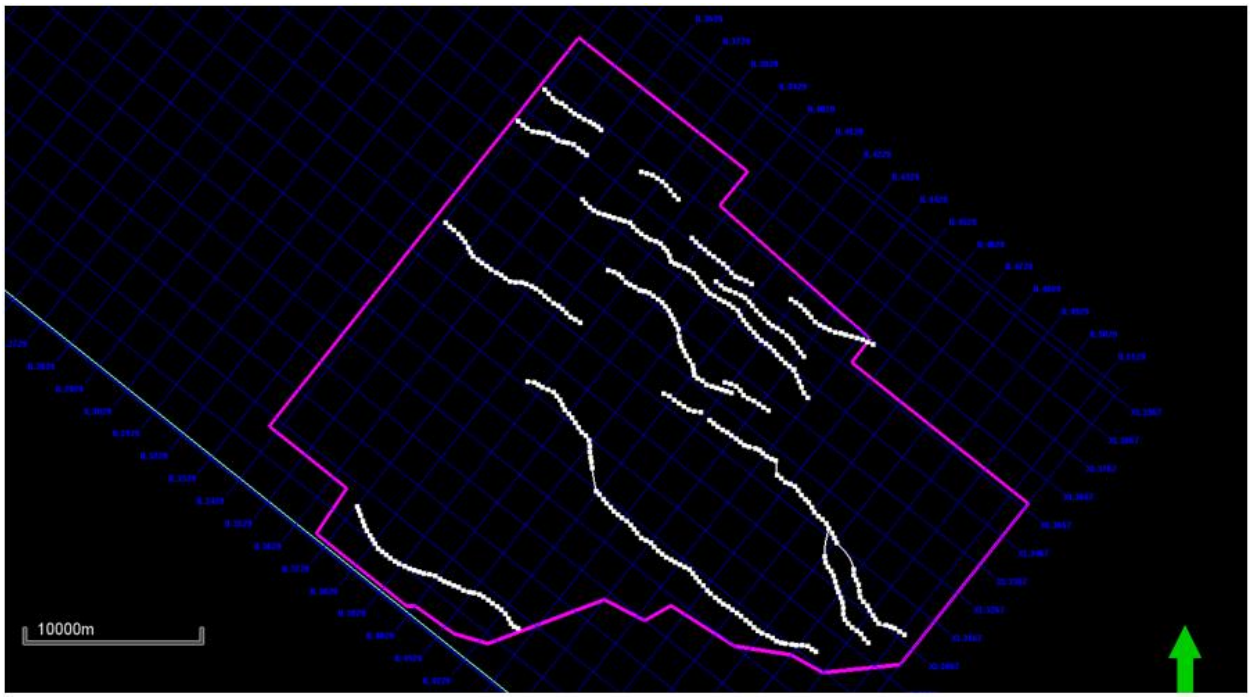

Figure 19 Map distribution of the major faults

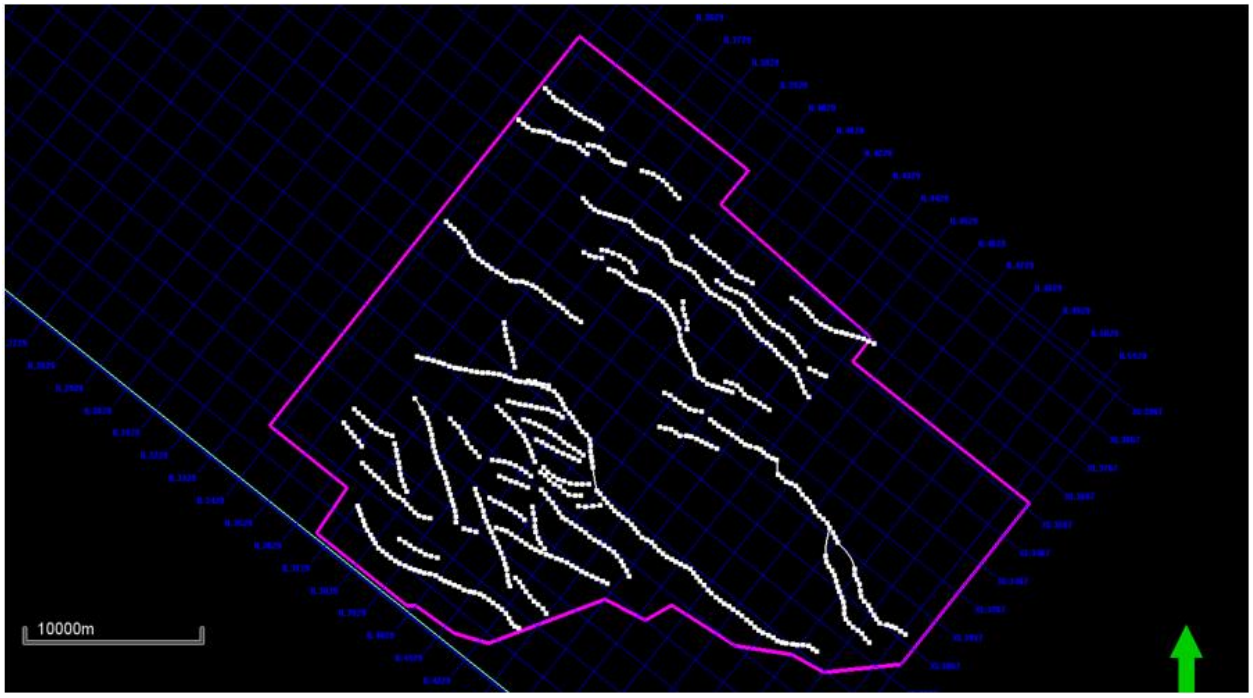

Figure 20 Map distribution of the major and the minor faults

4.1.4 Depth and Thickness Maps

The result of the horizons interpretation is presented in Figure 18 that illustrates the subsurface architecture in the WNB during the Late Jurassic until the early Tertiary. The seismic cross-section shows a different distribution, thickness, and depth trend of each Group within the WNB. The depth of each horizon and the thickness of the Chalk Group, Rijnland Group and Schieland Group are mapped and discussed in the next sub-chapter.

Most of the available wells are originally exploration wells targeting hydrocarbon and drilled in the structural high area. The high depth and thickness variation of the Nieuwerkerk Formation compounded by a high number of structural elements, causing the well penetration does not cover the entire SLDN sediments (Figure 28). As consequences, producing a thickness map from isopach map generated from the well lithology marker will result unreliable thickness model. Thus, the thickness map of Chalk Group, Rijnland Group, and Schieland Group are produced by the integration of the surface map and the lithology marker.

Schieland Group

The SLD horizon is characterized as a laterally fragmented hard-kick reflection with moderate to good seismic quality. At the most extreme area, the horizon has a significant depth difference within 50 m apart as illustrated by the red circle in Figure 18. This horizon can be traced by following an unconformity that separates the Altena Group and the Schieland Group. The unconformity was formed corresponding to Mid Kimmerian uplift and erosion during the Early to Middle Jurassic. The SLD horizon distributed all over the study area with depth varying from ~-900 to ~-3000 m.

The thickness has a significantly difference from one area to another that varying from 80 m to 1600 m. The maximum thickness is accumulated in the central-northern part of the study area and thinning to the point of absence towards the SW. The sediment in the SW overlies on the deeper Altena Group sediments, the Aalburg Formation, and characterized by a moderate soft-kick reflection in the seismic section.

Rijnland Group

The KN horizon can be traced as a continuous soft-kick reflection with moderate seismic quality overlying on the Schieland Group sediments. The depth of the KN horizon varies from

approximately -600 m depth in the NE and dipping towards SW with depth about ~-2000 m. The KN horizon is distributed all over the central part of the study area and getting difficult to be traced at the edges of the study area.

The Rijnland Group sediments are laterally continuous with highest sediments accumulation at the NW reaching about 700 m thick and getting thinner towards the proximal at the SE part with about 80 m thick. The KN and CK horizons are absent at the SE.

From the NE-SW perspective, the thickness trend of the Rijnland Group sediments shows an opposite trend as the Chalk Group sediments (Figure 18). The Rijnland Group sediments have a relatively homogeneous thickness from NE to the central part and thinning towards the SW. The lithology interpretation in well STW-01 (Appendix A) shows the KN sediments are absent in the SW part of the study area.

Chalk Group

The CK horizon shows a strong and continuous soft-kick reflection in the seismic cross-section. The depth is varying from ~-500 m in the NE and dipping to the SW with a depth up to ~-1900 m as depicted in Figure 25.

Figure 26 shows the thickness distribution of the Chalk Group sediments. The sediments are laterally continuous and thinning from SW to NE, with thickness up to 700 m thick in the SW and thinning at the limb of structural high and disappeared in the NE part.

North Sea Supergroup

The NSG horizon is characterized as a strong and continuous hard kick reflection. The NSG is overlain on the sediments of the Chalk Group in most of the study area. In the SE part of the study area, the entire Chalk and Rijnland Group sediments are absent. In those areas, the sediments of the North Sea Supergroup are directly overlying the Schieland Group.

The NSG horizon is slightly dipping from NE to SW with depth varying from ~-450 m to ~-1150m depth as illustrated in Figure 27.

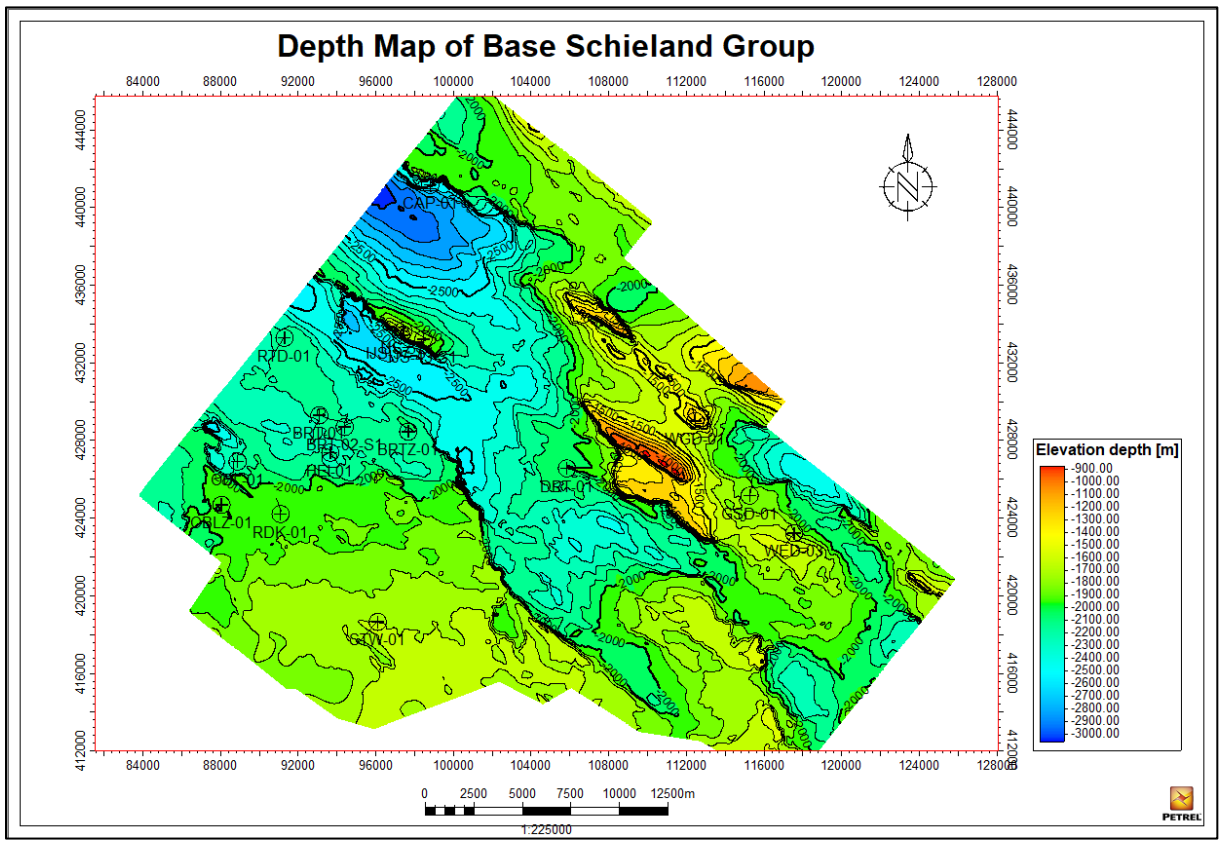

Figure 21 Depth Map of Base Schieland Group

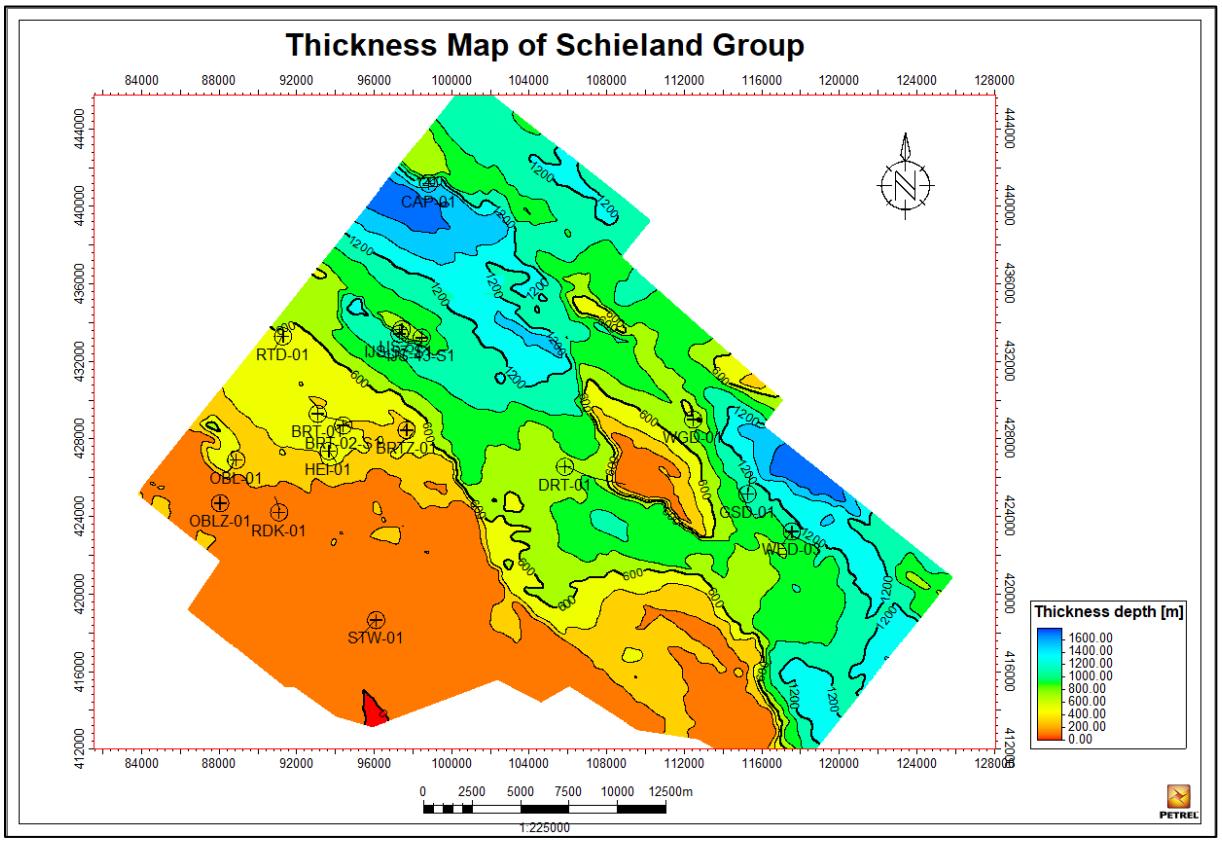

Figure 22 Thickness Map of Schieland Group

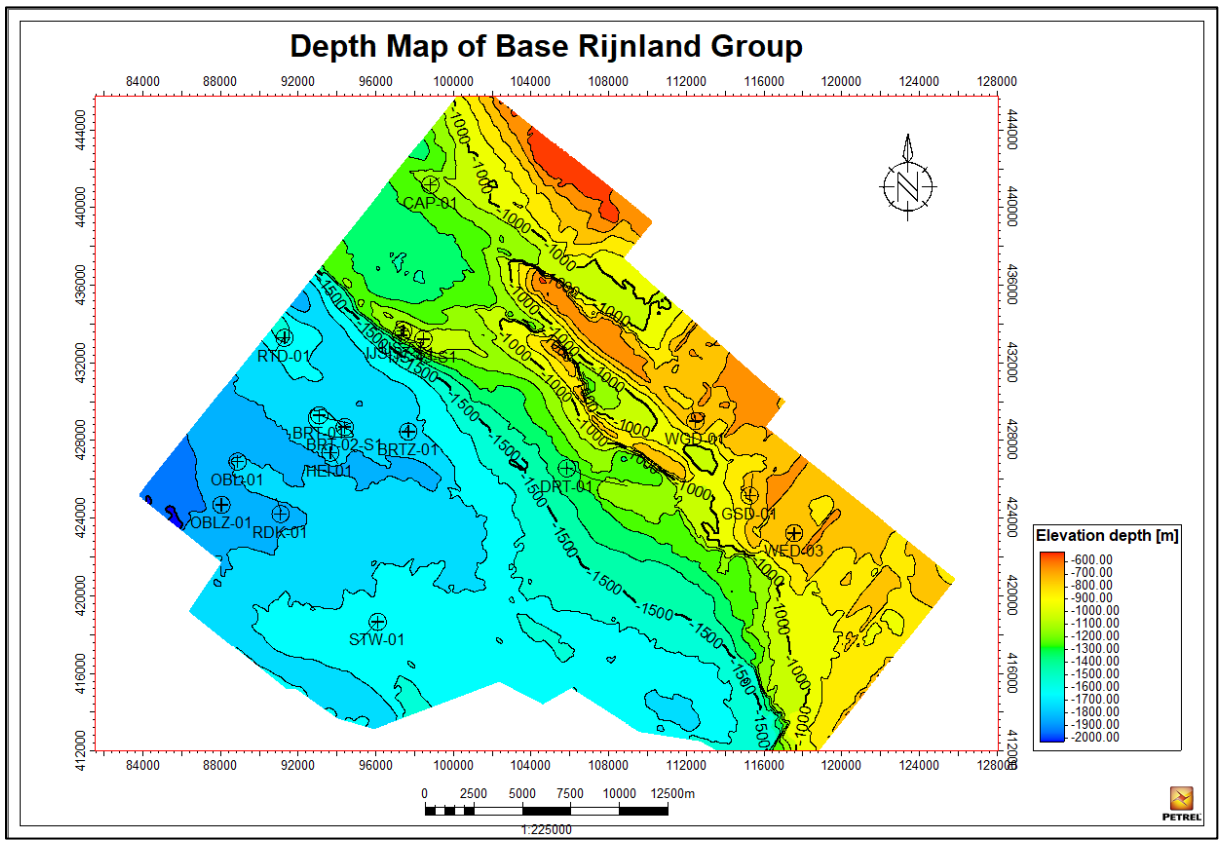

Figure 23 Depth Map of Base Rijnland Group

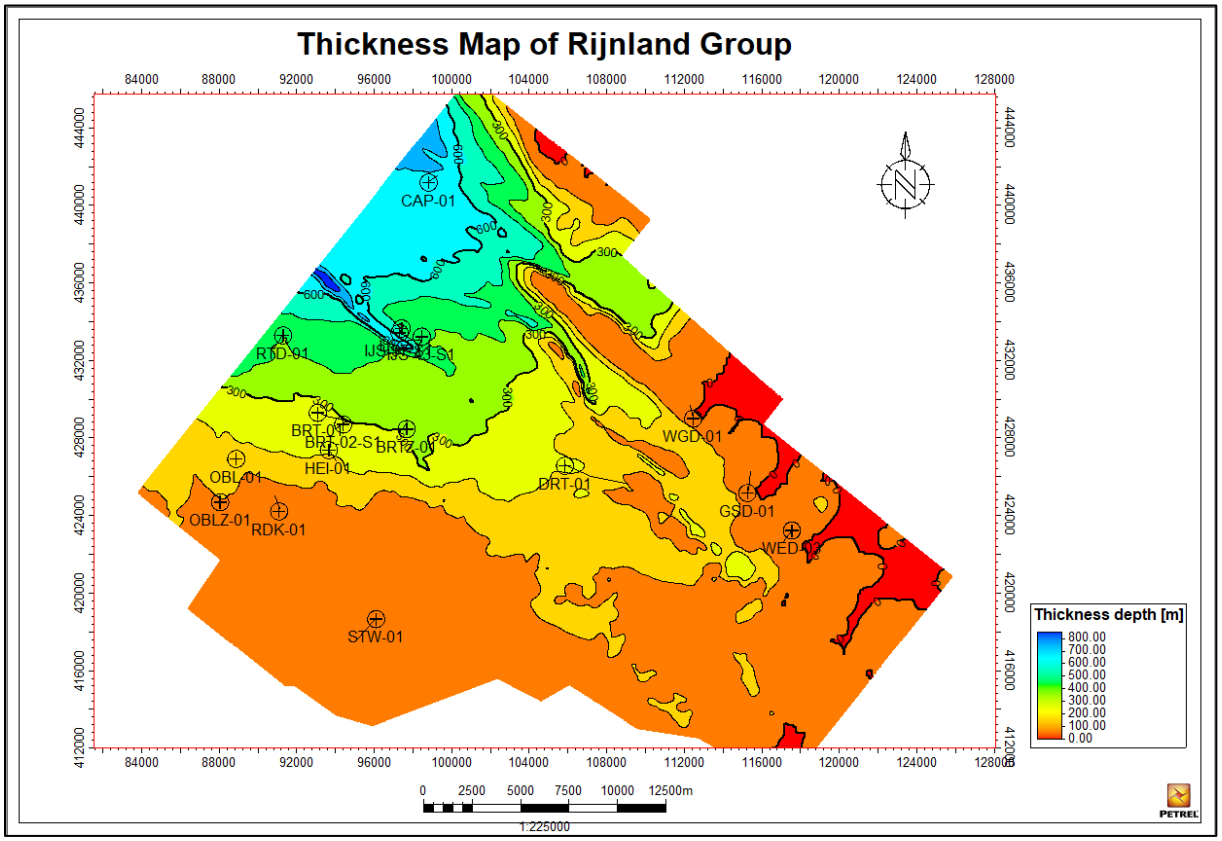

Figure 24 Thickness Map of Rijnland Group

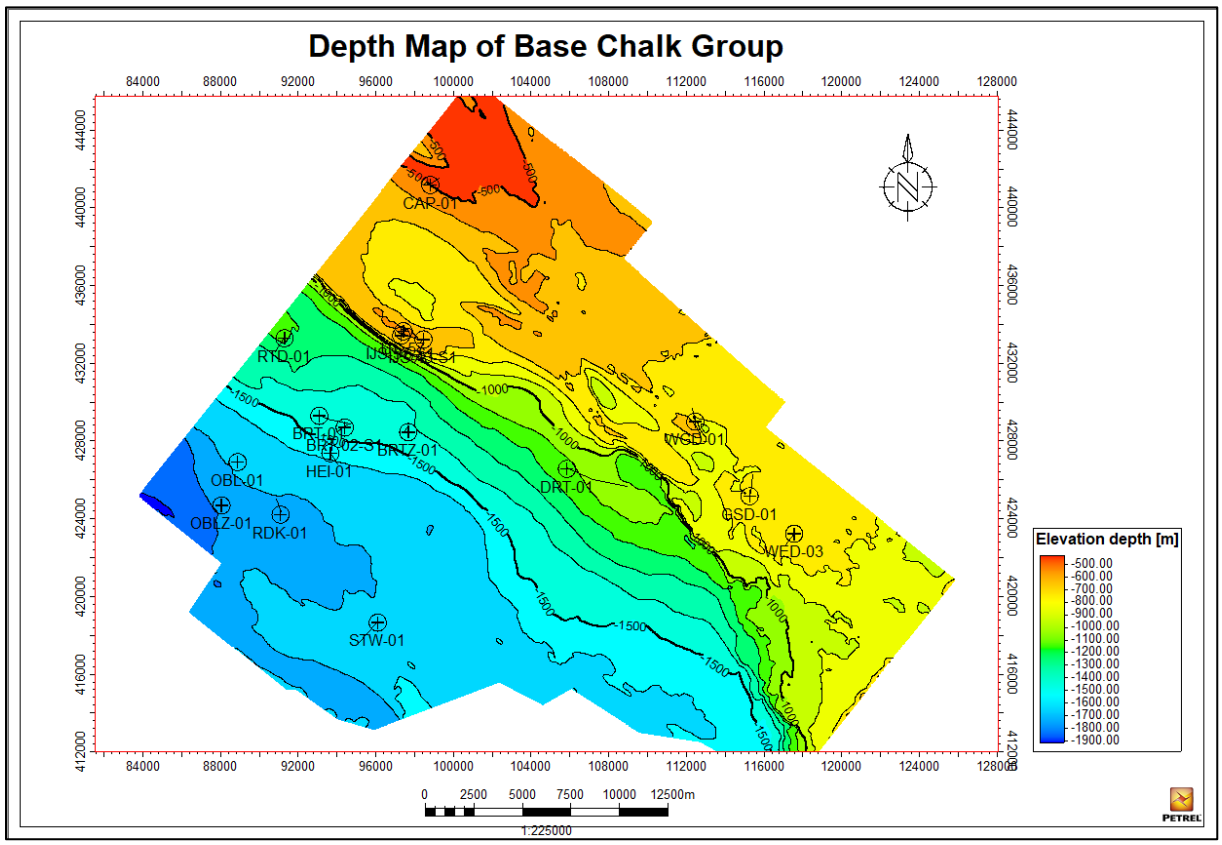

Figure 25 Depth Map of Base Chalk Group

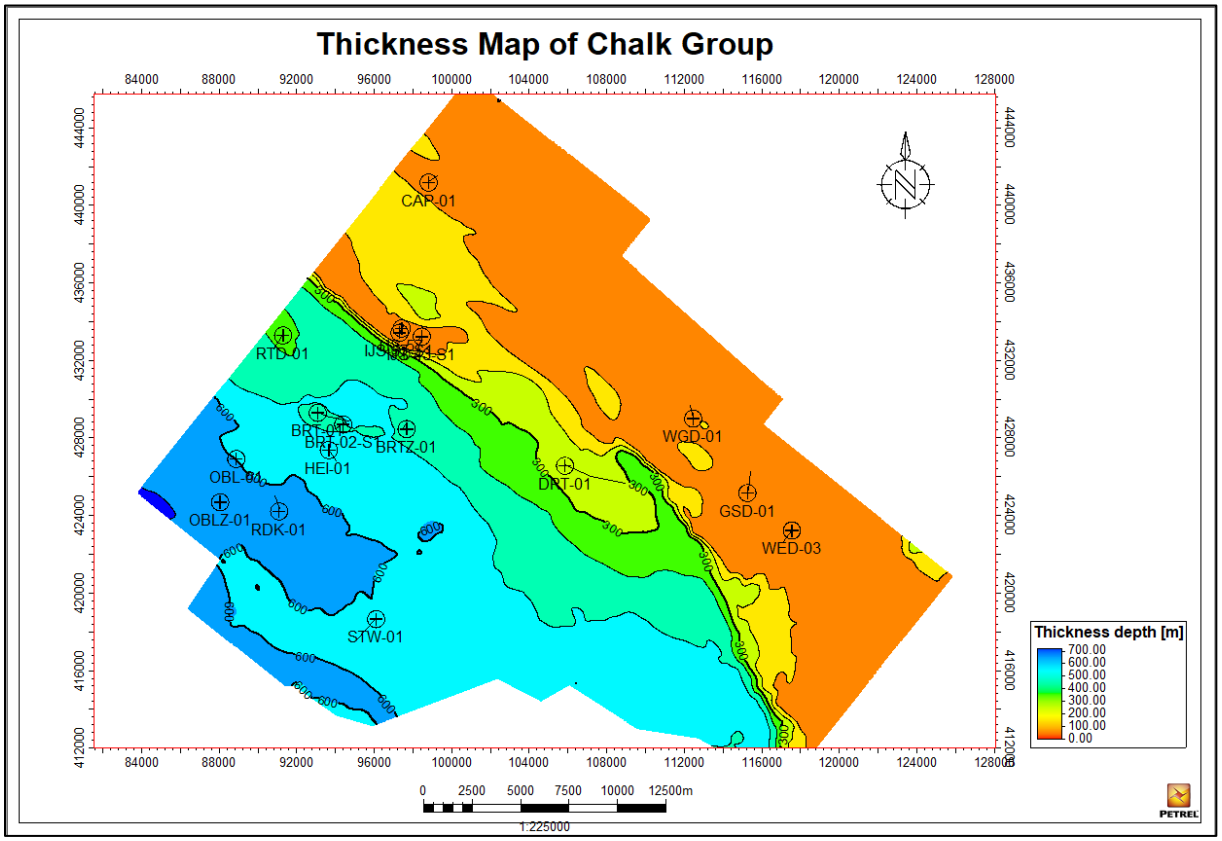

Figure 26 Thickness Map of Chalk Group

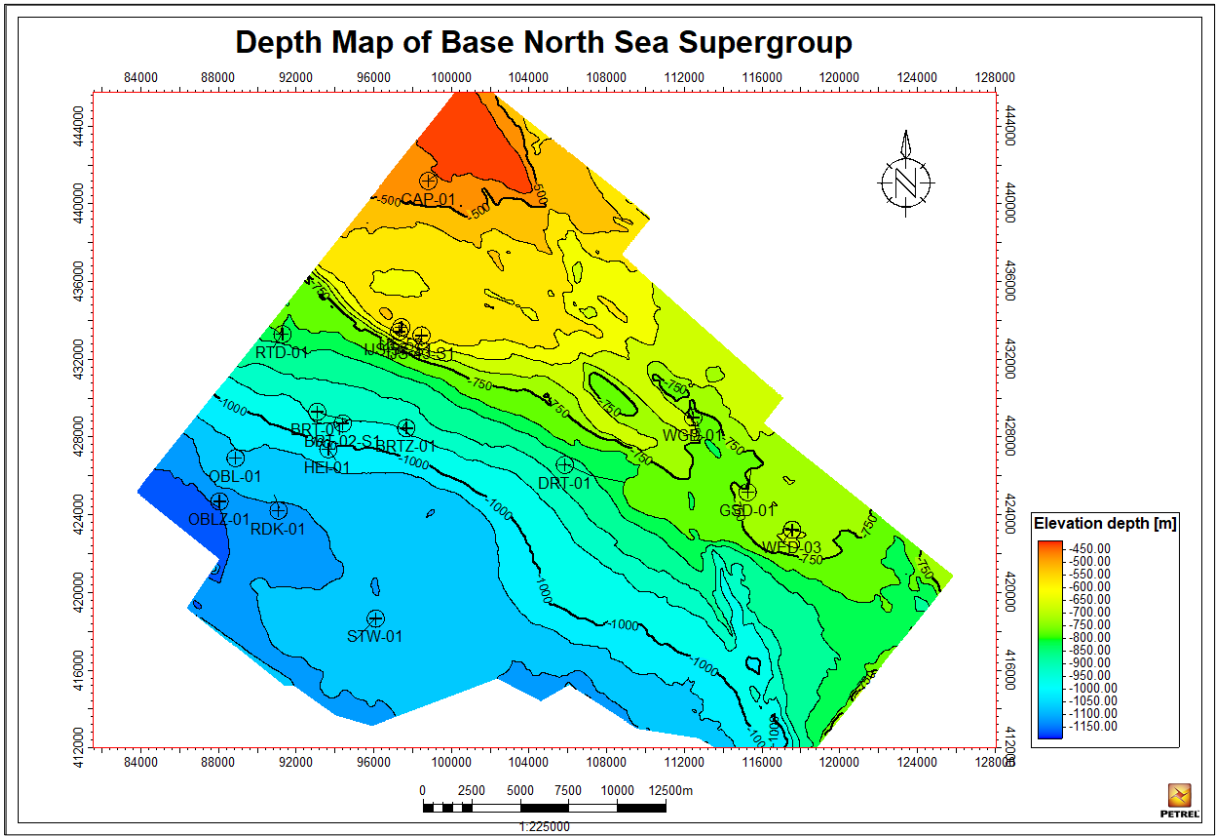

Figure 27 Depth Map of Base North Sea Supergroup

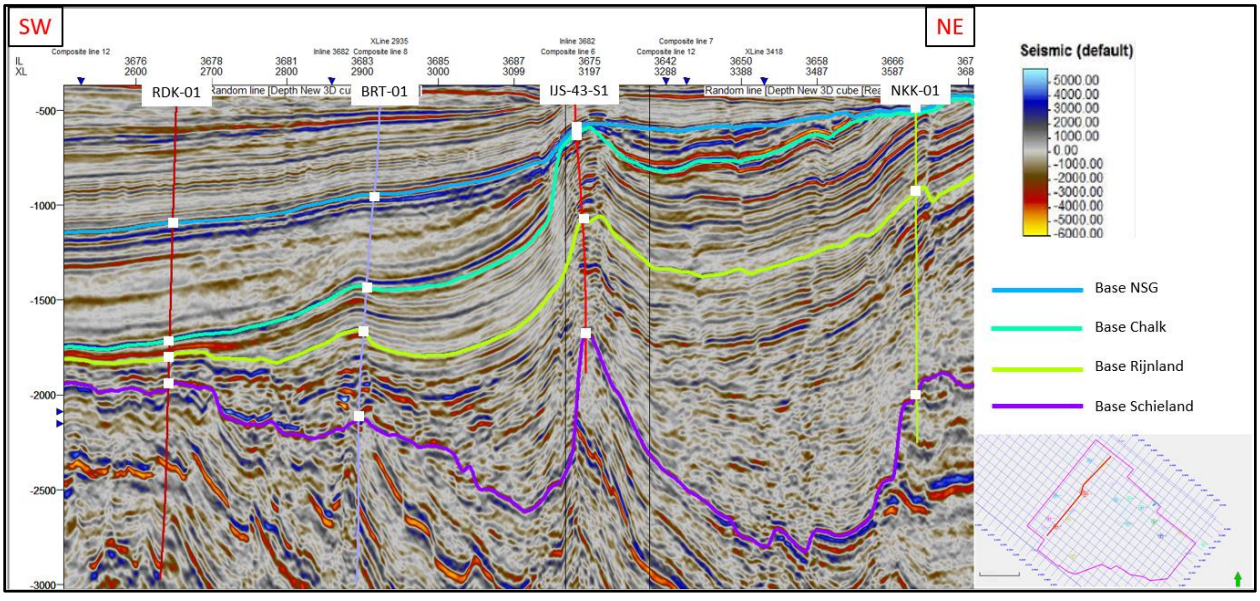

Figure 28 Well penetration in seismic cross-section

4.2 Reservoir Sedimentology

Figure 29 shows the workflow of sedimentological analysis in this study. The detailed discussion is presented in the following sub-sections.

Figure 29 Workflow of Reservoir Sedimentology

4.2.1 Core Description

The cores of the SLDN in the Drechtsteden area are limited and preserved as a set of fragments with length varying from 3 cm to 12 cm. It is difficult to study the depositional trend, recognizing structures of fluvial sediments such as cross-bedding and the boundary between layers. Lithofacies and depositional environment interpretation of the SLDN from the core description are tough due to the limited availability and quality of the cores. However, the result of the core descriptions can be used to get an insight of the potential aquifer quality.

Core description of Alblasserdam Member

15 core sections of Alblasserdam Member from well BLG-02, NKK-01, and ALD-01 are described. The length of each core section varies between 20 cm to 3.5 m with a gap at some parts. Three core sections will be discussed in this subchapter. The core sections are selected because it has indications of the good aquifer. The unselected core intervals are dominated by moderate to highly oxidized siltstone.

- Core B (-1342 to – 1345.2 m) well BLG-02

  This section consists of five core intervals. The core is characterized by three intervals of argillaceous sandstone with oxidized pyrite as the matrix. Followed by 25 cm long, fine-grained sandstone, well sorted and permeable signatures form the resin filling the pores. A bedding structure is present; however, the type of the bedding is difficult to be identified. Core at the top interval shows a high amount of weathered silt with an oxidized grain (pyrite) and oxidized clay pebbles.

- Core C (-1271 to -1273.4 m) well BLG-02

  This section consists of two core intervals, 20 cm at depth -1271 and 40 cm at depth -1273. The cores are characterized as fine-grained sandstone with a good sorting. The resin of the core is filling the pore of the core which indicates the core has good permeability. Bedding structures are observed in this core interval. Core at depth -1273 m, shows a small amount of white cement that present as a lamination with the fine-grained sandstone.

Figure 30 Cores of Alblasserdam Member at Well Bleskensgraaf-2 (BLG-02) at depth -1273 m and -1343 m

- Core G (-1505 to -1508.5 m) well NKK-01

  This section formed by four core intervals. Three core intervals that lie at depth -1506 – -1508.45 m show similar characteristic. The cores are characterized as fine-grained sandstone with well sorting and has an indication of a permeable layer as the resin fills the pores. A very fine-grained sandstone bounds the upper part. The transition of the boundary is unknown since the cores are fragmented.

Figure 31 Cores of Rodenrijs Claystone Member and Alblasserdam Member at Well Nieuwerkerk-1 (NKK-01) at depth -1230 m and -1506 m respectively

- Cores in well ALD-01

  This core section consists of six core intervals that distributed at depth -1214.5 to -1627.3 m. None of the cores shows a good aquifer indication. Most of the cores consist of a combination of very fine-grained sandstones with clay pebbles that lies on the oxidized silt and clay layers. At depth -1370 m, silt layer with ripples and sand layer can be found locally in between the layer.

Figure 32 Cores of Alblasserdam Member at Well Alblasserdam-1 (ALD-01) at depth -1469 m and -1370 m

Core description of Rodenrijs Claystone Member

Five scattered core sections of Rodenrijs Claystone Member from well BLG-02 and LEK-01 are described. Most of the core sections show a similar characteristic and dominated by highly weathered and oxidized siltstone. Thus, only two core sections that represent the overall core of SLDNR are discussed in the following sub-chapters.

- Core J (-1229 to -1231.9) well NKK-01

  This core section consists of four core intervals. At the bottom, the cores are characterized as argillaceous sandstone with organic-rich lamination. The cores are followed by 25 cm fine-grained sandstone with good sorting, and good permeability as indicated by a resin filled the pores. The cores at the upper intervals have a fining upward fine-grained to very fine-grained sandstone with clay pebbles and organic-rich fragments.

- Cores in well LEK-01

  This core section consists of two core intervals. Core depth -700 until -770.7 m are characterized as very fine-grained sandstone with good sorting and a permeable indication as the pores are filled by the resin. A parallel bedding structure is observed in this interval. Few rootlets and organic-rich are present as fragments and lamination. Oxidized grain (pyrite) are found at the top. Five centimetres of oxidized very-fine grained sandstone

present in between the layer. The top and the bottom boundaries are unknown since the core is not available.

The cores at the shallower interval consists of a coal layer and highly oxidized very fine sediment (silt). A high number of oxidized clay pebbles, rootlets, and coal fragments are found in the entire core interval.

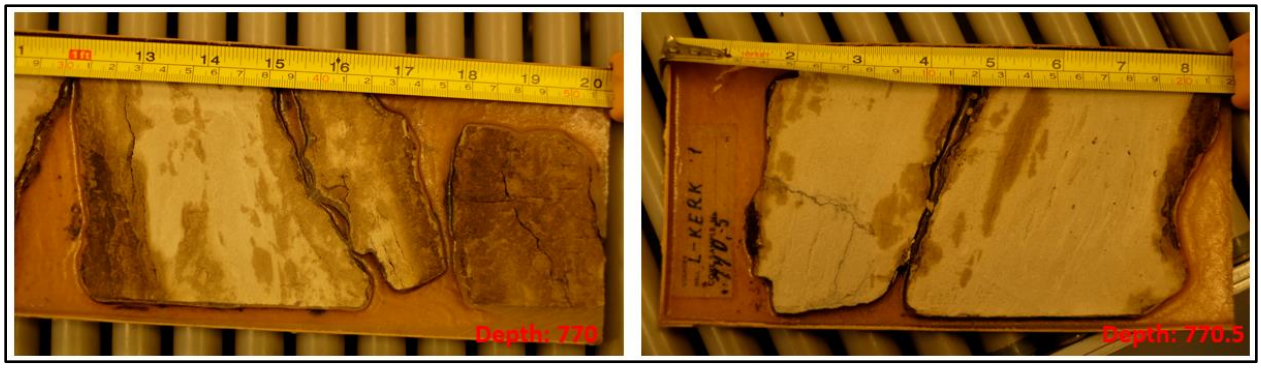

Figure 33 Cores of Rodenrijs Claystone Member at Well Lekkerkerk-1 (LEK-01) at depth -770 m and -770.5 m

4.2.2 Correlation of Gamma-ray and Core Description

From the core description, the SLDNA are characterized as interbedded of fine-grained sandstone, argillaceous sandstone, and silt. Another composition that can be observed are clay pebbles and oxidized very fine-grained layers. Ripples and bedding structures are observed at some cores; however, the type of the bedding cannot be identified since the core are preserved as fragments. From the gamma-ray log pattern, the SLDNA shows an interbedded of low and high gamma-ray response, with high thickness variation. The lateral continuity of the SLDNA is low as expressed by the seismic response in the seismic section. Based on the characteristics of the SLDNA shown in the cores, gamma-ray, and seismic response, high possibility of the SLDNA were deposited under fluvial setting.

Furthermore, the SLDNR also has similar characteristics to the SLDNA. However, the SLDNR has a higher number of oxidized layers. A significant rootlets, organic-rich fragments and lamination with very-fine grained layers indicate that the SLDNR were deposited under the fluvial setting that closes to the swamp environment.

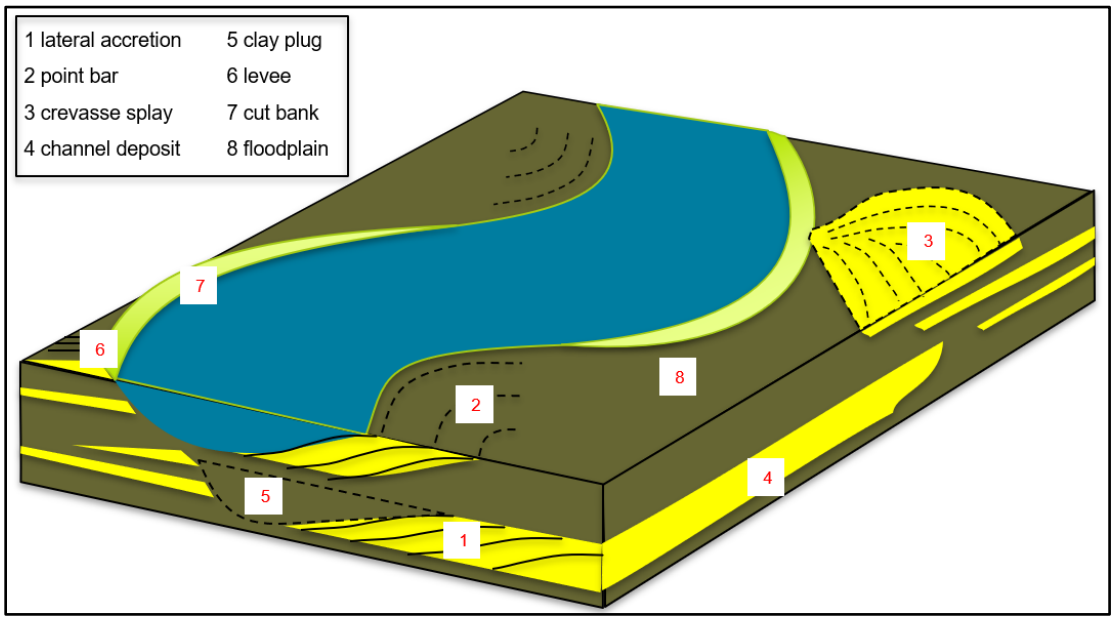

Figure 34 Main components and sub-environments of sinuous fluvial system

A fluvial system can be divided into three main sub-environments. There are channel, crevasse, and floodplain Figure 34. In this study, those three essential components of the fluvial system within the SLDNA is identified from the trend of the gamma-ray log response to obtain the distribution of sand-rich intervals within the study area. The characteristics of each sub-environments are resumed in Figure 35.

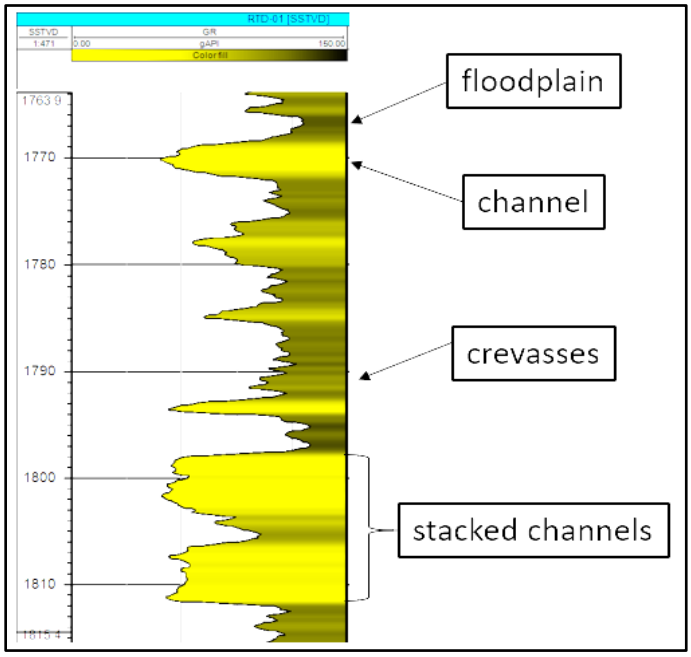

Figure 35 Recognition of fluvial lithology from gamma-ray log response

Channel

In the fluvial system, water flow is the main transport media of sediments from the source to the depositional environment or being trapped in the channel. The channel is bordered by natural dykes (levees). Within the channel, sedimentation occurs in the inner bend of the channel (point bar) and erosion in the outer bend (cut bank) which allows the channel to migrate sideways (Nichols, 2009).

In the gamma-ray log, a channel is characterized by a low and increasing upward interval. It can be formed as a single channel with thickness varies from 3 – 6 m and as a stacked-channels with thickness up to 25 m (Figure 35). A channel interval is observed from the SP log in well BLG-02 at depth -1267 m until -1275 (Figure 36). This interval is corresponding with Core C of well BLG-02. It can be concluded that 20 cm and 40 cm cores in Core section C of well BLG-02 are part of 8 m thick of channel.

Floodplain

The floodplain is the area of land between or beyond the channels that receive water only when the river is flooding. Commonly, the floodplain is composed of fine-grained sediments. In the gamma-ray response, it shows as a high gamma-ray interval.

Crevasse

A crevasse is a thin sheet layer of fine sand that spreads out on the floodplain as the result of levee breaches during flooding and formed a thin-bedded sand sheet. The existence of the crevasse will increase the connectivity between one river channel to the other. In the gamma-ray response, the crevasse shows as a thin low gamma-ray interval with a thickness less than 1 m (Figure 35).

Figure 37 shows Core B of well BLG-02 that corresponding with the high SP log response. From the SP log response and the core description, this interval could be interpreted as a floodplain of the fluvial system with crevasse. In addition, the gamma-ray and core description correlation of the SLDNR is presented in Figure 38.

From the gamma-ray and core description correlation, it can be concluded that the good aquifer indications can be found in the channel and crevasse. Thus, the potential aquifer with good aquifer properties is expected from the channels which characterized as low gamma-ray intervals. Table 4 provides the resume of the described cores and the core intervals with good aquifer properties.

Table 4 Described cores of the Alblasserdam Member

Well	Company	SLDN -m (MD) top	SLDN -m (MD) base	Base SLDNR -m (MD)	Core Depth (-m) From	Core Depth (-m) Until	Length (m)	Good Aquifer Indication -m (MD) From	Good Aquifer Indication -m (MD) Until	Length (m)
BLG-02	NAM	653	1510	1100	914.0	918.0	4.0			0.0
					1056.5	1060.8	4.3			0.0
					1120.8	1123.5	2.7	1121.8	1122.0	**0.2**
					1271.0	1271.2	0.2	1271.0	1271.2	**0.2**
					1273.0	1273.4	0.4	1273.0	1273.3	**0.3**
					1342.0	1345.2	3.2	1343.0	1343.5	**0.5**
					1499.5	1505.0	5.5			0.0
LEK-01	NAM	630	1362	1100	759.5	764.8	5.3			0.0
					770.0	770.7	0.7	770.0	770.7	**0.7**
NKK-01	NAM	968	1942	1450	1229.0	1231.9	2.8	1230.6	1230.9	**0.3**
					1505.0	1508.5	3.5	1506.0	1508.5	**2.5**
					1611.0	1615.6	4.6			0.0
					1717.5	1722.2	4.7	1720.5	1720.9	**0.3**
ALD-01	NAM	784	1650	1200	1214.5	1214.9	0.3			0.0
					1216.0	1216.5	0.5			0.0
					1297.5	1298.0	0.5			0.0
					1369.0	1370.5	1.5			0.0
					1373.0	1374.3	1.3			
					1469.0	1469.5	0.5			0.0
					1626.8	1627.3	0.5			0.0
							46.9			

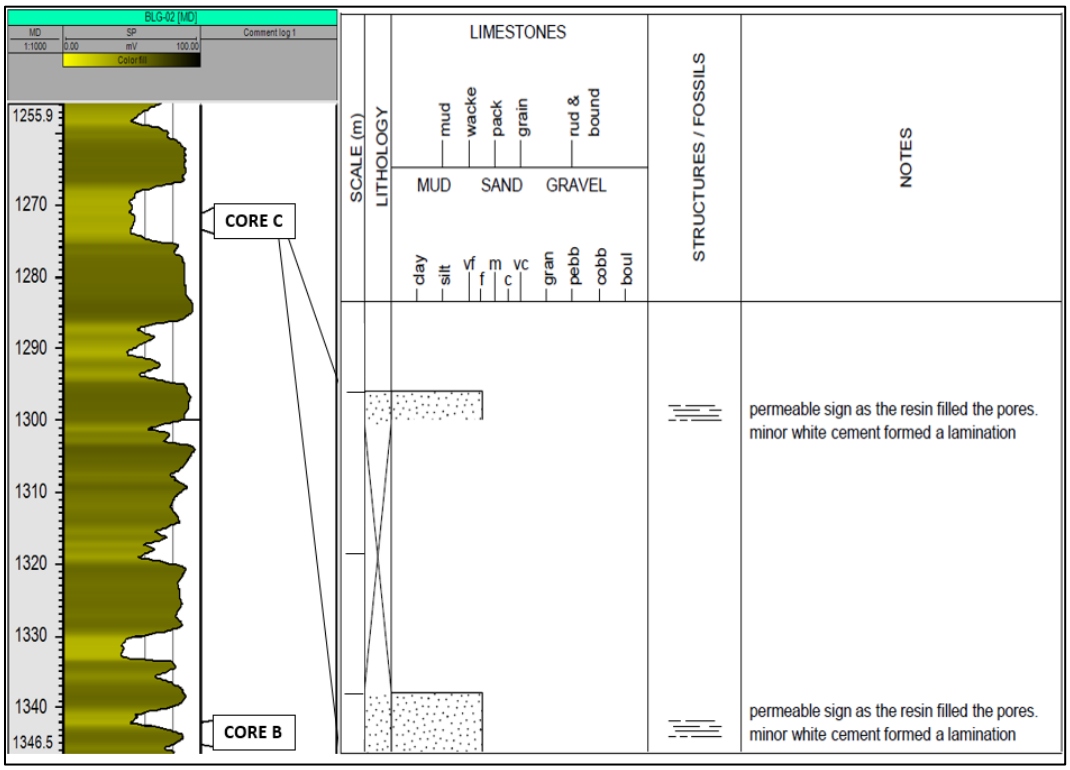

Figure 36 SP log and core description of well BLG-02 at depth -1271 and -1273 m

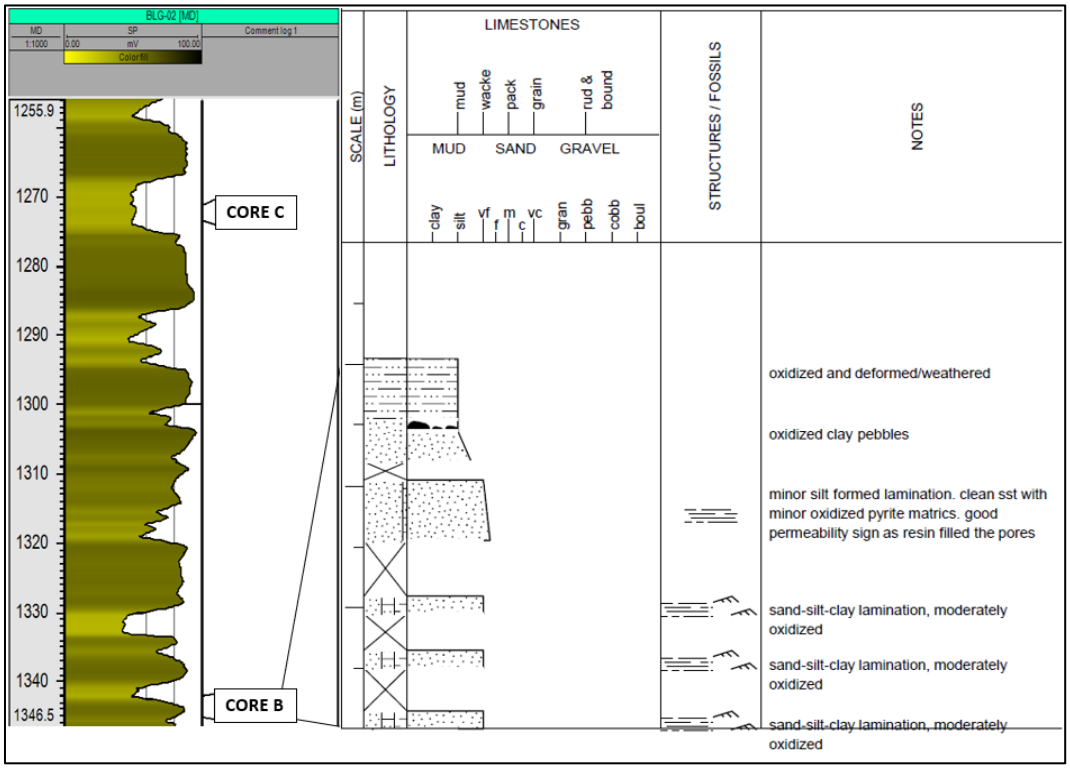

Figure 37 SP log and core description of well BLG-02 at depth -1343 m

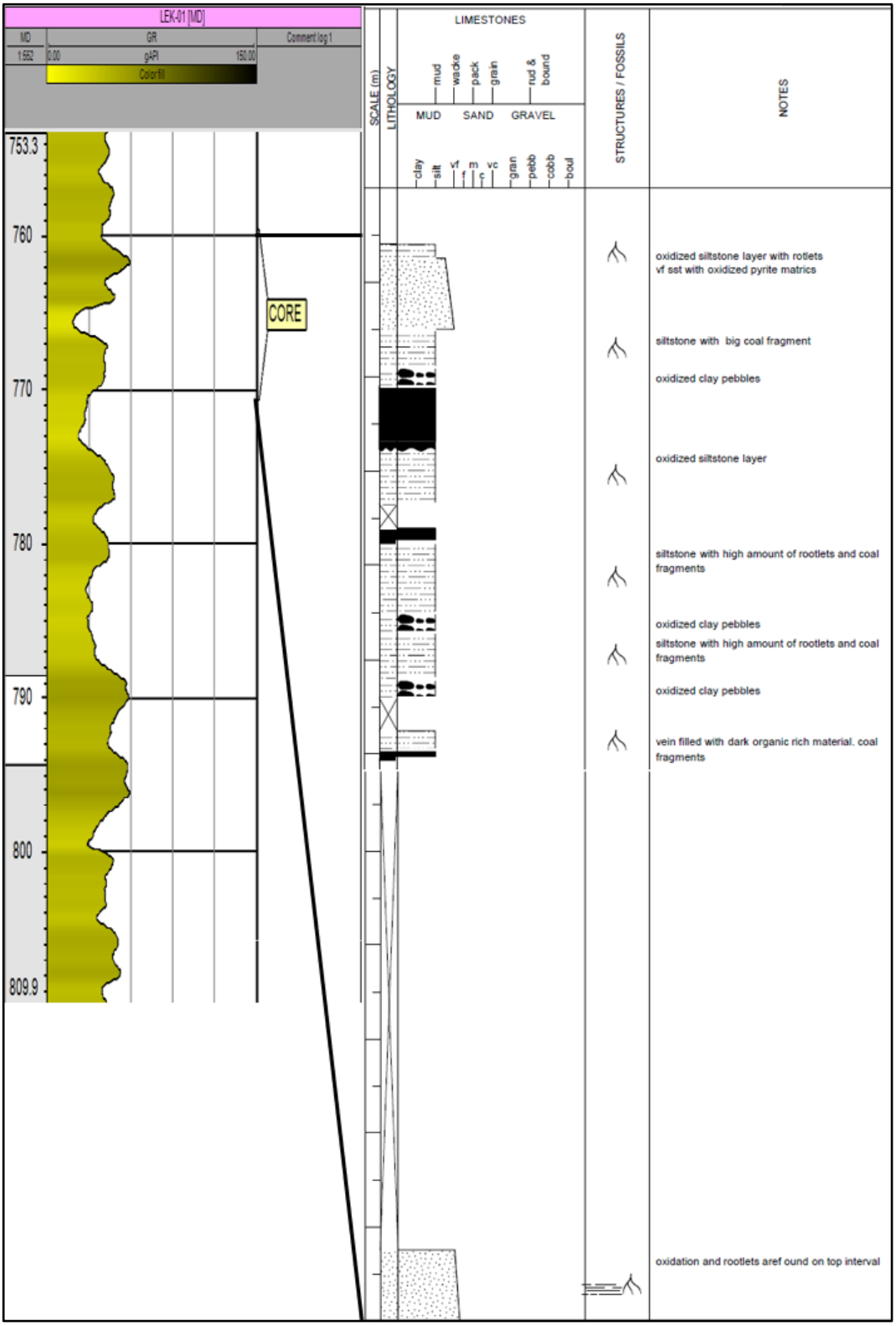

Figure 38 Gamma-ray log and core description of well LEK-01

4.2.3 Well Correlation of Nieuwerkerk Formation

Based on the core description study from the previous chapter, some cores of the SLDNA show good reservoir property indications in the low gamma-ray intervals. The intervals with good reservoir properties are expected from the channels that composed by sand-rich sediments. The connectivity between the channels can be improved by the existence of the crevasse in the floodplain. A further well correlation within the Nieuwerkerk Formation (SLDN) is performed to obtain the distribution of a high net to gross (N/G) interval sediments within the Drechtsteden. High variation in depth and thickness of the SLDN could cause inconsistencies in well correlation within the formation.

The well correlation is performed throughout the study area by utilizing the results of the seismic interpretation, well log analysis, and core descriptions. The results from seismic interpretation are used as the chronostratigraphic control.

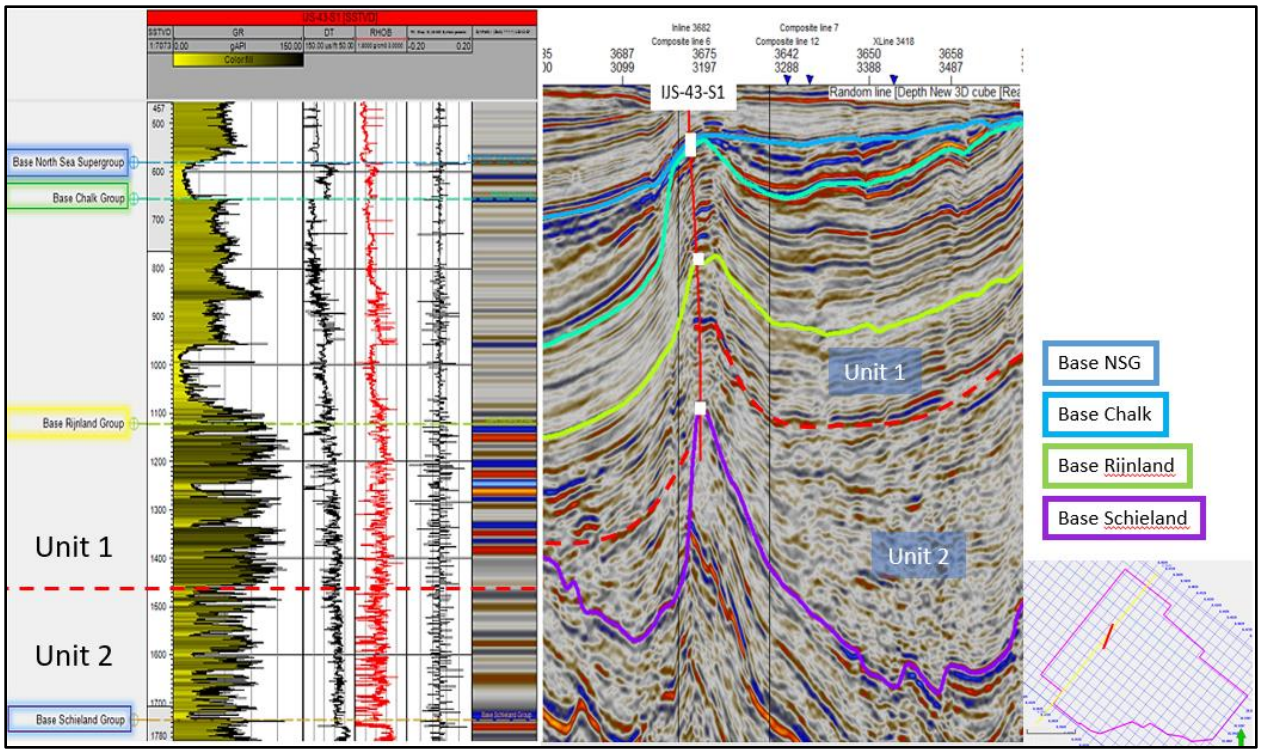

Figure 39 Unit 1 and Unit 2 character in the seismic cross-section at inline 3682

Within the SLDN layer that formed by the interpreted SLD and KN horizons in the previous chapter, two seismic facies can be distinguished with certain consistency as depicted in Figure 39. Unit 1 show laterally continuous reflections with relatively homogeneous thickness. On the other hand, the lower part (unit 2) is expressed with low lateral continuity with high thickness

variation. The seismic cross-section has a sufficient seismic quality to give an estimation boundary between unit 1 and unit 2.

A further well log analysis from gamma-ray, density, neutron and sonic log responses is performed to obtain the exact depth of the boundary between unit 1 and unit 2. From the well log analysis, unit 1 and unit 2 have a significantly different character, especially in the gamma-ray responses. Unit 1 has a higher gamma-ray value compare to the gamma-ray value of unit 2 (Figure 39).

Based on the literature, unit 1 matches description of Rodenrijs Claystone Member (SLDNR) of the SLDN Formation description by Boogaert and Kouwe (1993), Den Hartog Jager (1996), Devault and Jeremiah (2002), Herngreen and Wong (2007), and de Jager (2007). Thus, unit 1 needs to be excluded from the new Alblasserdam Member in the next processes.

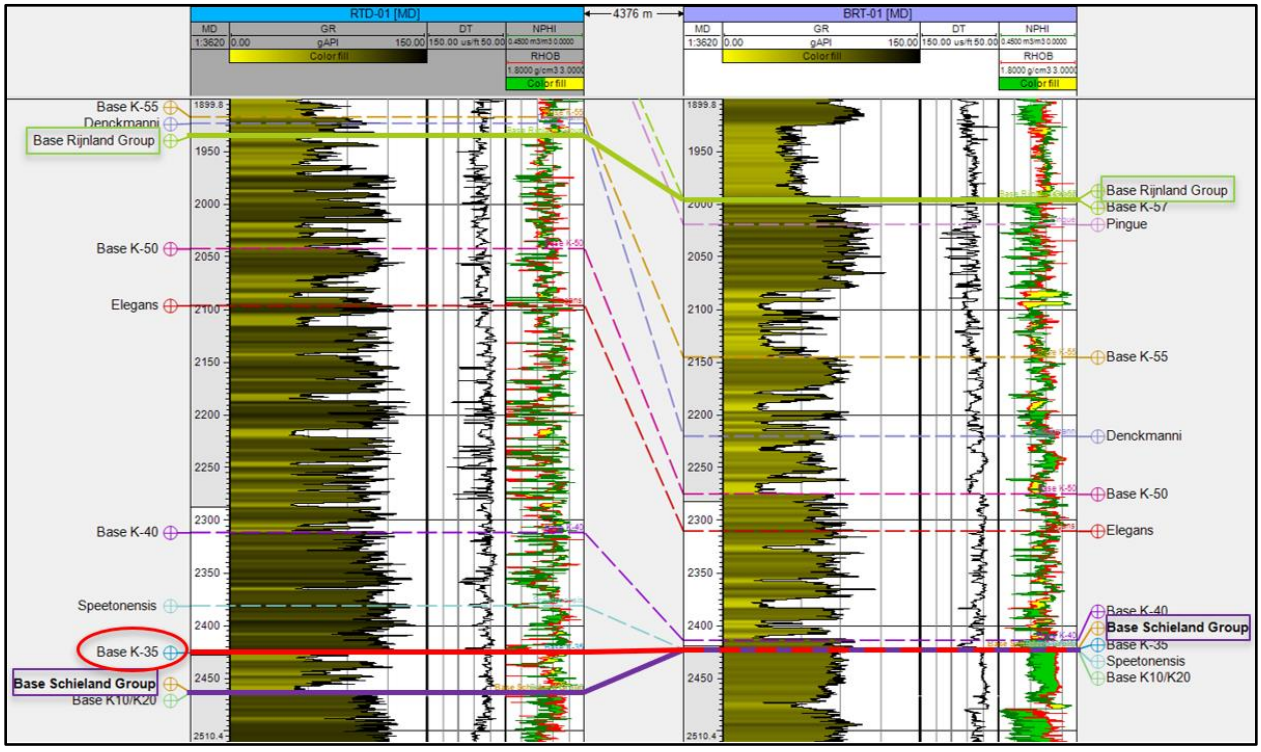

Figure 40 Log response characterization adopted from Devault and Jeremiah (2002)

A well correlation by Devault and Jeremiah (2002), containing wells RTD-01 and BRT-01 used in this study, is utilized as a guide to picking the boundary between unit 1 and unit 2 (Figure 40). The boundary between unit 1 and unit 2 corresponds to the Base K-35 in Devault and Jeremiah (2002). The result from well RTD-01 and BRT-01 is used as a guide to extrapolate the lithology marker in the other wells within the study area by integrating the seismic response as a chronostratigraphic control to reduce the inconsistency and uncertainties.

An update of the lithology interpretation of the available wells in the study area is made and presented in Table 5. In the seismic section, the Base of SLDNR shows as a moderate hard kick. The seismic reflection is fragmented and hardly can be traced to the point of absence on the SE side of the study area. The depth of the Base SLDNR varies from about ~-800 m in the NE side and dipping towards the SW side with depth reaching about ~-2200 m. Figure 41 shows the depth map of the Base SLDNR in the Drechtsteden.

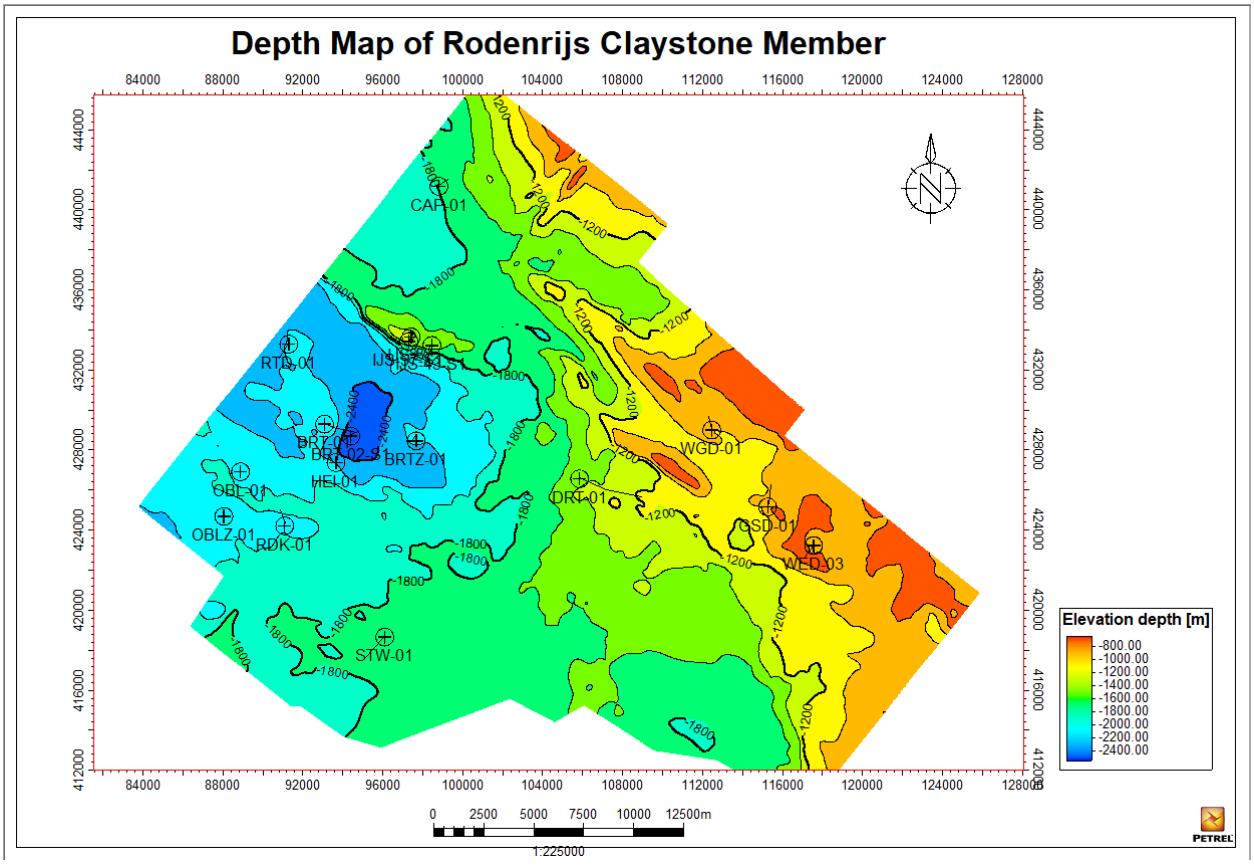

Figure 41 Depth Map of Rodenrijs Claystone Member

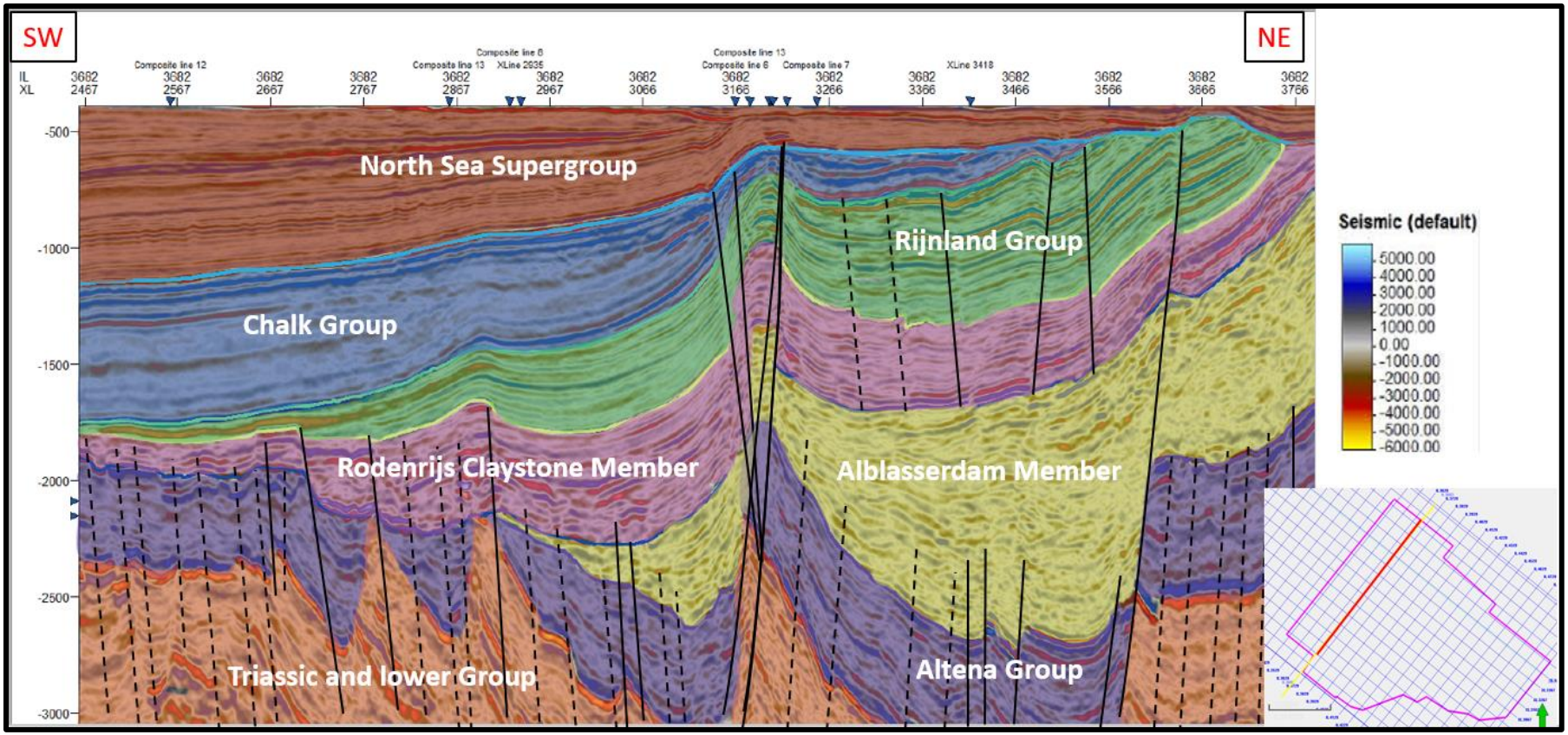

Figure 42 Updated Horizons and Faults Interpretations shown in seismic cross section at inline 3682

The results from seismic interpretation and lithology marker of the boundary between the SLDNR and SLDNA are used to update the thickness map model of the SLDN into the thickness map model of the SLDNR (Figure 43) and SLDNA (Figure 44).

The thickness trend of the SLDNR has the similar trend as the thickness of Rijnland Group (Figure 24). The SLDNR sediments are highly accumulated in the NW with thicknesses reaching about ~750 m and gradually thinning towards the south and SE side of the study area.

On the other hand, the thickness map of the SLDNA sediment has an irregular trend. The sediments are hardly can be found to diminish in the SW side. The maximum thickness is found at the northern SE area reaching about ~1600 m thick. The high thickness variations indicate that tectonic activities have a significant role in the deposition of the SLDNA.

Figure 45 shows the well correlation of the SLDNR and SLDNA across an NE-SW trending composite line. The SLDNR sediments are present in all wells and best developed at well RTD-01. On the other hand, the sediments of the SLDNA are absent on the SW side of the study area which can be observed in well BRT-01, OBL-01, RDK-01, and STW-01. The highest sediment accumulation is found in well IJS-43-S1 reaching a thickness of 250 m.

Two NW-SE well correlations covering the central and the NE side of the study area are created and illustrated in Figure 47 and Figure 46. The SLDNR sediments show a similar trend in the well correlation at the centre and on the NE side, which is gradually thinning in an SE direction. The SLDNA sediments are generally thickening in an SE direction. However, on the well correlation at NE side, the thickness of the SLDNA sediments has a significant difference between well in the NW (CAP-01 and WGD-01) to the wells in the SE (GSD-01 and WED-03).

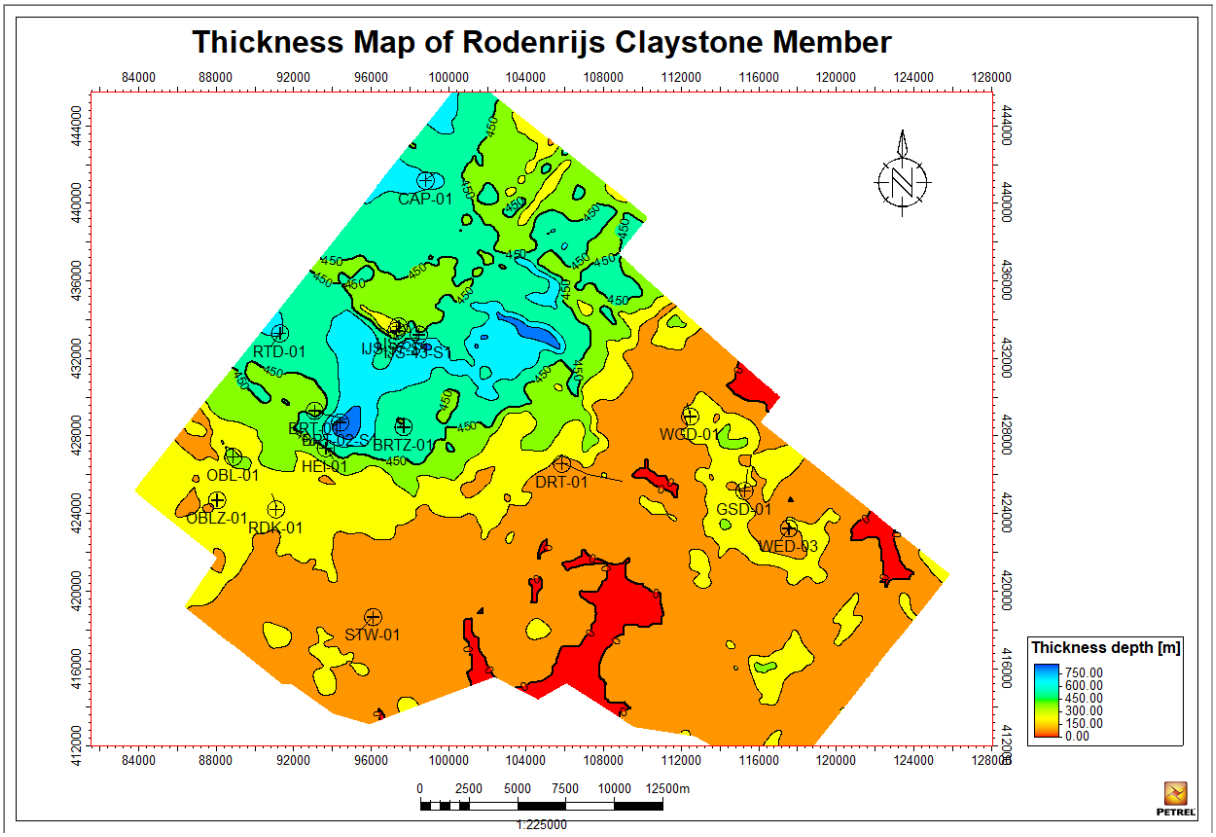

Figure 43 Thickness map of Rodenrijs Claystone Member

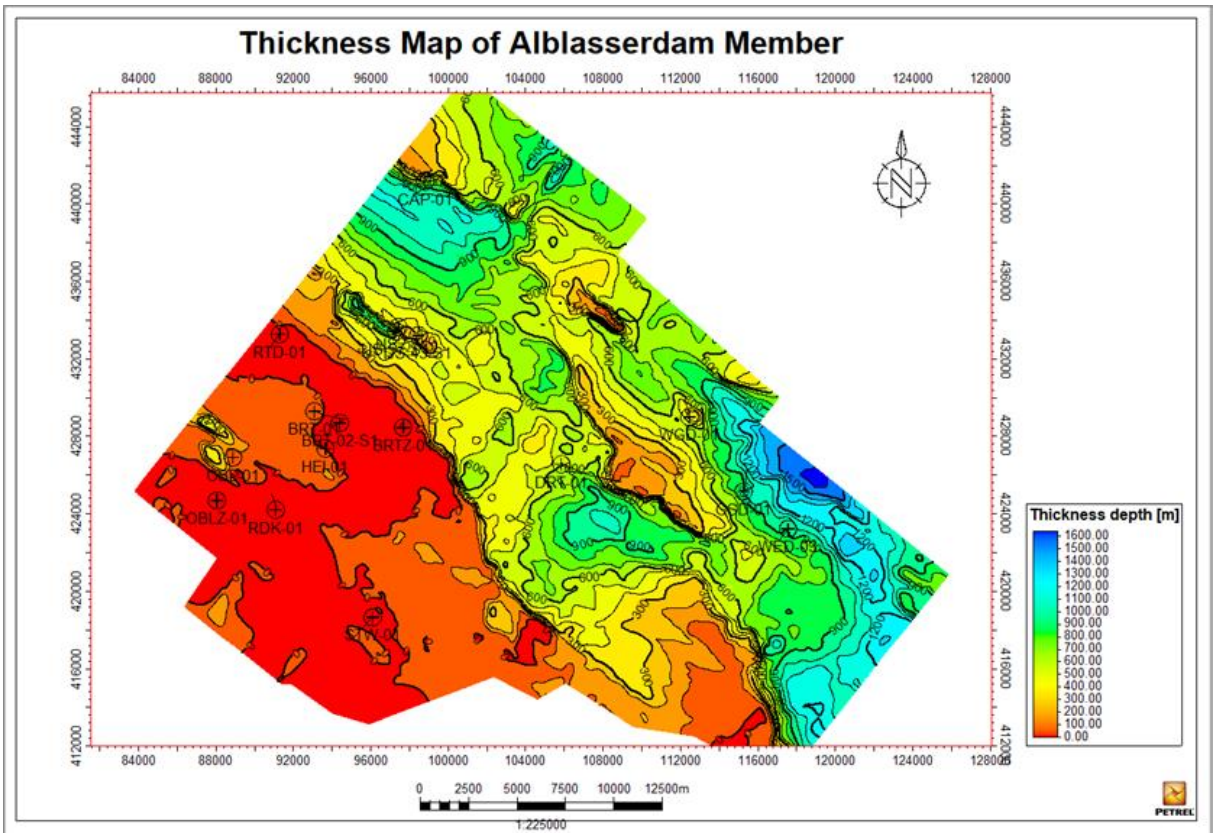

Figure 44 Thickness map of Alblasserdam Member

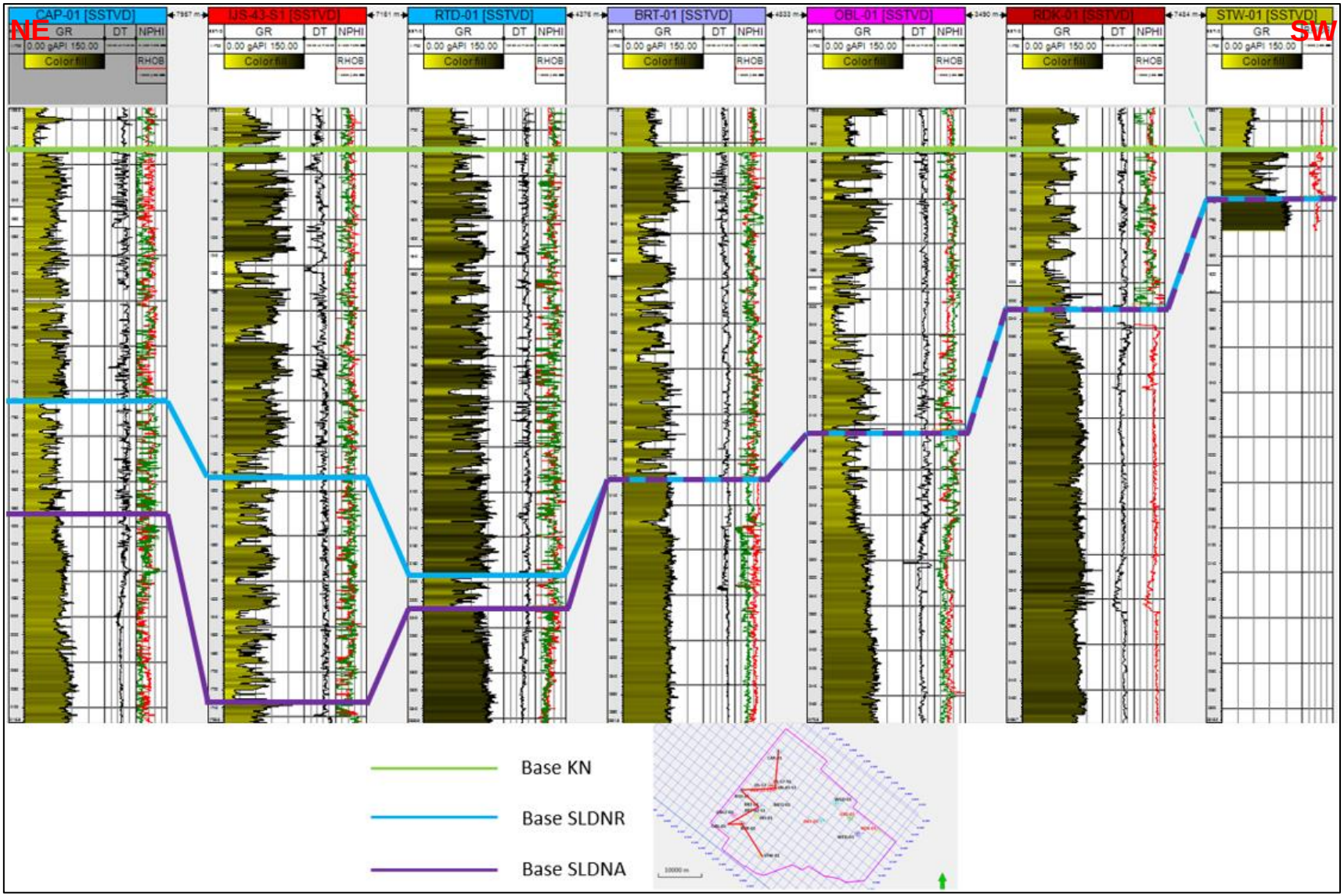

Figure 45 Well Correlation of Nieuwerkerk Formation NE-SW

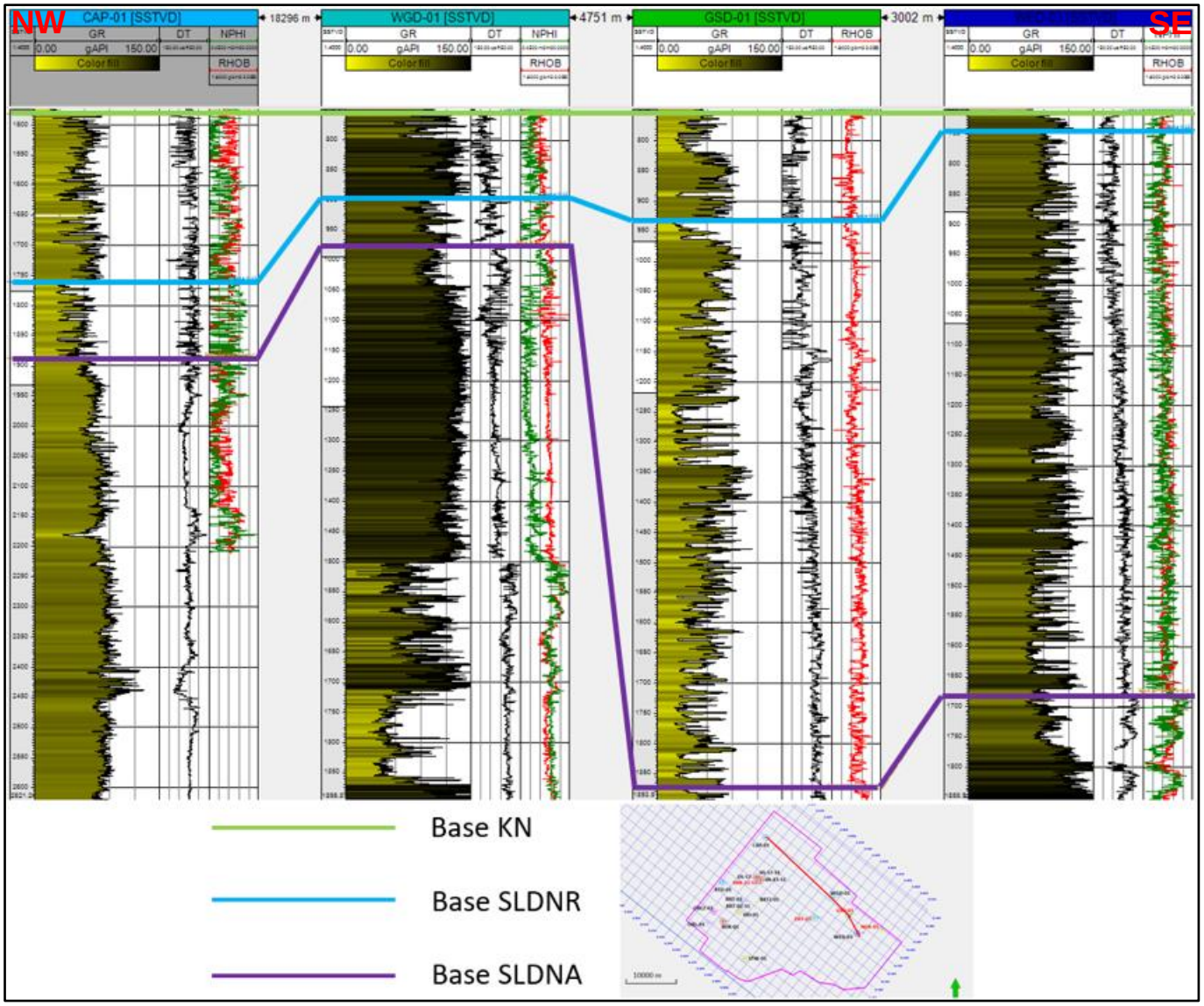

Figure 46 Well Correlation of Nieuwerkerk Formation NW-SE in Zone 3

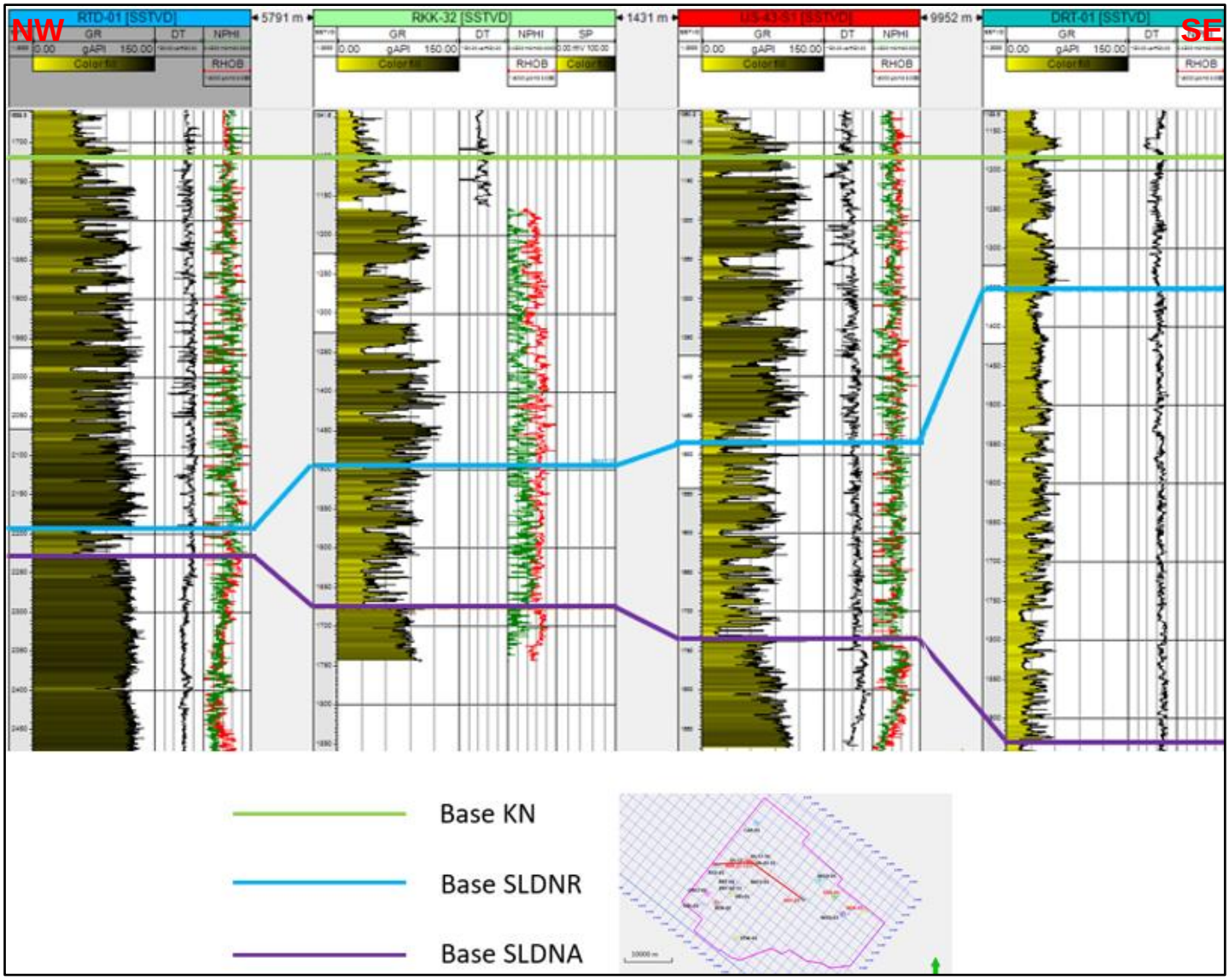

Figure 47 Well Correlation of Nieuwerkerk Formation NW-SE in Zone 2

Table 5 Lithology Marker Interpretation

Wells	Lithology Marker	Top MD	Base MD	Update Lithology Marker	Top MD	Base MD
ALD-01	Alblasserdam Member	784	1650	Rodenrijs Claystone Member	784	1178
				Alblasserdam Member	1178	1650
BLG-02	Alblasserdam Member	653	1510	Rodenrijs Claystone Member	653	756
				Alblasserdam Member	756	1510
BRT-01	Alblasserdam Member	1995	2422	Rodenrijs Claystone Member	1995	2422
				Alblasserdam Member	2422	2422
BRT-02-S1	Alblasserdam Member	1977	2565	Rodenrijs Claystone Member	1977	2565
				Alblasserdam Member	2565	2565
BRTZ-01	Nieuwerkerk Formation	1756	2181	Rodenrijs Claystone Member	1756	2181
				Alblasserdam Member	2181	2181
CAP-01	Alblasserdam Member	1482	1889	Rodenrijs Claystone Member	1482	1761
				Alblasserdam Member	1761	1889
DRT-01	Nieuwerkerk Formation	1402	2411	Rodenrijs Claystone Member	1402	1632
				Alblasserdam Member	1632	2411
GSD-01	Alblasserdam Member	763	1190	Rodenrijs Claystone Member	763	947
				Alblasserdam Member	947	2108
HEI-01	Alblasserdam Member	1945	2316	Rodenrijs Claystone Member	1945	2316
				Alblasserdam Member	2316	2316
IJS-43-S1	Alblasserdam Member	1160	1784	Rodenrijs Claystone Member	1160	1534
				Alblasserdam Member	1534	1784
IJS-57-S1	Alblasserdam Member	1182	1649	Rodenrijs Claystone Member	1182	1408
				Alblasserdam Member	1408	1649
LEK-01	Alblasserdam Member	630	1362	Rodenrijs Claystone Member	630	1100
				Alblasserdam Member	1100	1362
NKK-01	Alblasserdam Member	968	1942	Rodenrijs Claystone Member	968	1414
				Alblasserdam Member	1414	1942
OBL-01	Alblasserdam Member	1868	2187	Rodenrijs Claystone Member	1868	2187
				Alblasserdam Member	2187	2187
OBLZ-01	Alblasserdam Member	1914	2020	Rodenrijs Claystone Member	1914	2020
				Alblasserdam Member	2020	2020
RDK-01	Alblasserdam Member	1895	2075	Rodenrijs Claystone Member	1895	2075
				Alblasserdam Member	2075	2075
RKK-32	Alblasserdam Member	1163	2005	Rodenrijs Claystone Member	1163	1735
				Alblasserdam Member	1735	2005
RTD-01	Alblasserdam Member	1935	2463	Rodenrijs Claystone Member	1935	2425
				Alblasserdam Member	2425	2463
STW-01	Alblasserdam Member	2009	2078	Rodenrijs Claystone Member	2009	2078
				Alblasserdam Member	2078	2078
WED-03	Alblasserdam Member	722	1725	Rodenrijs Claystone Member	722	749
				Alblasserdam Member	749	1725
WGD-01	Nieuwerkerk Formation	811	1063	Rodenrijs Claystone Member	811	973
				Alblasserdam Member	973	1063

4.2.4 Well Correlation of Alblasserdam Member

From the updated lithology interpretation, the SLDNA is absent in SW side of the study area as can be observed in the well STW-01, BRT-01, BRT-02-S1, BRTZ-01, RDK-01, OBLZ-01, and HEI-01. On the other hand, the SLDA sediments are highly accumulated in the central and NE side of the study area with the NW-SE trend and bounded by the major faults.

The distribution of potential aquifer interval within the SLDNA is done by recognizing the characteristics log shapes of the mainly shale-rich interval and sandstone-rich interval that supported by core description to determine depositional environment and lithofacies within the SLDNA. The method is applied to all available wells, and a well correlation is made to predict the trend distribution of high N/G intervals in the Drechtsteden. Figure 48 shows the result of recognition of high N/G intervals in well IJS-43-S1 that has potential as a good aquifer.

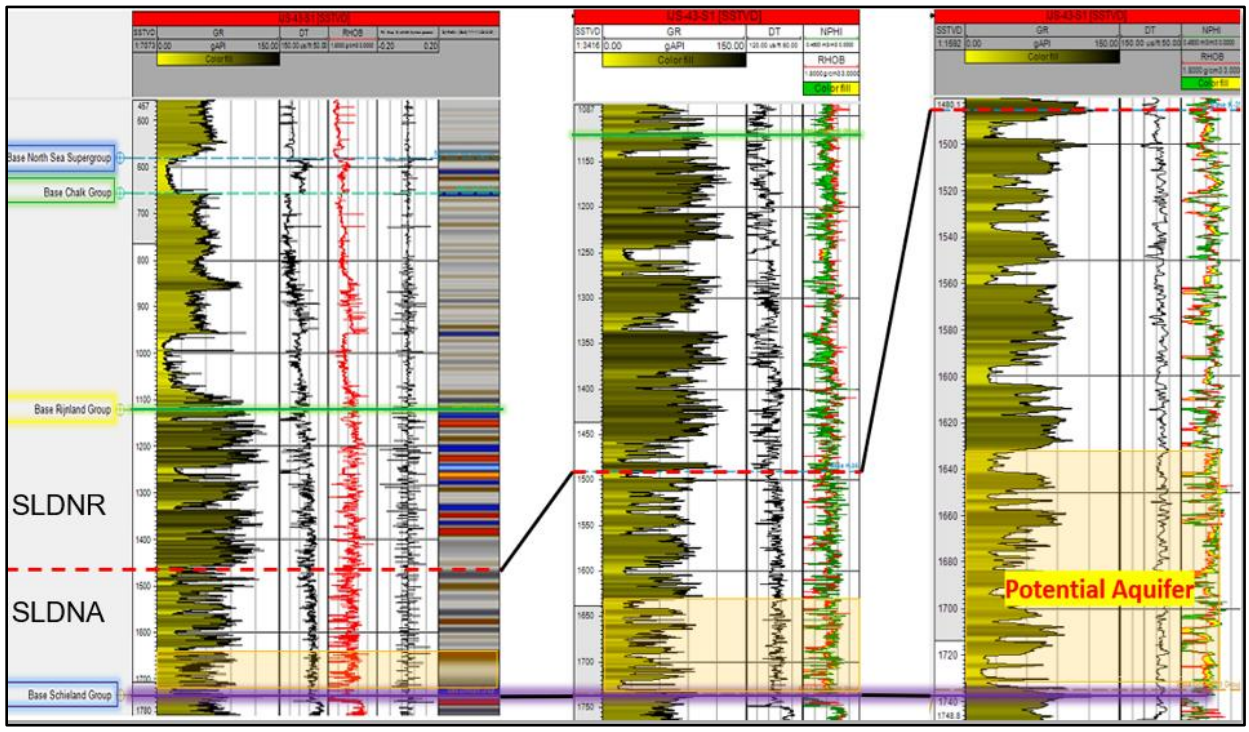

Figure 48 Potential Aquifer of the Alblasserdam Member in well IJS-43-S1

A high accumulation of high N/G interval at the base of the SLDNA are observed from five wells: RKK-32, IJS-43-S1, DRT-01, GSD-01 and WED-03. The high N/G interval is formed by stacked channels of the fluvial system with thickness varies from 64 m to 241 m and resumed in Table 6.

Table 6 Potential aquifer depth and thickness

Well	Lithology	Top (-m) MD	Base (-m) MD	Thickness MD	Top (-m) TVD	Base (-m) TVD	Thickness TVD
RKK-32	Rodenrijs Claystone Member	1163	1735	572	1103	1492	389
	Alblasserdam Member	1735	2005	270	1492	1678	186
	Aquifer 2	***1913***	***2005***	***92***	***1614***	***1678***	***64***
IJS-43-S1	Rodenrijs Claystone Member	1160	1534	374	1121	1485	364
	Alblasserdam Member	1534	1784	250	1485	1735	250
	Aquifer 2	***1680***	***1784***	***104***	***1631***	***1735***	***104***
DRT-01	Rodenrijs Claystone Member	1402	1632	230	1184	1353	169
	Alblasserdam Member	1632	2411	779	1353	1920	567
	Aquifer 2	***2197***	***2411***	***214***	***1762***	***1920***	***158***
GSD-01	Rodenrijs Claystone Member	763	947	184	754	929	175
	Alblasserdam Member	947	2108	1161	929	1876	947
	Aquifer 2	***1300***	***1435***	***135***	***1234***	***1338***	***104***
	Aquifer 1	***1857***	***2088***	***231***	***1660***	***1857***	***197***
WED-03	Rodenrijs Claystone Member	722	749	27	717	743	26
	Alblasserdam Member	749	1725	976	743	1680	937
	Aquifer 2	***1162***	***1246***	***84***	***1139***	***1220***	***81***
	Aquifer 1	***1373***	***1725***	***352***	***1439***	***1680***	***241***

Two potential aquifer intervals are observed in well GSD-01, and WED-03 as the wells penetrate the full SLDNA. Well RKK-32, IJS-43-S1, and DRT-01 were drilled on a structural high. Thus, only one potential aquifer interval is observed as the wells only penetrate the upper sediments of the SLDNA, as shown by seismic cross-section intersecting well GSD-01, WED-03, RKK-32, IJS-43-S1, and DRT-01 (Appendix B).

Furthermore, the well correlation is done by identifying stratigraphic base-level cycles of changing accommodation to sediment supply ratio (A/S cycles) from the trend of gamma-ray log responses. The falling or rising base level causing the falling and rising of A/S cycles (Devault & Jeremiah, 2002). A triangle pointing upward represents a high A/S that corresponding with increasing gamma-ray and a triangle pointing downward is represent a low A/S that corresponding with decreasing gamma-ray.

Analysis and recognition of a complete A/S cycles of the SLDNA are done in well GSD-01 (Figure 49). In general, the lower SLDNA is consists of single long period of A/S cycles and the upper SLDNA consist of several shorter A/S cycles. The gamma-ray response shows an overall fining upward interval is observed at the base of the SLDNA in well GSD-01 at depth -1857 up to -1338 m (A1 – A2 Figure 49). The similar trend of significant fining-upward that shown as a gradually

increasing upward gamma-ray response also indicated in well WED-03 (-1680 up to -1220 m depth). Followed by another fining upward interval (A3) which can be found in well WED-03 and the base of SLDNA in well RKK-32, IJS-43-S1, and DRT-01. Figure 50 shows the well correlation of the SLDN in the Drechtsteden with the distribution of potential aquifer. A further discussion about stratigraphy (A1, A2, and A3) and the structural trend of the SLDNA will be discussed in Chapter 5.

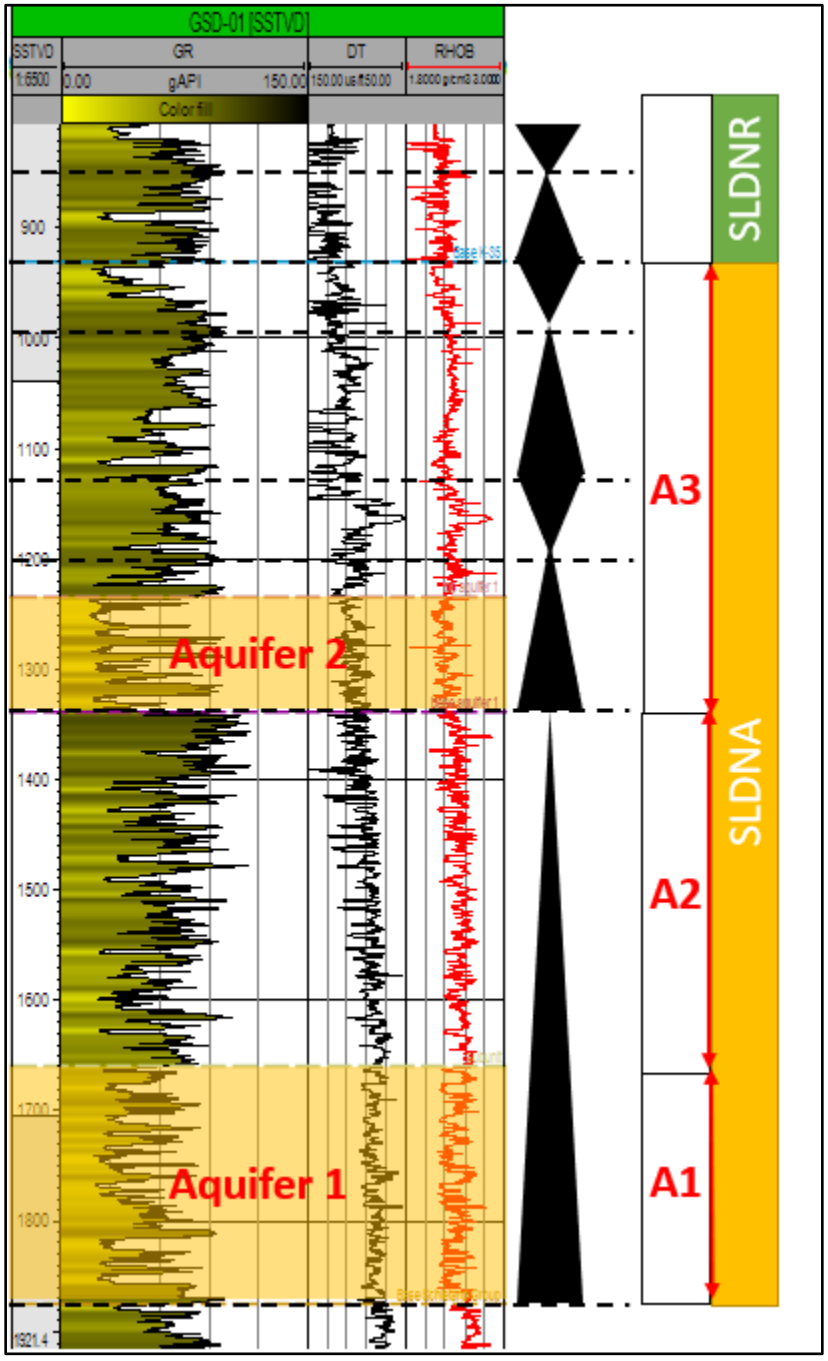

Figure 49 Recognition of cycles and subdivision in Alblasserdam Member

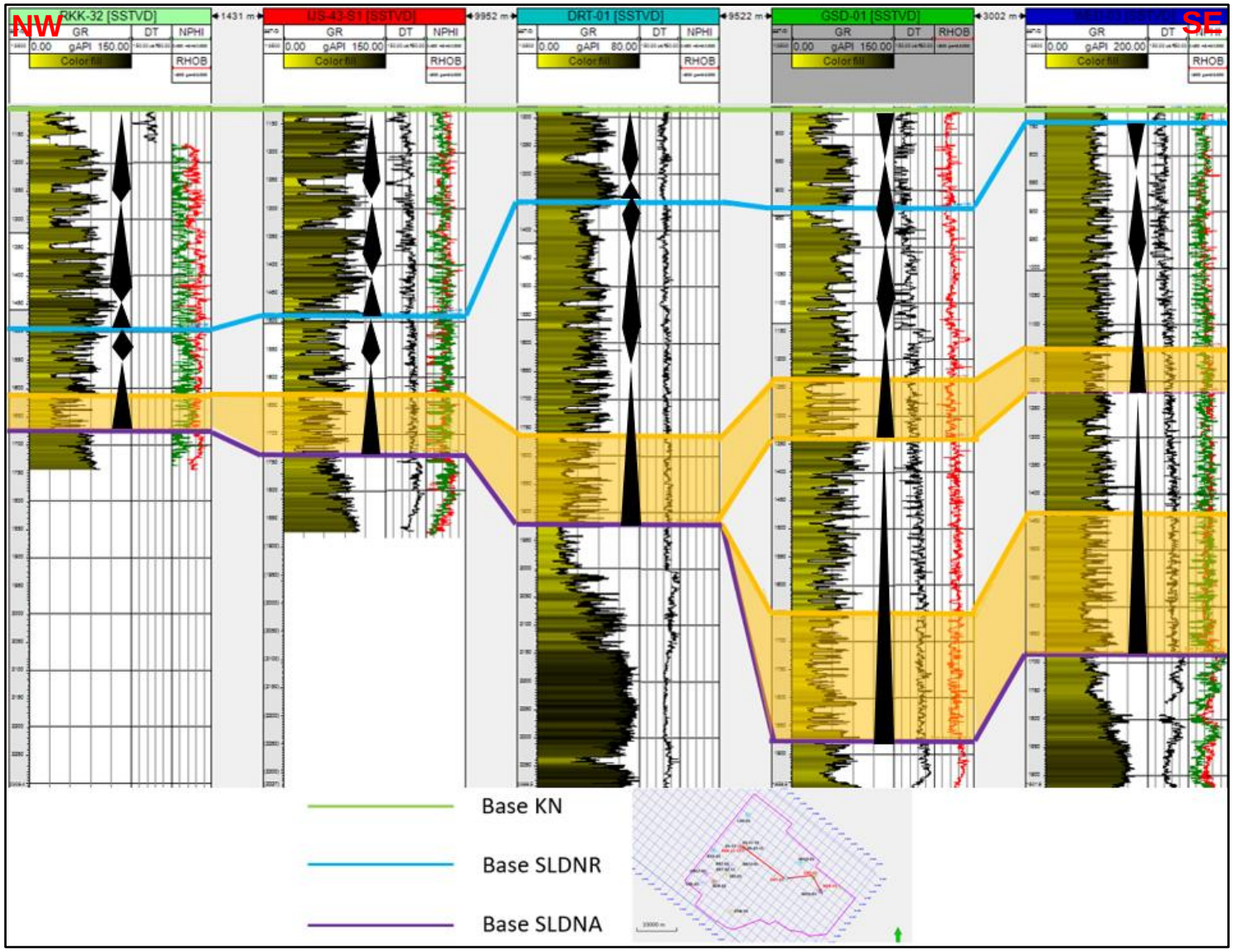

Figure 50 Potential aquifer distribution of the Alblasserdam Member

4.3 Petrophysical Evaluation

A petrophysical evaluation is done to map the reservoir properties of the potential aquifer in the study area. The petrophysical evaluation encompasses a volume of shale (vshale), net to gross (N/G), porosity and permeability profile of the SLDNA. The petrophysical evaluation is done in Petrel 2014 and Microsoft Excel software.

The petrophysical evaluation is performed in well RTD-01, CAP-01, IJS-43-S1, RKK-32, GSD-01, WED-03, and WGD-01. The wells are selected by considering:

- The availability of log data
- Location of the wells
- Penetrating the potential aquifer

4.3.1 Volume of Shale and Clean Sand

The vshale of a layer can be derived from the relationship of gamma-ray value at a certain depth with the maximum, and minimum gamma-ray value is determined from the shale and sand base line of the SLDNA interval in each well. Mathematically, the volume of shale and gamma-ray relationship can be expressed as follow:

$$V_{shale} = \frac{GR_d - GR_{min}}{GR_{max} - GR_{min}}$$

The value of the volume of shale is used to determine the ratio of clean sand contained in the SLDNA. The P10, P50, and P90 are calculated by setting the volume of shale cutoff equal to 0.5, 0.4 and 0.3 respectively.

4.3.2 Porosity Calculation

The porosity profile is calculated from the density log and neutron log. The matrix density of sand and shale dominated layers is equal to 2.65 and 2.7 g/cm^3 respectively (Tiab & Donaldson, 2004).

$$\Phi_{ND} = \sqrt{\frac{\Phi^2_{density} + \Phi^2_{Neutron}}{2}}$$

$$\Phi_{density} = \frac{\rho_{ma} - \rho_{log}}{\rho_{ma} - \rho_{mf}}$$

Moreover, the fluid density equal to:

- 1 g/cc water-bearing zone
- 0.8 g/cc oil-bearing zone
- 0.25 g/cc gas-bearing zone

The determination of water, oil, and gas bearing intervals is done by analysing the resistivity logs, density-neutron logs and the well report contained in the well dataset. The maximum measured porosity is equal to 30%. Thus, the result of the calculated porosity is filtered by allowing the maximum calculated porosity equal to the maximum measured porosity.

4.3.3 Permeability Determination

The permeability value is derived from porosity and permeability relations that derived from core measurements data from 33 wells in the WNB. Only 11 of the wells are located within the Drechtsteden. The core data from the other wells are assumed to be representative for both the SLDNA and SLDNR due to inconsistencies in the boundary interpretation in the public database (www.nlog.nl).

A Swanson regression technique is applied to find a correlation between the porosity and the permeability of the SLDNA. The Swanson regression gives a better result in a large dataset (>200 plugs) (Betts, 2017). In this study, the data is clustered based on the porosity value. The X10 (10^{th} percentiles), X50 (50^{th} percentiles), and X90 (90^{th} percentiles) of the permeability value in every cluster are calculated using Microsoft Excel. The result from the Swanson regression technique is determined as the medium case. The low and high case is calculated using the following operations.

$$K_{Swanson} = 0.3\,X10 + 0.4\,X50 + 0.3\,X90$$

$$K_{High\ case} = 0.1\,X10 + 0.4\,X50 + 0.5\,X90$$

$$K_{Low\ case} = 0.5\,X10 + 0.4\,X50 + 0.1\,X90$$

The porosity-permeability relations of the SDLNA and SLDNR can be written as:

Rodenrijs Claystone Member

$$K_{SLDNR\_Low}(\log mD) = -0.0083\,\Phi_{ND}{}^2 + 0.427\,\Phi_{ND} - 2.0541 \qquad R^2 = 0.9796$$

$$K_{SLDNR\_Medium}(\log mD) = -0.0072\,\Phi_{ND}{}^2 + 0.4047\,\Phi_{ND} - 2.3183 \qquad R^2 = 0.9799$$

$$K_{SLDNR\_High}(\log mD) = -0.0061\,\Phi_{ND}{}^2 + 0.3763\,\Phi_{ND} - 2.5998 \qquad R^2 = 0.977$$

Alblasserdam Member

$$K_{SLDNA\_Low}(\log mD) = -0.0008\,\Phi_{ND}{}^2 + 0.1466\,\Phi_{ND} - 0.2479 \qquad R^2 = 0.9665$$

$$K_{SLDNA\_Medium}(\log mD) = -0.0013\,\Phi_{ND}{}^2 + 0.1702\,\Phi_{ND} - 0.7199 \qquad R^2 = 0.9799$$

$$K_{SLDNA\_High}(\log mD) = -0.0015\,\Phi_{ND}{}^2 + 0.1808\,\Phi_{ND} - 1.2498 \qquad R^2 = 0.9782$$

Two sets of regression relations are produced. The first relation is derived from the core data of the SLDNR and the second relation is from the SLDNA (Figure 51).

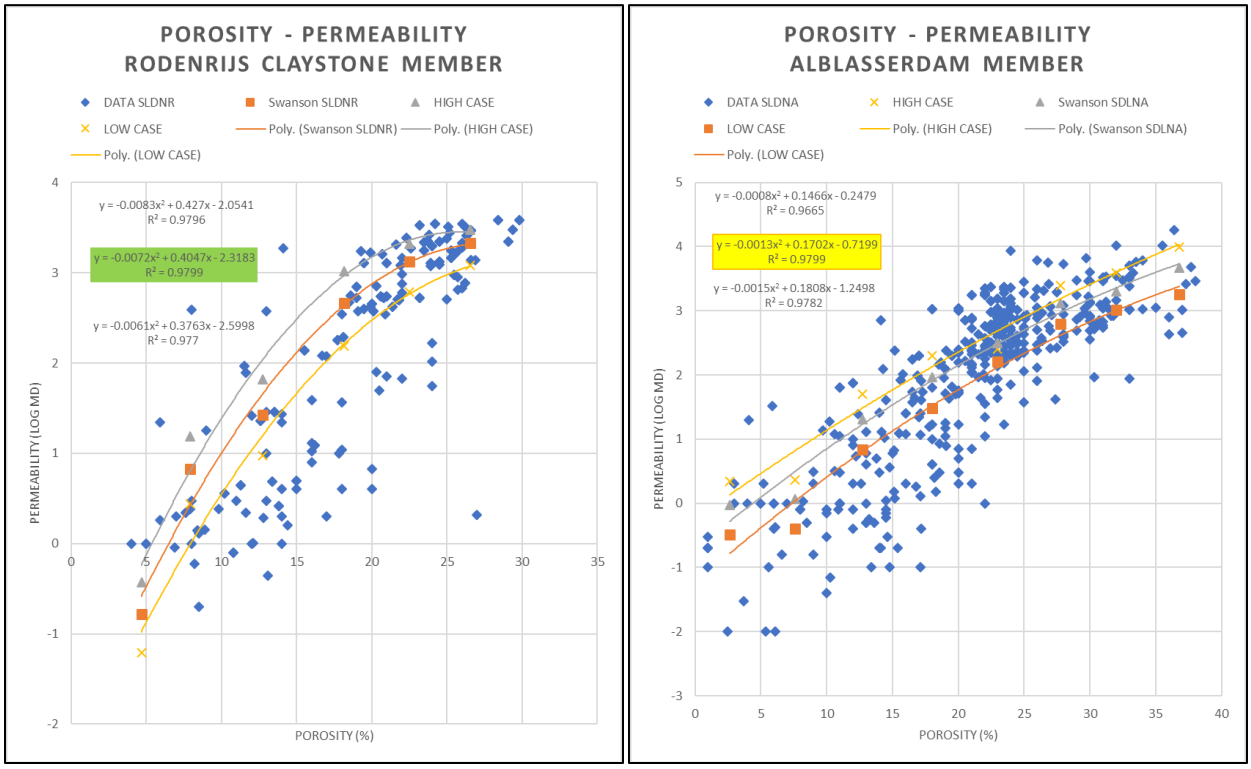

Figure 51 Porosity and Permeability plot of Rodenrijs Claystone Member

4.3.4 Results of Petrophysical Evaluation

The result of the N/G ratio, porosity, and permeability evaluation are presented in one well-section. Figure 52 shows the result of the petrophysical evaluation as well GSD-01. An interbedded of sand and shale intervals are observed within the SLDNA. The permeability profile shows high values in the sand-rich intervals and low in the shale-rich intervals. The highly stacked sand-rich and high permeability intervals are shown in the aquifer 2 and aquifer 1. The result of the petrophysical evaluation in the other well can be found in Appendix C.

The resume of the average petrophysical properties of the SLDNR and SLDNA from the seven wells are shown in Table 7. In this study, the volume of shale cut-off 0.4 is used as the base case to divide the sand-rich and shale-rich intervals. A layer with the volume of shale higher than 0.4 is interpreted as shale, and lower than 0.4 is interpreted as sand. Furthermore, the net aquifer is defined as sand-rich intervals with permeability higher than 1mD.

The SLDNR has a low N/G ratio that varies between 0.06 to 0.28. The overall SLDNA has higher N/G ratio compared to the SLDNR, especially within the Aquifer 1 and Aquifer 2 intervals that give significant higher N/G ratio varying from 0.44 up to 0.75.

The average porosity and permeability values of SLDNR and SLDNR are varied from one well to the other. The wells are distributed all over the Drechtsteden area and penetrate the SLDN which experienced different tectonic activities before, during, and after the deposition. The tectonic activities might affect the properties of the SLDN, especially in the highly inverted area. Further analysis of properties changes will be discussed in the next chapter.

Table 7 Petrophysical Evaluation of the Nieuwerkerk Formation

Lithology	Well	Depth				Thickness				N/G			Avg Porosity	Average Permeability (mD)		
		MD		TVD		Gross	NET SAND (vshale cut off)									
		Top	Base	Top	Base		0.3	0.4	0.5	Low	Med	High	(%)	Low	Med	High
Rodenrijs Claystone Member	RTD-01	1935	2425	1721	2192	471	74.2	89.5	104.5	0.16	0.19	0.22	10	2	4	10
Rodenrijs Claystone Member	CAP-01	1482	1761	1482	1760	278	15.6	24.6	35.7	0.06	0.09	0.13	8	0	1	1
Rodenrijs Claystone Member	RKK-32	1163	1735	1103	1492	389	62.6	73.8	87.3	0.16	0.19	0.22	11	3	7	18
Rodenrijs Claystone Member	IJS-43-S1	1160	1539	1121	1485	364	36.9	43.5	50.2	0.10	0.12	0.14	12	3	8	20
Rodenrijs Claystone Member	GSD-01	763	947	754	929	175	36.1	48.4	66.4	0.21	0.28	0.38	11	4	10	27
Rodenrijs Claystone Member	WED-03	722	749	717	743	26	0	1.6	4.9	0.00	0.06	0.19	9	0	1	2
Rodenrijs Claystone Member	WGD-01	811	973	756	895	139	12.7	18.2	22.7	0.09	0.13	0.16	11	2	5	13
Alblasserdam Member	RTD-01	2425	2463	2192	2229	37	12.5	16.5	20.5	0.34	0.45	0.55	15	25	63	103
Alblasserdam Member	CAP-01	1761	1889	1760	1886	126	21.7	31.5	40	0.17	0.25	0.32	13	10	25	48
Alblasserdam Member	RKK-32	1735	2005	1492	1678	186	62.6	76.9	94.8	0.34	0.41	0.51	16	46	113	182
Alblasserdam Member	IJS-43-S1	1539	1784	1485	1735	250	55.3	68.3	80.2	0.22	0.27	0.32	16	20	54	117
Alblasserdam Member	GSD-01	947	2108	929	1876	947	214.3	269.3	343.6	0.23	0.28	0.36	14	20	49	78
Alblasserdam Member	WED-03	749	1725	743	1680	937	139.9	246.3	350.6	0.15	0.26	0.37	15	17	41	66
Alblasserdam Member	WGD-01	973	1063	895	976	81	4.9	13.7	27.1	0.06	0.17	0.33	14	13	33	52
Aquifer 2	RTD-01															
Aquifer 2	CAP-01															
Aquifer 2	RKK-32	1913	2005	1614	1678	64	40.4	48.1	53.5	0.63	0.75	0.84	18	90	223	353
Aquifer 2	IJS-43-S1	1680	1784	1631	1735	104	49	62	76.4	0.47	0.60	0.73	15	96	287	944
Aquifer 2	GSD-01	1300	1435	1234	1338	104	56	62.9	69.6	0.54	0.60	0.67	17	89	226	414
Aquifer 2	WED-03	1162	1246	1139	1220	81	26.5	35.9	45.6	0.33	0.44	0.56	17	80	196	311
Aquifer 2	WGD-01															
Aquifer 1	RTD-01															
Aquifer 1	CAP-01															
Aquifer 1	RKK-32															
Aquifer 1	IJS-43-S1															
Aquifer 1	GSD-01	1857	2088	1660	1857	197	80.2	99.3	123.3	0.41	0.50	0.63	15	55	136	214
Aquifer 1	WED-03	1473	1725	1439	1680	241	117.2	135.9	152.9	0.49	0.56	0.63	16	47	118	196
Aquifer 1	WGD-01															

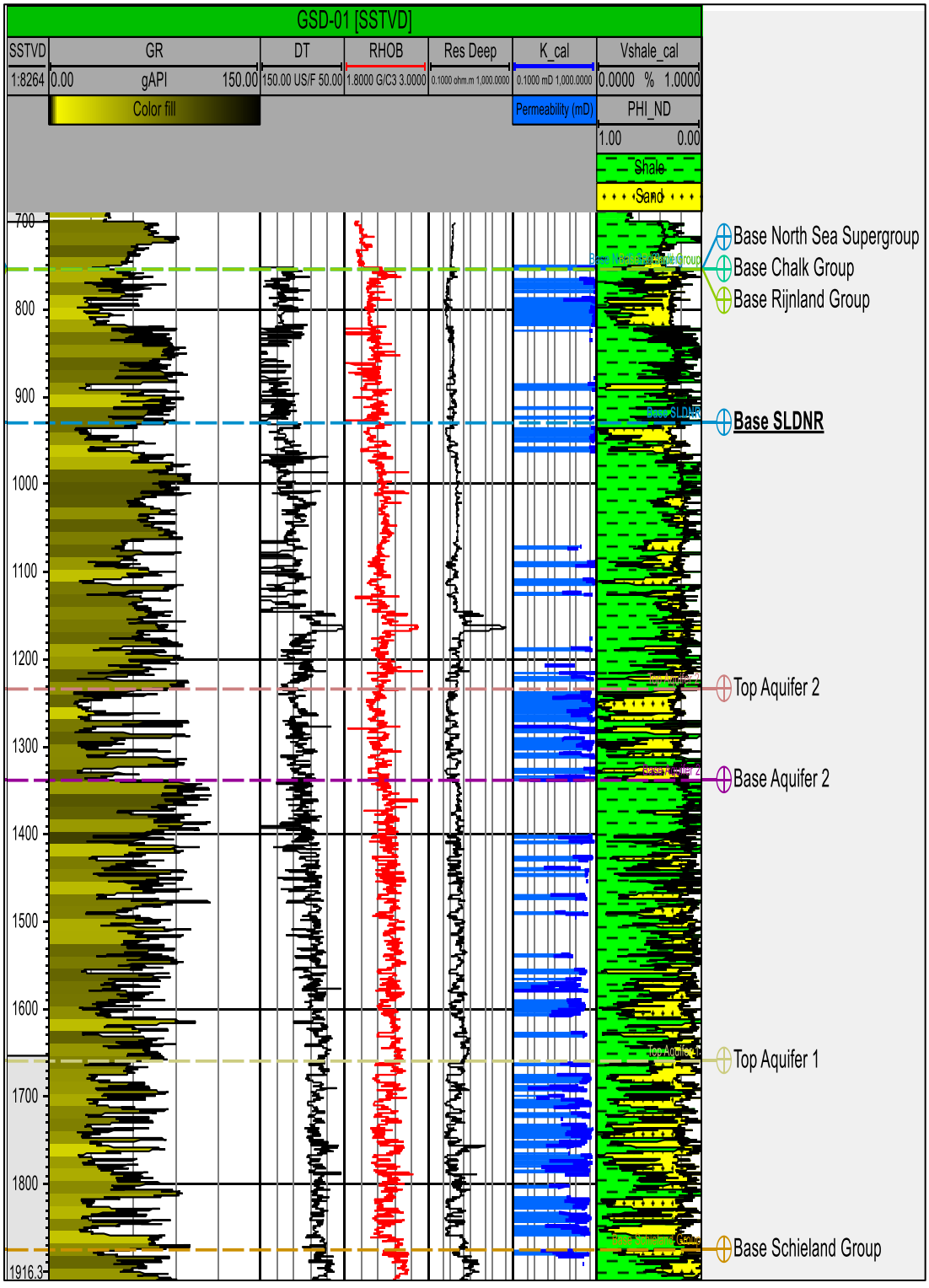

Figure 52 Result of petrophysical evaluation in well GSD-01

5. Discussion

In this chapter, the structural, stratigraphy and reservoir properties of the Alblasserdam Member will be modelled. The model is used to determine the best location to place the injection and production geothermal wells.

5.1 Distribution of Alblasserdam Member in Drechtsteden

The results and a brief discussion in previous chapters indicate that there are potential aquifers found within the SLDNA. However, it is also observed that the SLDNA has high structural and stratigraphy heterogeneities in lateral and vertical direction.

A lateral zonation and vertical subdivision of the SLDNA is performed by utilizing the well correlation, depth, thickness, and faults map from the previous chapters. A lateral zonation is used to map the structural trend within the SLDNA. Followed by a vertical subdivision to observed and divide the stratigraphy of the SLDNA during the deposition and the influence of tectonics activities on the depositional trend of the SLDNA. In the end, the high N/G interval of the SLDNA as a potential geothermal aquifer in the Drechtsteden can be predicted.

5.1.1 Structural Architecture of Alblasserdam Member

The subsurface architecture of the SLDN within the study area shows a complex geometry. The result of tectonic activities is recorded as high variations in depth, thickness and continuity of the SLDN and illustrated in Figure 21 and Figure 22. As discussed in the Faults Interpretation chapter, based on the time occurrence the faults are grouped into the old, new, and reactivated faults. And based on the magnitude of fault displacement, the faults are divided into the major and minor faults. In general, there are two sets of major faults, South and North major faults. The faults are striking toward NW-SW and divide the study area into three zones as illustrated in Figure 53, Figure 54, and Figure 55.

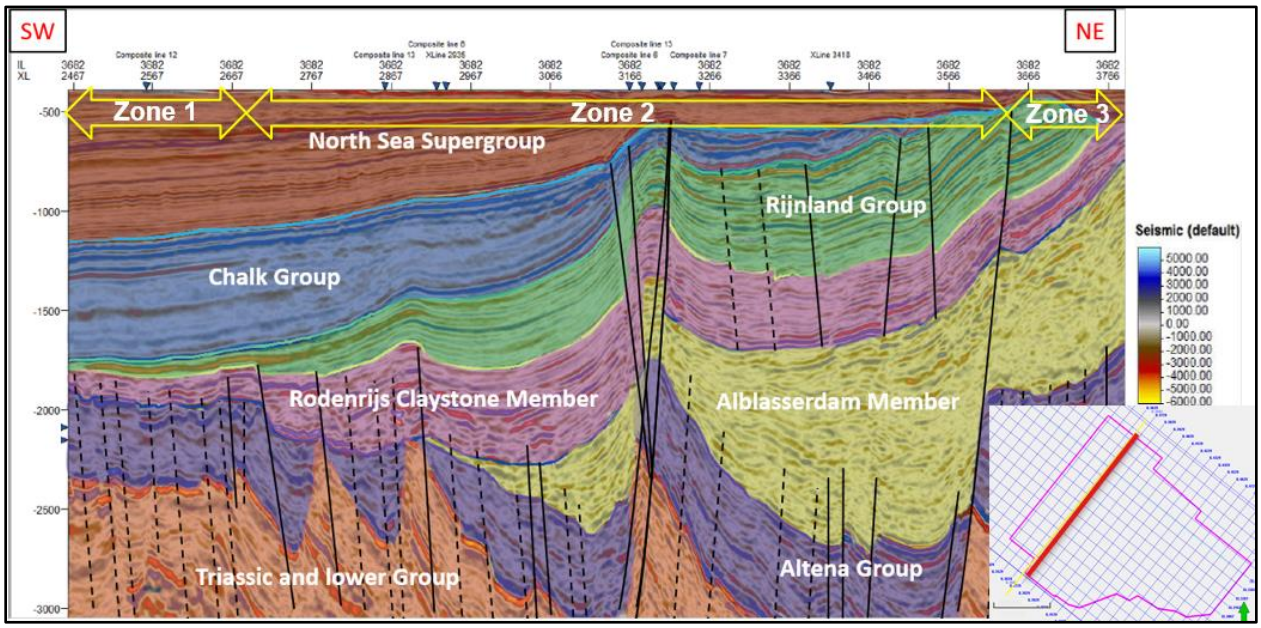

Figure 53 Zonation of Drechtsteden in the seismic cross section at inline 3682

Drechtsteden Zone 1

Drechtsteden Zone 1 (Zone 1) is the area between the South major faults to the southernmost part of the study area. The sediments of the SLDN are less likely to be found in this area. This area experienced a high degree in uplift and erosion before the sediments of the SLDN were deposited. This observation is confirmed by the lithology interpretation from available wells in this area that indicate by the absences of the upper sediments of the Altena Group. The seismic responses show the sediments of the SLDN were gradually filling up the depositional space and overflowing the higher area during the deposition of the Rijnland Group.

The old faults group (23) are densely distributed in the base of the SLDN sediments. Furthermore, the fragmented base of the SLDN sediments is caused by the differentiation in subsidence during the rifting period. A small inversion effect indicates by only a few of the faults were reactivated and resulted in a small bulge structure in the base of the Chalk Group and Rijnland Group sediments (Figure 18).

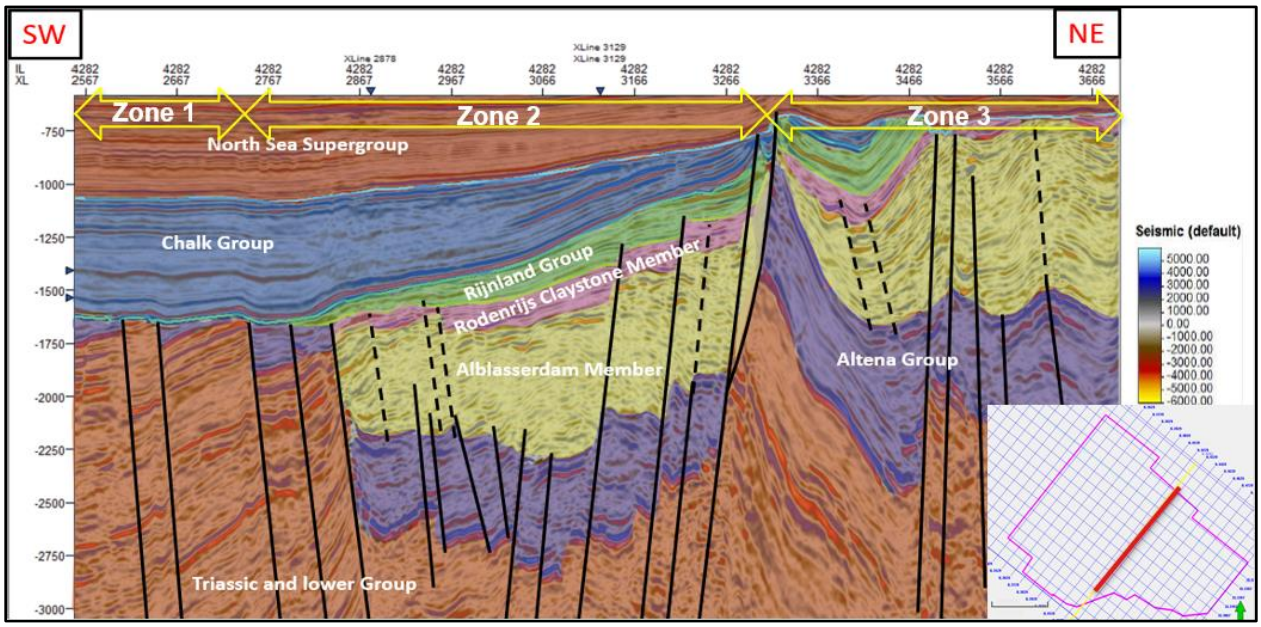

Figure 54 Zonation of Drechtsteden in the seismic cross section at inline 4282

Drechtsteden Zone 2

Drechtsteden Zone 2 (Zone 2) is the area between the two major faults and located in the central part of the study area. The SLDN sediments lie at a depth between -2000 m up to -3000 m depth, which is the deepest depth of the SLDN sediments in the study area. Also, the sediments are highly accumulated in this zone, varies from about ~900 m up to about ~1600 m in NW-most of the study area.

The sedimentation of the SLDN sediments was controlled by a local subsidence rate and fault activities. Some of the old faults were active during the deposition of the SLDNA sediments. One of obvious evidence is depicted in Figure 18, at the NW part of Zone 2 (inline 3682) the sediments show a growing trend towards to the North major faults thus the sediments in the northern part is thicker than the sediments in the southern part. The faults are normal faults with different fault displacement and only found locally in some area in the Drechtsteden. The variation of fault displacements indicates by the thickness heterogeneities of the SLDNA sediments in one area to another.

Furthermore, the fault activities and subsidence rate have a linear correlation. The sediments accumulation in the area with the active fault is higher than the area with no fault activities. The thicker sediments will lead to a higher subsidence rate as the overburden in this area is higher than the area with thinner accumulated sediments. In Zone 2 of the Drechtsteden, the fault

activities and subsidence rate are higher at the NW side as indicate in the seismic section and a thickness map of the SLDNA (Figure 44).

A set of reactivated faults are found in the NW part of the Zone 2 formed during the inversion period. The faults penetrate the Triassic up to the Tertiary sediments. These faults are forming a fragmented anticline structure and can be interpreted as an indication of structural history in the WNB that experienced a transition from normal to the transpressional regime. A moderate effect of the inversion period can be observed as an inclining trend of the KN and CK horizons in Zone 2 (Figure 54). The effect of the inversion is gradually higher from SW to NE as in line with the depth trend of the KN and CK horizons.

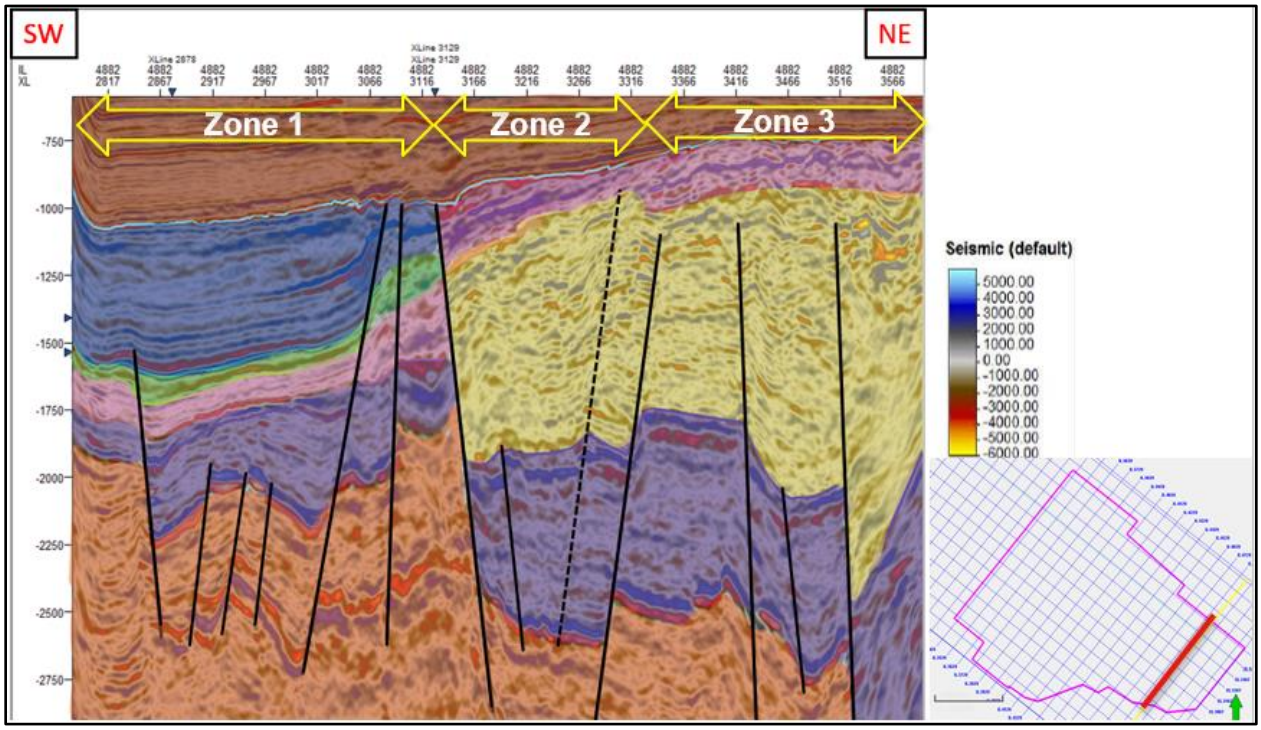

Figure 55 Zonation of Drechtsteden in seismic cross section at inline 4882

Drechtsteden Zone 3

Drechtsteden Zone 3 (Zone 3) is an area located between the North major faults to the northernmost part of the study area. The SLDNA sediments in this area have a thickness that varies from less than 200 m up to 1600 m thick; the highest thickness accumulation is found in the SE part of Zone 3. The depth varies from -900 to -2000 m depth which is about 1 km shallower depth compared to the depth of Zone 2. The high depth difference compared to the Zone 2 indicates that Zone 3 is the highly inverted area during the inversion period. Similar indications are also expressed in the depth map of the North Sea Supergroup (Figure 27), Chalk Group (Figure 25), and Rijnland Group (Figure 23). From the log response, seismic reflection, well correlation, and thickness trend, the SLDNA in Zone 3 has similar characteristics and cycles compared to the SLDNA in Zone 2. Thus, it is possible that Zone 2 and Zone 3 were initially formed as a single-fragmented area before significantly uplifted during the inversion period.

From the seismic analysis, the general trend of tectonic activities in the Drechtsteden in each zone and timing relative to the deposition of the SLDNA as may be found in Table 8.

Table 8 Summary of the magnitude, timing, and the affected area of tectonic activities in the Drechtsteden

Tectonic Activities	**Zone 1**	**Zone 2**	**Zone 3**
Before Deposition	High	Low	Low
During Deposition	Low	High	High
After Deposition	Low	Moderate	High

5.1.2 Stratigraphy of Alblasserdam Member

Distribution of the potential aquifer of the SLDNA in the Drechtsteden is predicted by reconstructing the depositional setting of the SLDNA. From the seismic interpretation and well correlation, a reconstruction of the depositional setting of the SLDNA before inversion period is presented in Figure 58. In general, the sediment of SLDNA sediments are highly accumulated in the Zone 2 with SE-NW trend. Moreover, the thickness trend of the SLDNR shows a gradual thinning towards SE. Based on the core description of the SLDNA and SLDNR, it can be concluded that during the Cretaceous the marine environment is at the NW and the continental environment is at the SE.

Based on the seismic and well log characteristic within the SLDNA, the SLDNA is divided into Alblasserdam – 01 (A1), Alblasserdam – 02 (A2), and Alblasserdam – 03 (A3). The reconstruction is supported by the depth, thickness, and structural maps from the previous chapters.

- *Alblasserdam - 01 (A1)*

  A1 are the basal sediments of the SLDNA that unconformably overlie the eroded Altena Group sediments. It is characterized by thickly stacked channels as can be observed in gamma-ray log responses at the base of well GSD-01 and WED-03 (Aquifer 1). The wells at the NW side do not penetrate this interval. Thus the continuity towards the NW cannot be observed from the well log response.

  Well GSD-01 and WED-03 are located in Zone 3 of the study area. The seismic characteristics of A1 at the base of SLDNA in Zone 3 shows a low and scattered reflection. A similar seismic response can be observed at the base of SLDNA in Zone 2.

  The thickly stacked channels indicate the sediment supply is higher than the available space (low A/S) caused cannibalization of coarser sediments to the finer sediments. Thus, only the coarser sediments are preserved. The A1 is interpreted as the basal syn-rift sediments and expected to have a wide distribution in the base of Zone 2 and Zone 3 of the Drechtsteden and consist of stacked fluvial channels with thickness average of about ~200 m thick and thinning toward SW direction (Zone 1).

- *Alblasserdam-02 (A2)*

The seismic response of A2 shows a higher reflectivity compare to A1. The A2 is interpreted as a syn-rift sediment deposited during intense local fault activities and subsidence rate. The local fault movement and subsidence rate controlled the deposition of the sediments and formed a local structural low and structural high area.

During this period, the deposition of the SLDNA sediments was continued only in the structural low area as it is more favourable for sediment to be deposited in the relatively lower topography. In the seismic section, growing sediment trends are observed as consequences of the fault activities. The active fault gives accommodation for sediments to be deposited. Also, the A/S cycle analysis shows a single high A/S cycle during the deposition of A1 and A2. The period of A/S cycle in the lower SLDNA (A1 and A2) is longer than the A/S cycles in the upper SLDNA (A3). This characteristic implies high tectonic activities was occurred and controlled the depositional trend of the lower SLDNA sediments (A1 and A2).

On the other hand, a sedimentation was hiatus at the structural high area as can be observed from the core description of the SLDNA in well ALD-01. A red bed of siltstone is found at depth -1626.8 m indicates that the sediments were exposed to the surface (Figure 56). The boundary between the red bed and the grey sediments cannot be analyzed as the limitation of the core preservation.

The fault movement and subsidence rate were higher than the sediment supply as expressed by the complete preservation of the fluvial components in gradually increasing gamma-ray log responses in well WED-03 and GSD-01 (Figure 49). The sand rich interval of the A2 is expected as an isolated channel with low lateral continuity following the distribution of the structural low area where the fluvial sediments were continuously deposited.

Figure 56 Oxidized siltstone core of SDLNA in well ALD-01

- *Alblasserdam-03 (A3)*

A3 has a relatively higher and continuous seismic reflectivity compared to A2 and A1. The A3 is interpreted as late syn-rift to early post-rift sediments that distributed all over the Drechtsteden area including some area of Zone 1. Fault activity decreased during this period as indicates by the character of the seismic response and shorter period of A/S cycles. The subsidence rate controls the trend of sedimentation and the position of the main fluvial system.

In general, the total SLDNA sediments at the SE Drechtsteden are highly accumulated in Zone 3. On the other hand, the SLDNA sediments at the NW part is highly accumulated at the central part of the study area (Zone 2) with SE-NW trend.

A well correlation in Zone 3 (Figure 46) shows thick loosely stacked channels (aquifer 2) in well WED-03 at depth -1139 until -1220 m. Toward NW direction the similar loosely stacked channels are observed in well GSD-01 at depth -1234 until -1338 m. However, the gamma-ray response in well CAP-01 which located at the boundary between Zone 2 and Zone 3 shows no indication of thick loosely stacked channels. Also, a well correlation is done in Zone 2 (Figure 47), shows a similar characteristic of the thick loosely stacked channels at the base of well DRT-01, IJS-43-S1, and RKK-32. However, the aquifer 2 is absent in well RTD-01 that located at the SW tip of the Zone 2.

During the deposition of A3, the area in Zone 2 is lower than the area in Zone 3 and Zone 1 because of the higher fault activities during the deposition of the previous SLDNA sediments (A1 and A2), resulting in a higher sediment accumulation. The high sediment accumulation induced a higher subsidence rate as a higher overburden load of the accumulated sediments. Also, the well correlations in Zone 3 and Zone 2 show that a high N/G interval (Aquifer 2) are found at the SE side of Zone 3 (WED-03 and GSD-01) and absent in the NW side. Nevertheless, the Aquifer 2 is found in the SE side of Zone 2 (well IJS-43-S1, RKK-32, and DRT-01).

The well correlation in Figure 50 shows that Aquifer 2 reaches the maximum thickness up to 158 m thick in well DRT-01. On the other hand, the thickness of the Aquifer in well RKK-32 and WED-03 is only 64 m and 81 m respectively. Thus, it can be concluded that the main fluvial system was shifted from SE side of Zone 3 Southwestward to the NW side of Zone 2 following the formed structural low with the overlapping point at the well DRT-01.

This observation is supported by a palynological analysis in the WNB (Willems et al., 2017) (Vondrak, Donselaar, & Munsterman, 2018), indicate a shifting position of the prevailing meander belt from the east to the west side of the basin during the Ryazanian and Valanginian Figure 57. In this study, the east and west side of the basin correspond to the Zone 3 and Zone 2 respectively.

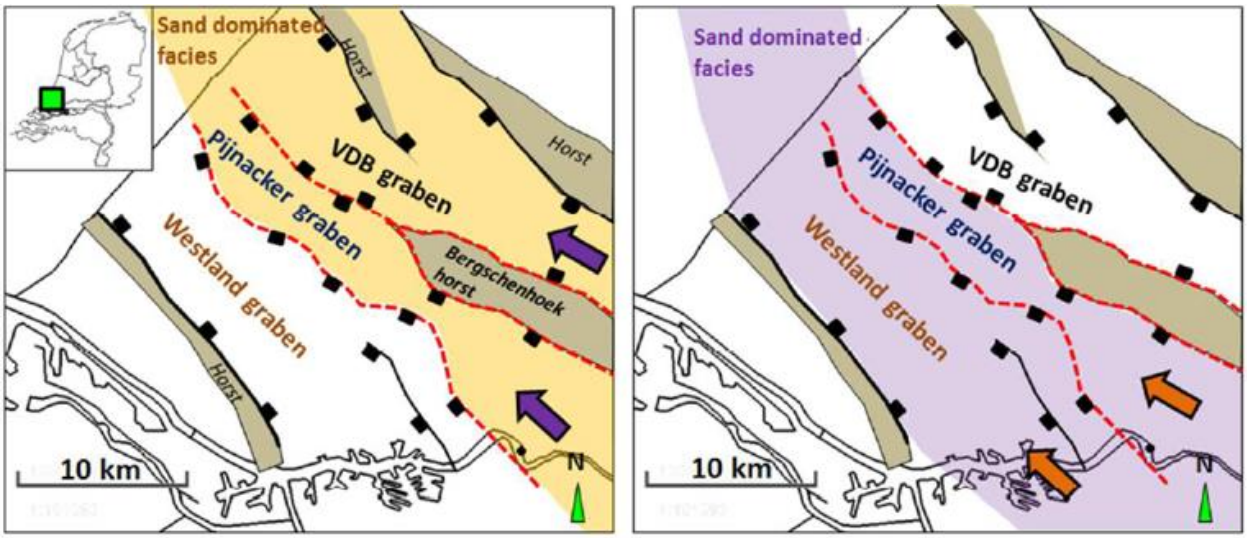

Figure 57 Map of sand dominated facies during Late Ryazanian (left) and Valanginian (right) (Willems et al., 2017)

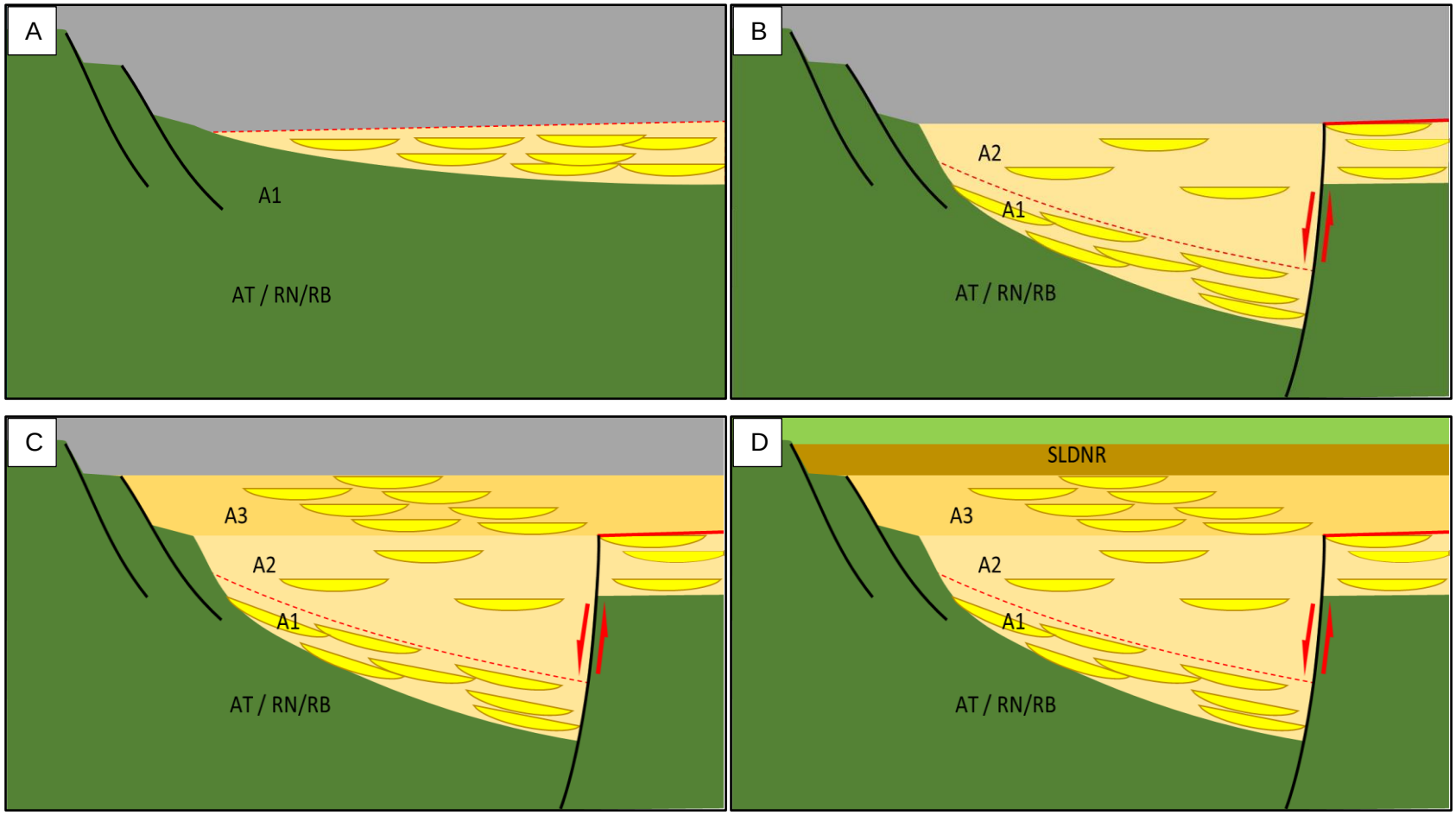

Figure 58 Reconstruction model of depositional Alblasserdam Member before the inversion period

5.2 Reservoir Properties

5.2.1 Porosity and Permeability profile of Nieuwerkerk Formation

From the log analysis and petrophysical evaluation, two intervals of sand-rich sediments have been identified within the Alblasserdam Member. Those intervals have a potential to serve as a geothermal aquifer. A geothermal aquifer commonly has an aquifer temperature >70^{o}C and thickness preference higher than 30 m (Lokhorst & Wong, 2007).

However, the high tectonic activities occurred during and after the deposition of the SLDNA might affect the reservoir properties of the Aquifer 1 and Aquifer 2. Figure 59 shows the average porosity with the depth of the SLDNA and SLDNR in the Drechtsteden. Commonly, the porosity values will decrease at the deeper level. However, the average porosity plot of the SLDNA does not show a regular decreasing trend with depth. By classifying the well based on the location of the wells, the porosity trend of the SLDNR and SLDNA can be observed.

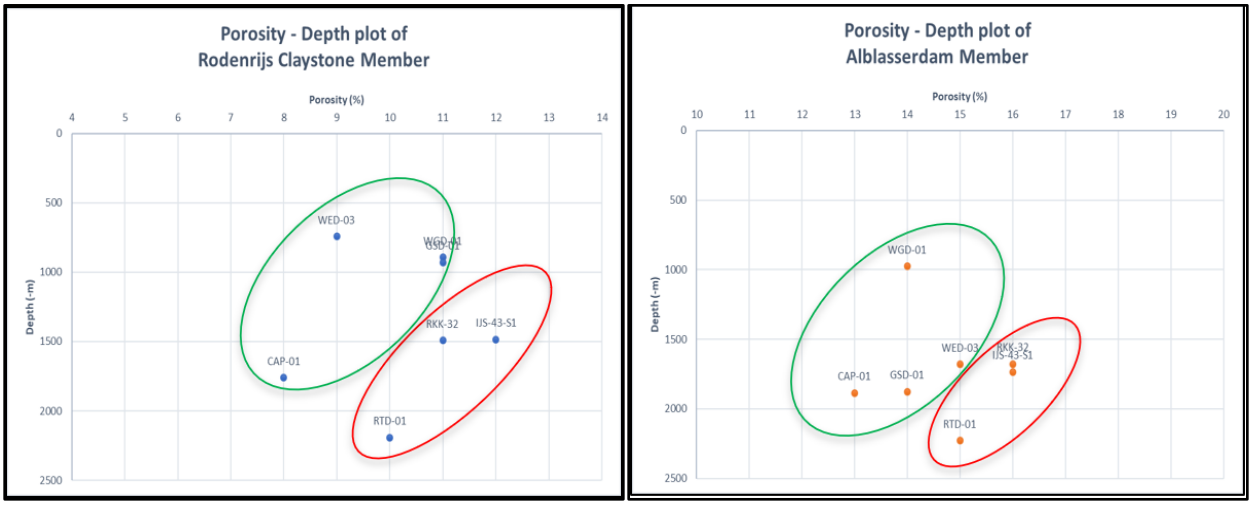

Figure 59 Porosity vs depth of Rodenrijs Claystone Member and Alblasserdam Member

Wells RKK-32, IJS-43-S1, and RTD-01 are located in Zone 2 of the Drechtsteden (red circle). The average porosity of the SLDNA and SLDNR decreases with depth.

On the other hand, well CAP-01, WED-03, GSD-01, and WGD-01 (green circle) are located in Zone 3. It is hard to observe the trend of the average porosity of the SLDNR and SLDNA in this area. In conclusion, the reservoir properties of the SLDNA in the study area is affected by tectonic activities and differs in each area in line with the magnitude and timing of the tectonic occurrences.

High tectonic activity occurred during and after the deposition of the SLDNA. High thickness accumulation resulting in higher compaction as the bed load becomes higher than the adjacent area. In the highly inverted area, the properties of the SLDNA might affected by the tectonic activities. At the same depth, the overall average porosity in Zone 3 is lower than the average porosity trend in the Zone 2. This is caused by the SLDNA at Zone 3 was deposited and buried at the deeper level before being inverted to the shallower level. In the previous chapter, a lamination of white cement is found in the core description of the SLDNA. Thus, the lower porosity is possibly caused by the precipitation of minerals after the inversion.

Furthermore, various average permeability values of SLDNA are observed. The value of the permeability is in line with porosity. A layer with high porosity value is expected to have a high permeability value. However, the average permeability and average porosity of a layer does not show an observable trend, because the average permeability is also affected by the ratio of sand-rich and shale-rich interval within the layer. The higher volume of shale will have lower average permeability. Figure 60 illustrates the average permeability profile of the SLDNA in the seven wells as a function of porosity and N/G ratio.

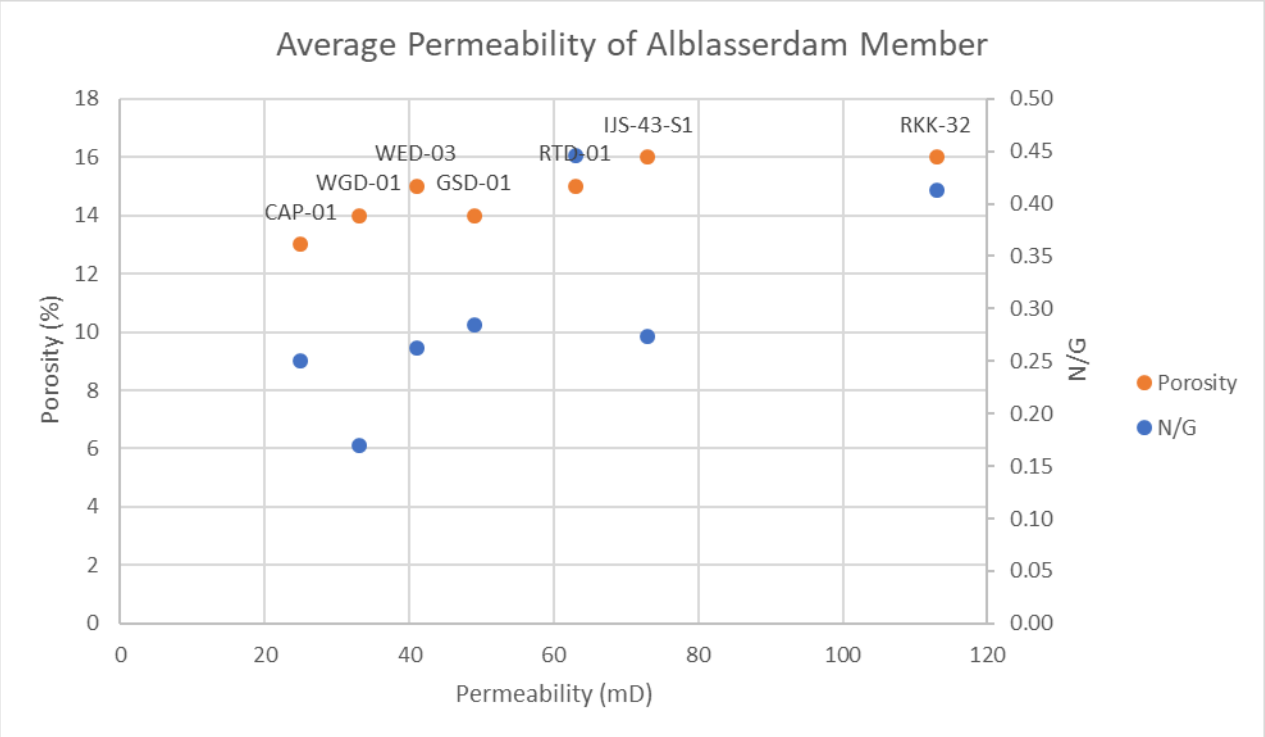

Figure 60 Average Permeability profile of Alblasserdam Member as a function of porosity and N/G ratio

5.2.2 Aquifer Temperature

The recent subsurface temperature study stated that the average thermal gradients in the onshore Netherlands is 31.3 °C/km and the average surface temperature is equal to 10.1°C (Bonté et al., 2012). Based on this data the aquifer temperature can be calculated as:

$$T_{aquifer} = depth\,.km * 31.3\ {}^{\circ}\mathrm{C}/_{km} + 10.1\ {}^{\circ}\mathrm{C}$$

The subsurface temperature at the Top and Base of the SLDNA is presented in Figure 61 and Figure 62. The subsurface temperature of the sand-rich interval in well RKK-32, IJS-43-S1, DRT-01, GSD-01, and WED-03 is given in Table 9.

Table 9 Temperature at the potential aquifers in the Drechtsteden

Well	Update Lithology Marker	Top	Base	Thickness	T min	T max
		(-m) TVD			°C	
RKK-32	Aquifer 2	1614	1678	64	60.62	62.62
IJS-43-S1	Aquifer 2	1631	1735	104	61.15	64.41
DRT-01	Aquifer 2	1762	1920	158	65.25	70.20
GSD-01	Aquifer 2	1234	1338	104	48.72	51.98
	Aquifer 1	1660	1857	197	62.06	68.22
WED-03	Aquifer 2	1139	1220	81	45.75	48.29
	Aquifer 1	1439	1680	241	55.14	62.68

Note that most of the wells were drilled at the structural high formation. However, the potential geothermal aquifers are expected to be at the structural low (Figure 28). Thus, the aquifer temperature also expected to be higher than the aquifer temperature reported in the investigated wells.

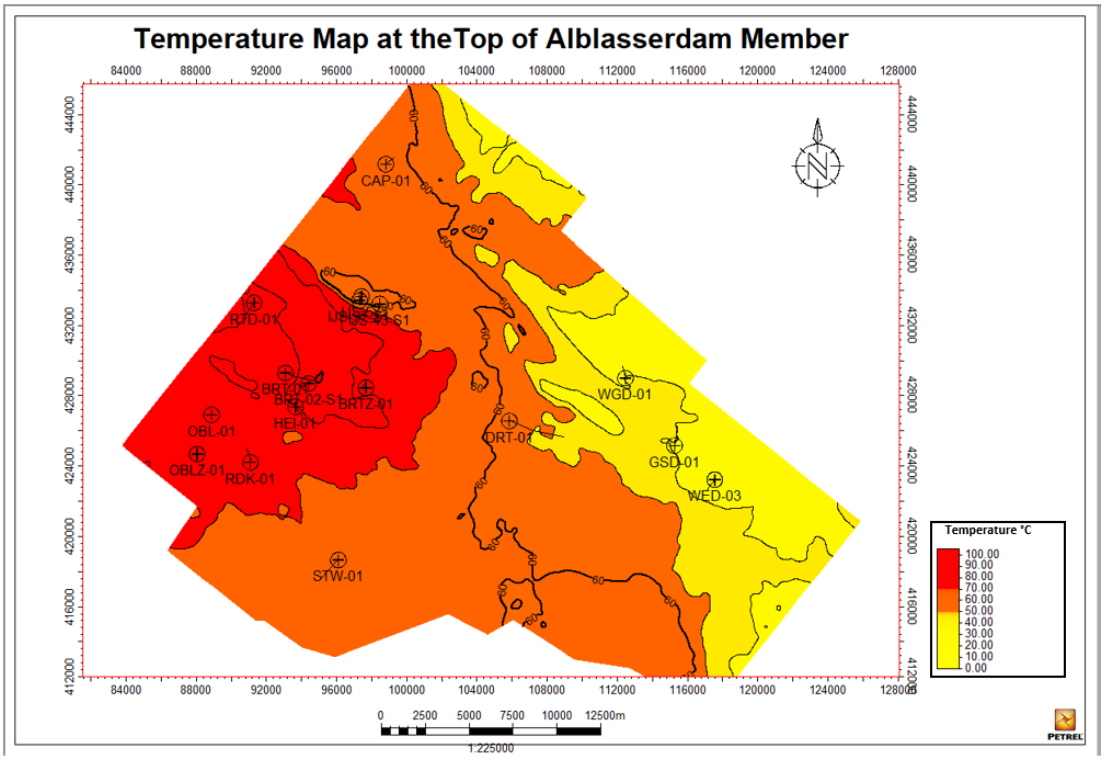

Figure 61 Temperature Map at the Top of Alblasserdam Member

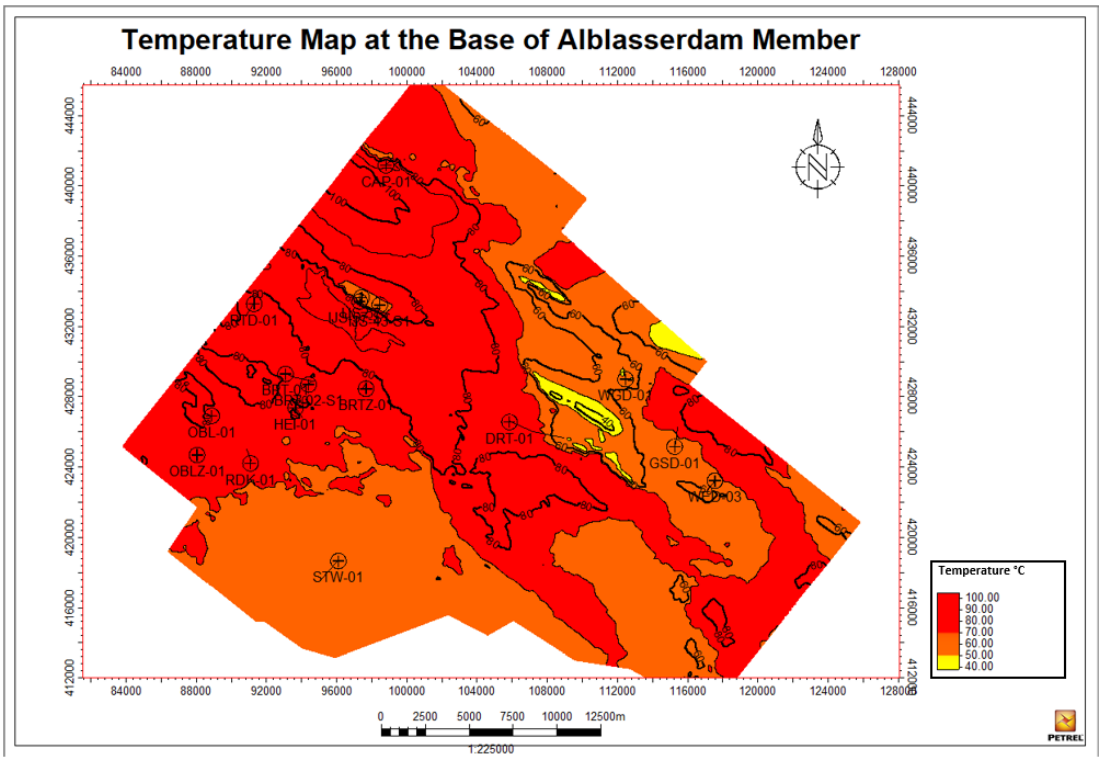

Figure 62 Temperature Map at the Base of Alblasserdam Member

5.3 Proposed Geothermal Doublet Location

Based on the result of the aquifer architecture of the SLDNA in Drechtsteden, two potential areas with three possible scenarios of the good geothermal aquifer are proposed. The areas are chosen based on the following criteria:

- High accumulation of sand-rich intervals
- Sufficient depth to produce heat >70 ^{o}C
- Absences of the fault

5.3.1 Area of Potential Geothermal Aquifers

Area 1

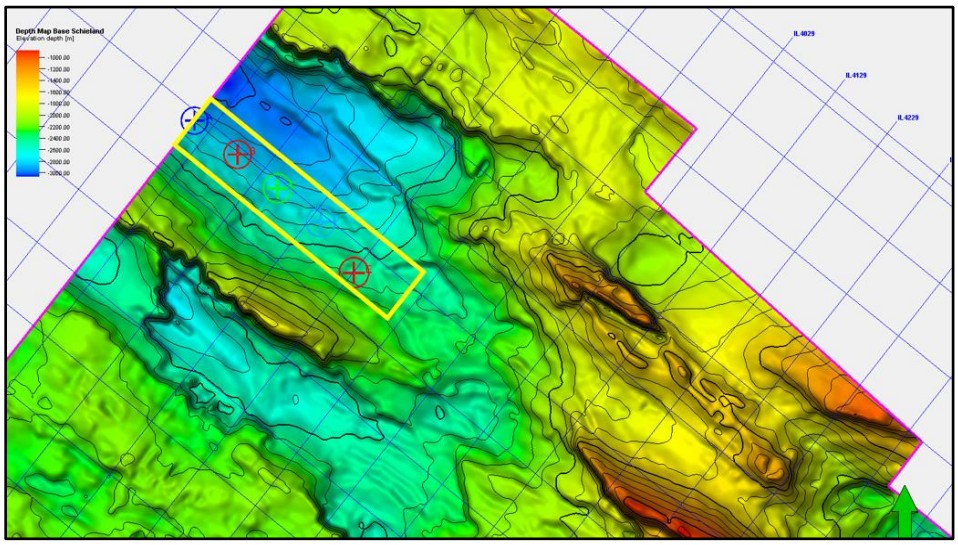

Figure 63 Area 1 of doublet placement in Drechtsteden with five possible locations of the geothermal doublet

The first area is located on the NW side of the Zone 2 in Drechtsteden (yellow square in Figure 63). The area is formed by polygonal of Inline 3402 – 3730 (~6.56 km) and Xline 3314 – 3354 (800 m), with total area of about ~52 km^2.

Figure 63 shows the depth map of the SLDNA and five possible well locations. The base of the SLDNA is slightly dipping towards NW. The production well will be placed in the deeper interval to obtain higher aquifer temperature. Four doublet configurations can be placed in this area with a minimum distance between the well equal to 1500 m as listed in Table 10. The depth of Aquifer 1 and 2 in this area are deeper than -2000 m. Thus the aquifer temperature is satisfied the

minimum geothermal aquifer temperature criteria. Also, the depth is also complying with the TNO requirement of geothermal exploitation for greenhouses and housing purposes.

Table 10 Coordinates of doublet placement in Drechtsteden

Well	X (RD-New)	Y (RD-New)
A	95200	439500
B	96500	438500
C	97700	437500
D	99000	436500
E	100000	435000

Area 2

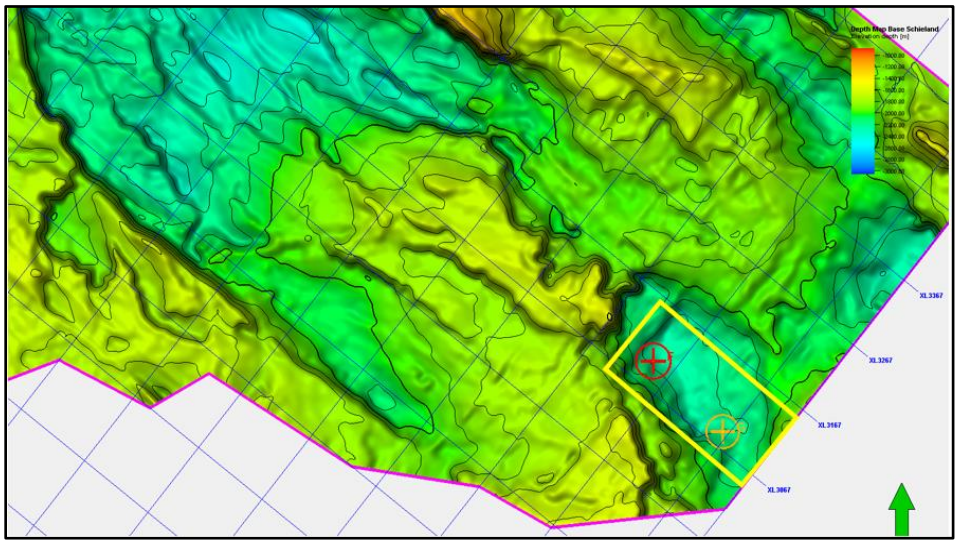

Figure 64 Area 2 of doublet placement in Drechtsteden

The second area is on the SE side of Zone 3 in the subsurface of Drechtsteden. The depth of Aquifer 1 is varying from -1600 m to -2000 m with maximum aquifer temperature equal to 73 ^{o}C. The produced heat from Aquifer 1 in this area can be used as geothermal energy for greenhouses. On the other hand, the depth of Aquifer 2 is varying from -1100 m to -1300 m with maximum aquifer temperature equal to 51^{o}C. These parameters are not satisfying the minimum depth and temperature requirement by TNO. In the subsurface, the injection well is placed at coordinate (118715, 413822) and the production well at (117005, 415522) Figure 64.

5.3.2 Scenario of Doublet Placements

Scenario 1

The first proposed geothermal doublet scenario is producing the heat from the Aquifer 2 in Area 1. Based on the structural and depositional analysis in the previous chapter, Aquifer 2 is lies at the base of Alblasserdam – 03 (A3). From the seismic section (Figure 65), the depth of Aquifer 2 in this area is varying from about ~-2000 m to ~-2200 m.

The values of the aquifer properties are estimated from the petrophysical evaluation data in the previous chapter. The thickness of clean sand and porosity values for the low, medium and high case of Aquifer 2 are estimated from X10, X50, and X90.

Furthermore, based on the result of the petrophysical evaluation in the previous chapter, the porosity-permeability relation does not represent the average permeability values of Aquifer 1 and Aquifer 2. It is caused by the data used in the porosity-permeability relation are including the entire interval of the SLDNA which contain low N/G intervals. Thus, the permeability value at low, medium and high case are estimated from X,10, X50, and X90 of the average permeability in Aquifer 2. The resume of the aquifer properties in Scenario 1 is presented in Table 11.

The actual permeability value of Aquifer 2 in Zone 2 could be lower than the expected values. A lower of permeability value in Zone 2 are possibly caused by fault sealing. Thus, the existence of the fault is considered in the determination of the doublet placement area.

Table 11 Aquifer Properties in Scenario 1

Scenario 1			
Aquifer Properties	Low	Medium	High
Gross Thickness (m)	69	93	104
N/G ratio	0.45	0.60	0.75
Net Aquifer (m)	31	56	78
Porosity (%)	16	17	18
Permeability (mD)	83	225	785
Depth (-m)	2000	2100	2200
Aquifer Temperature (°C)	73	76	79

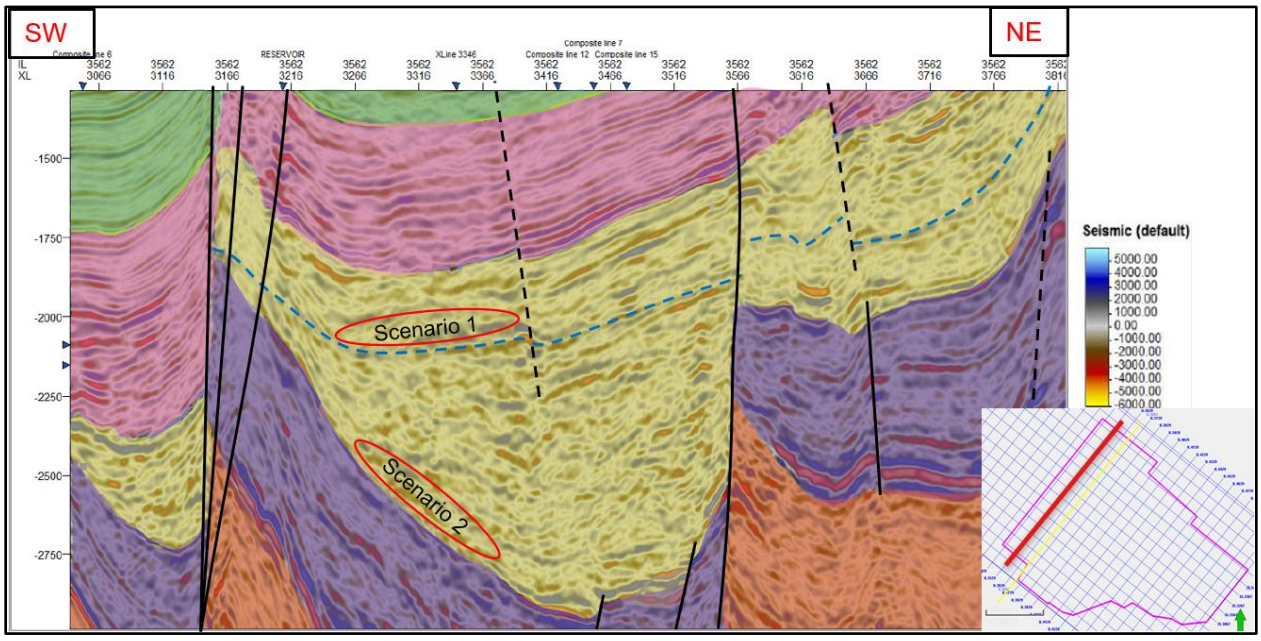

Figure 65 Aquifer target of a Production well in Scenario 1

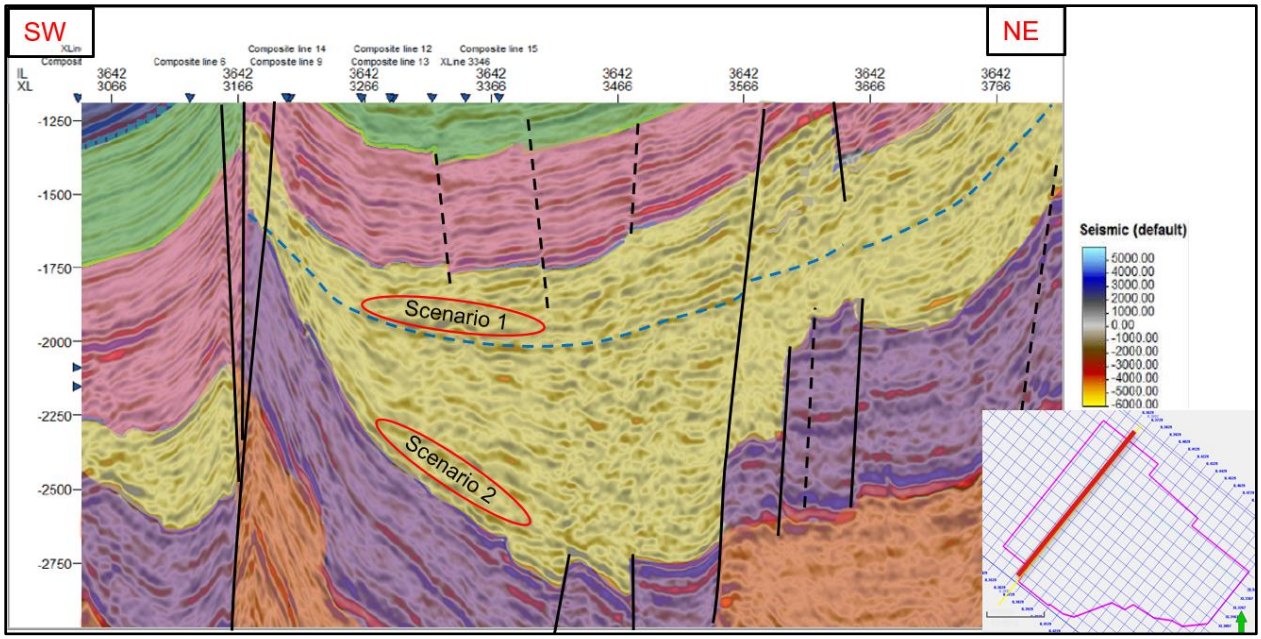

Figure 66 Aquifer target of an Injection well in Scenario 1 and Scenario 2

Scenario 2

The second proposed geothermal doublet scenario is producing the heat from the Aquifer 1 in Area 1 (Figure 65). From the seismic section, the depth of Aquifer 1 in this area is varying from about ~-2400 m to ~-2600 m. The values of the aquifer properties are estimated from the petrophysical evaluation data in the previous chapter. The thickness of clean sand for the low, medium and high case values in Aquifer 1 are estimated from X10, X50, and X90 from the petrophysical evaluation data.

In the petrophysical evaluation, the wells used are in the Zone 3 which were highly inverted to the shallower level, and mineral precipitation may occur after the inversion. The porosity of Aquifer 1 in this area (Zone 2) is expected to be higher than the average porosity from the petrophysical evaluation.

Compared to the properties of Aquifer 2 in the same location, Aquifer 1 has a higher net thickness. However, the average porosity and permeability of Aquifer 1 are lower than in the Aquifer 2. The lower porosity and permeability values are caused by lower N/G ratio and possibly due to higher compaction in Aquifer 1 that located about 500 m deeper than Aquifer 2. The resume of the aquifer properties in Scenario 2 is presented in Table 12.

Table 12 Aquifer Properties in Scenario 2

Scenario 2			
Aquifer Properties	Low	Medium	High
Gross Thickness (m)	201	219	237
N/G ratio	0.45	0.53	0.63
Net Aquifer (m)	90	117	149
Porosity (%)	15	16	17
Permeability (mD)	48	127	212
Depth (-m)	2400	2500	2600
Aquifer Temperature (^{o}C)	85	88	91

Scenario 3

The third proposed geothermal doublet scenario is producing the heat from Aquifer 1 in Area 2. From the seismic section (Figure 67), the depth of Aquifer 1 in this area is varying from about ~-1800 m to ~-2000 m. The wells used in the petrophysical evaluation of Aquifer 1 are located in this area. Thus, the values of the aquifer properties are estimated from the petrophysical evaluation data in the previous chapter. The thickness of clean sand, porosity and permeability values for the low, medium, and a high case of Aquifer 1 are estimated from X10, X50, and X90 from the petrophysical evaluation data.

Furthermore, Zone 3 is the area that highly affected by the inversion pulses and changed the reservoir properties of the SLDNA. The SLDNA in this area is strongly uplifted and has a high possibility of mineral precipitation occurred after the inversion period. The mineral precipitation is forming cement that clogged the pores and reducing the porosity and permeability values of the SLDNA in this area. The resume of the aquifer properties in scenario 1 is presented in Table 13.

Table 13 Aquifer Properties in Scenario 3

Scenario 3			
Aquifer Properties	Low	Medium	High
Gross Thickness (m)	201	219	237
N/G ratio	0.45	0.53	0.63
Net Aquifer (m)	90	117	149
Porosity (%)	14	15	16
Permeability (mD)	29	76	127
Depth (-m)	1800	1900	2000
Aquifer Temperature (°C)	66	70	73

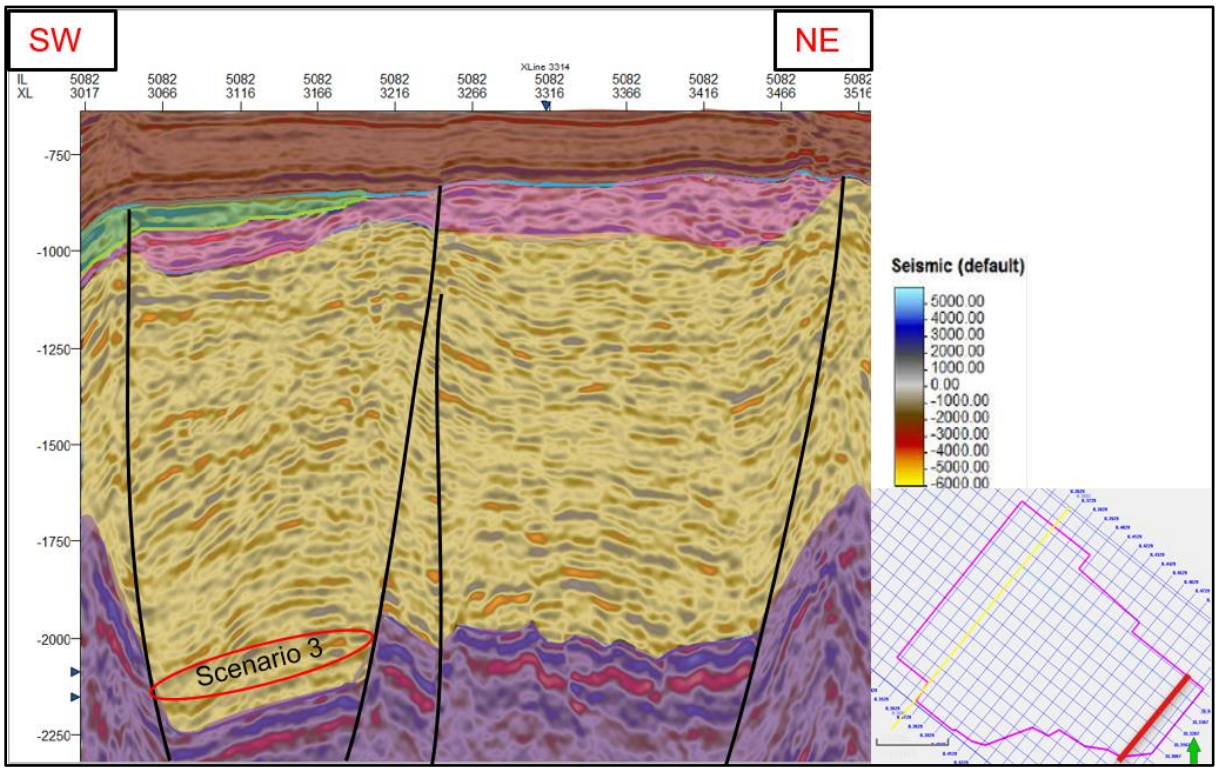

Figure 67 Aquifer target of a Production well in Scenario 3

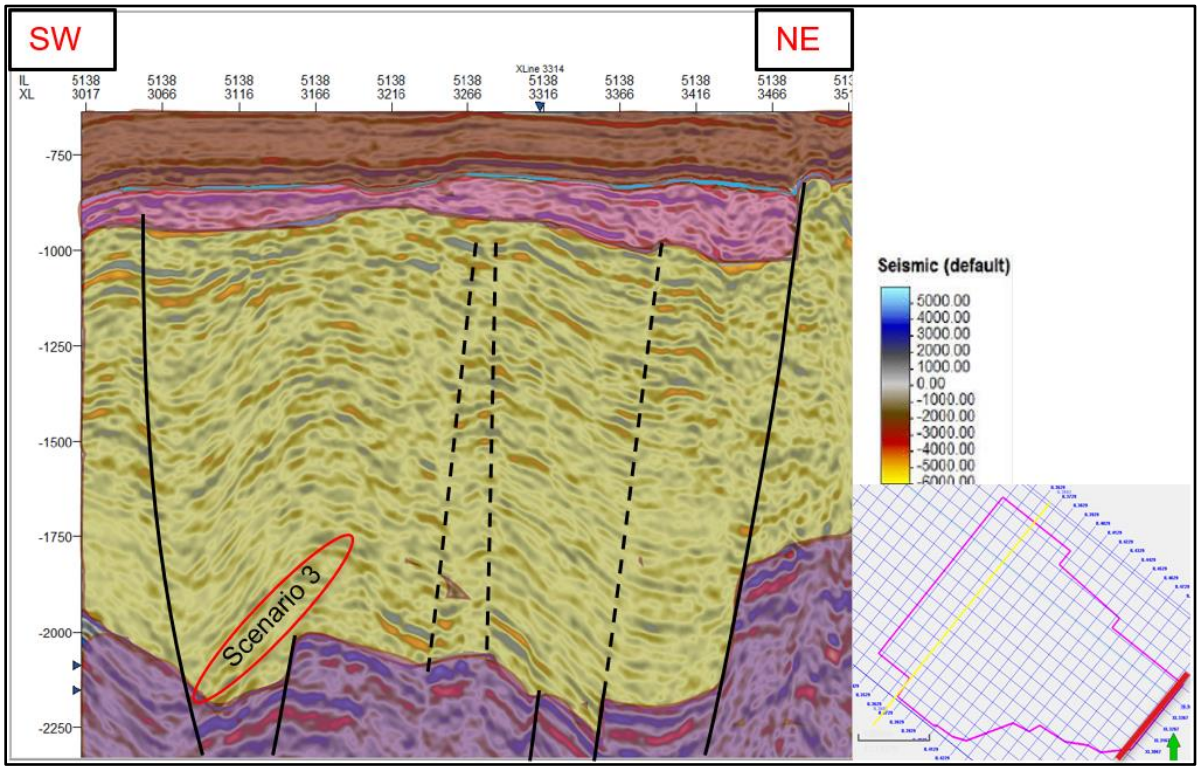

Figure 68 Aquifer target of an Injection well in Scenario 3

5 Conclusions

In this study, the architecture of the Alblasserdam Member in the Drechtsteden is modelled by integrating the seismic interpretation, reservoir sedimentology and petrophysical evaluation by utilizing the seismic, well log and core data. Based on the results and discussion, several main ideas can be concluded as follow:

- The seismic response of the Alblasserdam Member shows a high thickness and depth variations. It implies that the deposition of the Alblasserdam Member was affected by tectonic activities.
- A lateral zonation and stratigraphy analysis are done to classify the character and frequency of tectonic activities and observe the depositional distribution of the Alblasserdam Member in the Drechtsteden.
- The sediments of the Alblasserdam Member are highly accumulated in Zone 2 and SE side of Zone 3 in the Drechtsteden. The thickness distributions of the sediments are following the trend of the major faults toward SE-NW.
- Before the deposition of the Alblasserdam Member, high tectonic activities occurred in Zone 1. This area was a structural high formed as the result of Mid Kimmerian pulse during the Jurassic. The accumulation of the Alblasserdam Member is low to the point of absent in Zone 1.
- During the deposition of the Alblasserdam Member, high tectonic activities occurred in Zone 2 and Zone 3. High tectonic activities influenced the deposition of the lower Alblasserdam Member as illustrated by long periods of high A/S cycles. Also, the seismic, well correlation, and core data show high thickness variations of the sediments, red-beds, and fault activity overprint. The tectonic activities correspond to the syn-rift phase of Late Kimmerian tectonic pulse.
- After the deposition of the Alblasserdam Member, high tectonic activities occurred in Zone 3. It is expressed by a shallower level of the Alblasserdam Member and the absence of Rijnland and Chalk Group sediments. The tectonic activities are corresponding to the inversion period (Alpine Inversion). During this period, the normal rifting faults were reactivated into reverse faults, forming a transpressional flower structure.
- From the integration of well correlation and seismic interpretation, two high sand intervals are observed within the Alblasserdam Member with the trend of main fluvial channel toward SE-NW which are in line with the trend of sediments thickness and fault orientation. There are Aquifer 1 and Aquifer 2.

- In general, Aquifer 1 has a higher clean sand thickness, but lower average permeability compared to Aquifer 2. This might be caused by lower N/G ratio, the compaction and mineral precipitation after the inversion period, especially in the highly inverted area.
- Fault activities and subsidence rate have a linear correlation. High normal faults activities are resulting in a high accumulation of the basal Alblasserdam Member (A1 and A2). The high sediments accumulation is resulting in a high overburden and inducing a high subsidence rate. In the area with higher subsidence rate, a structural low will be formed and become a favourable area for a fluvial channel to flow.
- The main fluvial channel of the Alblasserdam-03 (A3) was shifted southward from Zone 3 to Zone 2 caused by high local faults movements and subsidence rate differences. In this study, the overlapping point is observed in well DRT-01 with a total thickness equal to 158 m.
- Three scenarios of doublet placement are proposed. Producing the heat from Aquifer 2 in the potential Area 1 is the best scenario in this study. The aquifer parameters in Scenario 1 are complying with the TNO requirement of geothermal exploitation for greenhouses and housing purposes.

References

Bonté, D., Van Wees, J. D., & Verweij, J. M. (2012). Subsurface temperature of the onshore Netherlands: New temperature dataset and modelling. *Geologie En Mijnbouw/Netherlands Journal of Geosciences*, *91*(4), 491–515. https://doi.org/10.1017/S0016774600000354

de Jager, J. (2003). Inverted basins in the Netherlands, similarities and differences. *Geologie En Mijnbouw/Netherlands Journal of Geosciences*, *82*(4), 355–366. https://doi.org/10.1017/S0016774600020175

de Jager, J. (2007). Geological development. *Geology of the Netherlands*, 5–26.

Devault, B., & Jeremiah, J. (2002). Tectonostratigraphy of the Nieuwerkerk Formation (Delfland subgroup), West Netherlands Basin. *American Association of Petroleum Geologists Bulletin*, *86*(10), 1679–1707.

Donselaar, M. E., Groenenberg, R. M., & Gilding, D. T. (2015). Reservoir Geology and Geothermal Potential of the Delft Sandstone Member in the West Netherlands Basin. *World Geothermal Congress 2015*, (April), 9.

Herngreen, G. F. W., & Wong, T. E. (2007). Cretaceous. In *Geology of the Netherlands* (pp. 127–150).

Jeremiah, J. M. (2000). Lower Cretaceous turbidites of the Moray Firth: sequence stratigraphical framework and reservoir distribution. *Petroleum Geoscience*, *6*(4), 309–328. https://doi.org/10.1144/petgeo.6.4.309

Lokhorst, A., & Wong, T. E. (2007). Geothermal energy. In *Geology of the Netherlands* (pp. 341–346). https://doi.org/10.1016/S0140-6701(03)80021-8

Nichols, G. (2009). *Sedimentology and Stratigraphy* (Second Edi). West Sussex: John Wiley & Sons.

Rondeel, H. E., Batjes, D. A. J., & Nieuwenhuijs, W. H. (1996). *Geology of Gas and Oil under the Netherlands*. : https://doi.org/10.1007/978-94-009-0121-6

Tiab, D., & Donaldson, E. . (2004). *Petrophysic: Theory and Practice of Measuring Reservoir Rock and Fluid Transport Properties* (second edi).

Vondrak, A., Donselaar, M. E., & Munsterman, D. K. (2018). Reservoir architecture model of the Nieuwerkerk Formation (Early Cretaceous , West Netherlands Basin): diachronous

development of sand-prone fluvial deposits. *Geological Society London Special Publications*.

Willems, C. J. L., Vondrak, A., Munsterman, D. K., Donselaar, M. ., & Mijnlieff, H. F. (2017). Regional geothermal aquifer architecture of the fluvial (the) Lower Cretaceous Nieuwerkerk Formation , derived from palynological cuttings analysis. *Netherlands Journal of Geosciences*.

Wong, T. E. (2007). Jurassic. In *Geology of the Netherlands* (pp. 107–125).

Appendixes

A. Well Database

Well database of wells in the Drechtsteden area that penetrating the Nieuwerkerk Formation. The data consist of list off wells with the availability of gamma-ray, porosity, density, sonic, resistivity and core data.

Well	Depth From	Depth Until	Cretaceous (Alblasserdam/delfland/Schieland)	Jurassic	Triassic	Info	GR	NPHI	RHOB	DT	RES	Check Shot	CORE
ALD-01	0	1650	Alblasserdam			CAL, SP, RES, Alblasserdam							675.5-1628
ALM-01	0	2370				Alblasserdam included							
BLG-01	0	1516				CAL, SP, RES, Alblasserdam							
BLG-02	0	1604				CAL, SP, RES, Alblasserdam							785.5-1502
BLK-01	0	2300				DLISS data, no Alblasserdam							
BRAK-01	0	2689				Alblasserdam							1154.2-2478.5
BRT-01	0	3365				production profile, dipmeter, lithology, cronological test							1696-1704.7, 1930-1938.7, 1939-1948
BRT-02-S1	1321	3177				Chemistry data, neutron photos, temperature							3006 - 3023
BRT-02-S2	1508	3295				report, temperature							
BRTZ-01	0	3259				production profile, lithology, formation test							2664 - 2789
BRTZ-02-S2	1668	3101				no ascii/LAS file available, nieuwerkerk included							
BRTZ-03	0	3035				nieuwerkerk included							
BRTZ-04	0	2860				nieuwerkerk included							
DRT-01	0	4290				nieuwerkerk included							
GSD-01	0	2575				ablasserdam included							
HEI-01	0	2316				ablasserdam included							
IJS-03	0	1872				alblasserdam included							
IJS-03-S1	1560	2132				unidentified log data, only two data available, alblasserdam							
IJS-16	0	1911				composite well, petrophysics, SP							
IJS-17	0	1615				composite well, petrophysics, SP, temperature							
IJS-20	0	1173				composite well, petrophysics, SP							
IJS-30	0	1600				petrophysical data							
IJS-31-S2	826	1185				Caliper, SP, Conductivity							
IJS-33-S1	778	1153				composite well, SP							
IJS-36-S1	650	1574											
IJS-36-S3	404	1553				composite well, petrophysics, SP							
IJS-37	0	1600				composite well, petrophysics, SP							
IJS-38	0	1600				composite well							
IJS-39	0	1200				SP							
IJS-39-S1	803	1600				composite well, petrophysics, SP							
IJS-41	0	1228				SP							
IJS-41-S1	877	1640				composite well, petrophysics, SP, temperature							
IJS-43	0	1600				composite well, petrophysics							
IJS-43-S1	392	1932				composite well							
IJS-47	0	1689				composite well, SP, petrophysics							
IJS-48	0	1639				composite well, SP, petrophysics							
IJS-49	0	1656				composite well							
IJS-52-S1	310	1158				composite well, SP							
IJS-57	0	1132				composite well, SP, petrophysics							679.3-1069.4
IJS-57-S1	765	1649				1182-1649							
LEK-01	0	1965				Biostartigraphy and palynology reports available, Core interval undetermined							764.2-1114.2 ?
MOL-02	0	2432				DLIS, Dip Log Available							
NMD-01	0	2804				DLIS Format							
NKK-01	0	2554				Core interval undetermined							469-470 , 603-608, 971-975, 1005-1710, 2207-2241 ??
OBL-01	0	2714				DLIS							
OBLZ-01	0	2745				DLIS, Core analysis, description and lab reports are available, Core interval determined from report							2202-2296
RDK-01	0	3053				DLIS, Core description, analysis, biostratigraphy reports and photos are available							2722-2735, 2800-2814, 2816-2825
RKK-01	0	2424				DLIS, Res-microlog-short&long and SP, GR-RHOB-DT-NPHI In Different format, Conventional core analysis is availaible							827-2392
RKK-09-S2	395	1115				DLIS, different format well logs, Res-microlog-short&long and SP, neutron log available							
RKK-24-S1	0	1112				DLIS, different format well logs							
RKK-26	0	1591				DLIS, Res-microlog-short&long and SP						Interval Transit Time	
RKK-27	0	1832				DLIS, different format well logs							
RKK-30	0	1620				DLIS, different format well logs							
RKK-31	0	1609				DLIS, different format well logs							
RKK-32	0	2101				DLIS						Interval Transit Time	
RKK-32-S1	1551	2401				DLIS						Interval Transit Time	
STR-01	0	2779				Different format well logs (non NAM - Amoseas)							
STW-01	0	3101				DLIS, Core Analysis available							2445-2455. 2546-2563
WED-01	0	2275				Res-microlog, Induction log resistivity long-short, dipmeter log available							719-1997 ??
WED-03	0	3125				DLIS, Core photos and por-perm analysis available							2821-2982
WGD-01	0	2394				DLIS, Core description and photos available, Wellshot file unidentified yet							1379-1775

B. Seismic

B.1 Seismic Data Information

Axis	Min	Max	Delta
X	50766.53	130959.96	80193.44
Y	400271.25	474053.37	73782.13
Z	-6004.00	4.00	6008.00
Lat	51°34'57.34...	52°15'17.9768"N	0°40'20.6345"
Long	3°51'40.154...	5°02'26.4441"E	1°10'46.2899"

Description	Value
Original CRS:	Netherlands-RD-New (MENTOR:Netherlands-RD-New:RD / Netherlands New / Onshore) [SIS,501575]
Origin X:	50780.58
Origin Y:	447102.47
End first inline X:	72275.25
End first inline Y:	474039.32
End first crossline X:	109451.24
End first crossline Y:	400285.30
Number of inlines:	3754
Number of crosslines:	1724
Inline length:	34461.79
Inline interval:	20.00
Crossline length:	75060.60
Crossline interval:	20.00
Inline rotation from north:	38.59
Survey type:	3D survey
Inline range:	1429 to 5182 step 1
Crossline range:	2267 to 3990 step 1

Copy to output sheet: ☑ List 1 ☑ List 2 ☐ Reset

B.2 Seismic Horizon Interpretation

B.2.1 Horizon Interpretation of Base Rijnland Group

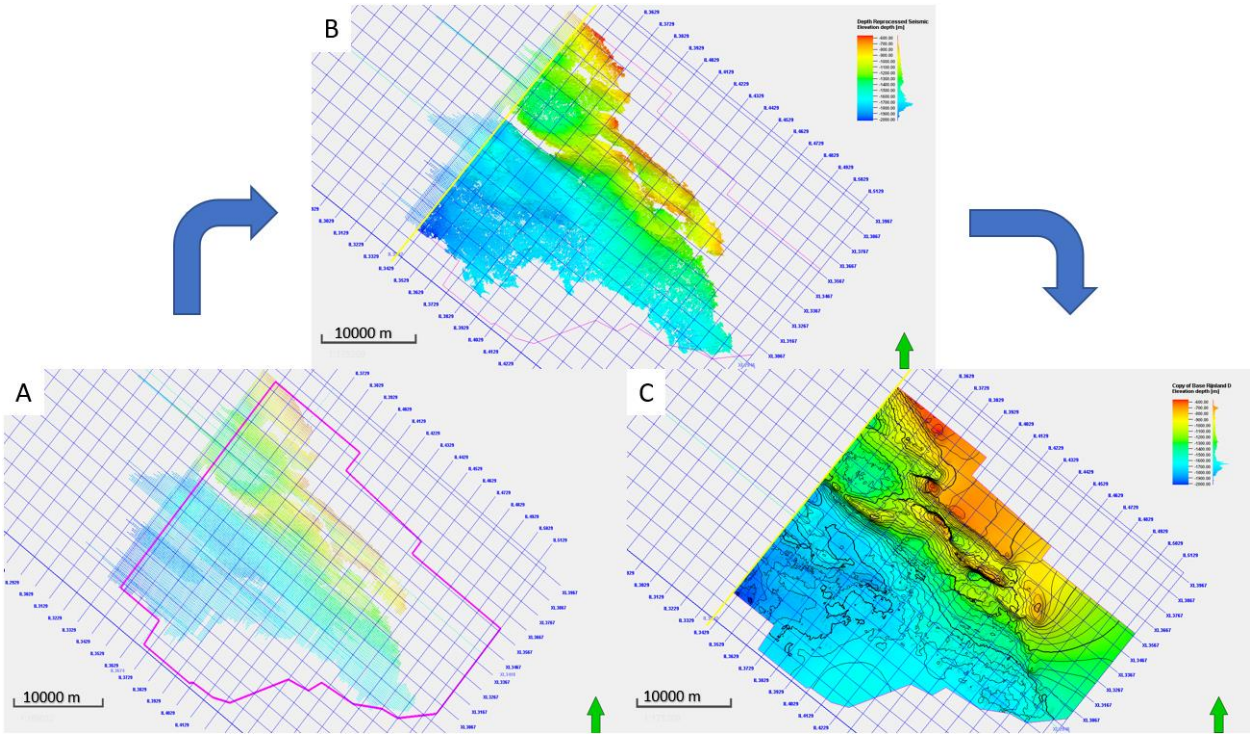

Figure 69 Steps in horizons interpretation at Base Rijnland Group A) Result of 2D interpretation across inline and crossline; B) Result from 3D guided auto-tracking; C) Surface Map

B.2.2 Horizon Interpretation of Base Chalk Group

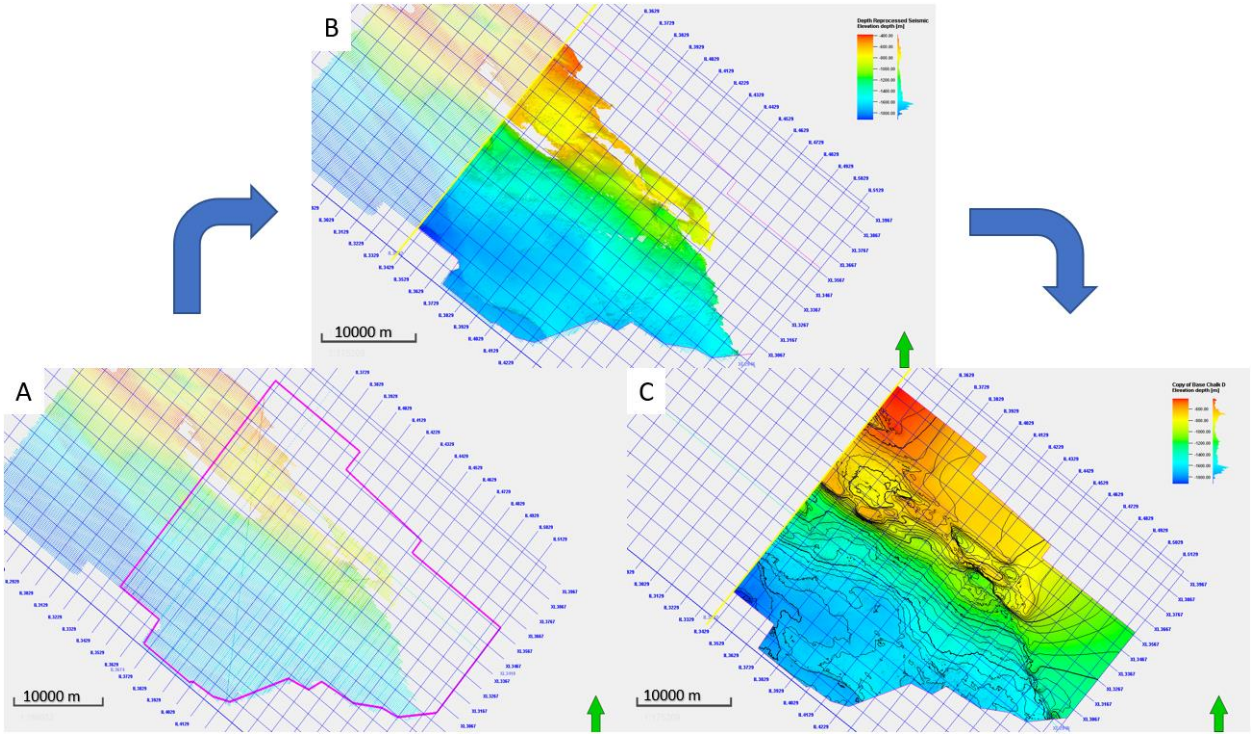

Figure 70 Steps in horizons interpretation at Base Chalk Group A) Result of 2D interpretation across inline and crossline; B) Result from 3D guided auto-tracking; C) Surface Map

B.2.3 Horizon Interpretation of Base North Sea Supergroup

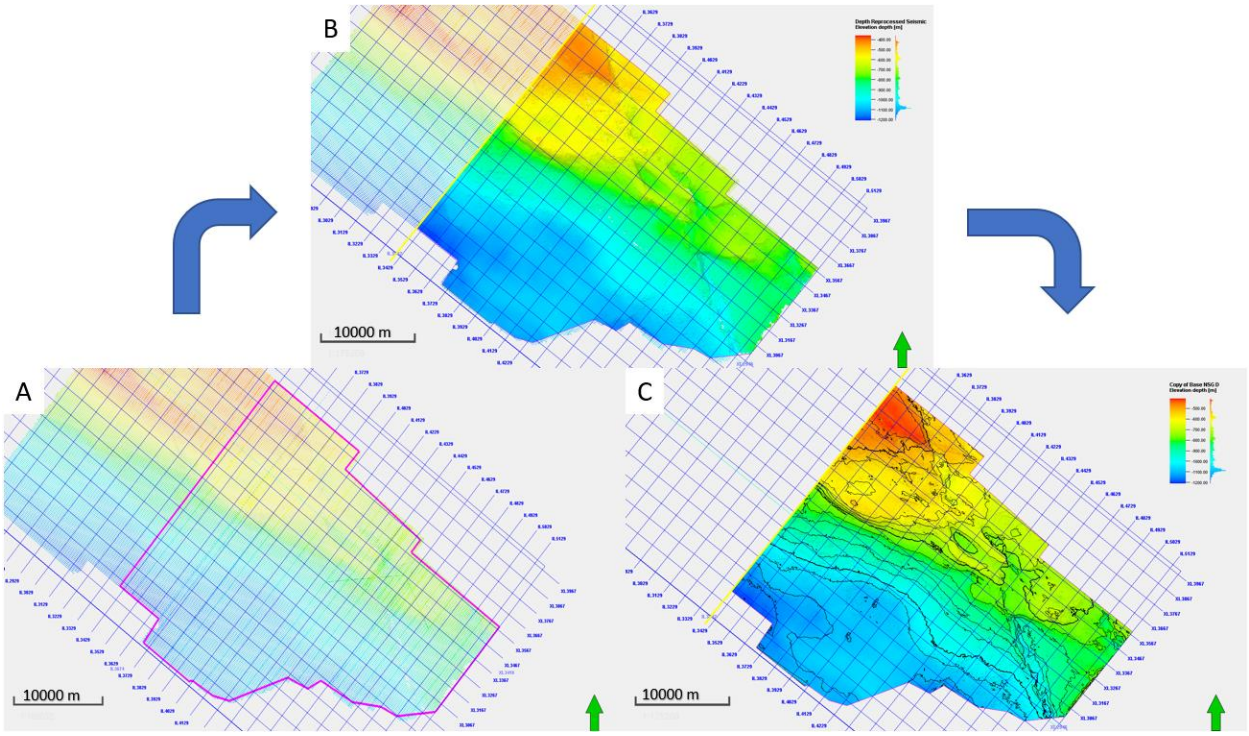

Figure 71 Steps in horizons interpretation at Base North Sea Supergroup A) Result of 2D interpretation across inline and crossline; B) Result from 3D guided auto-tracking; C) Surface Map

B.3 Seismic Cross-section

The seismic cross-section is made in every 20 inline (4 km) to show the high structural heterogeneities in the Drechtsteden, the West Netherlands Basin.

B.3.1 Seismic Cross-section at inline 3482

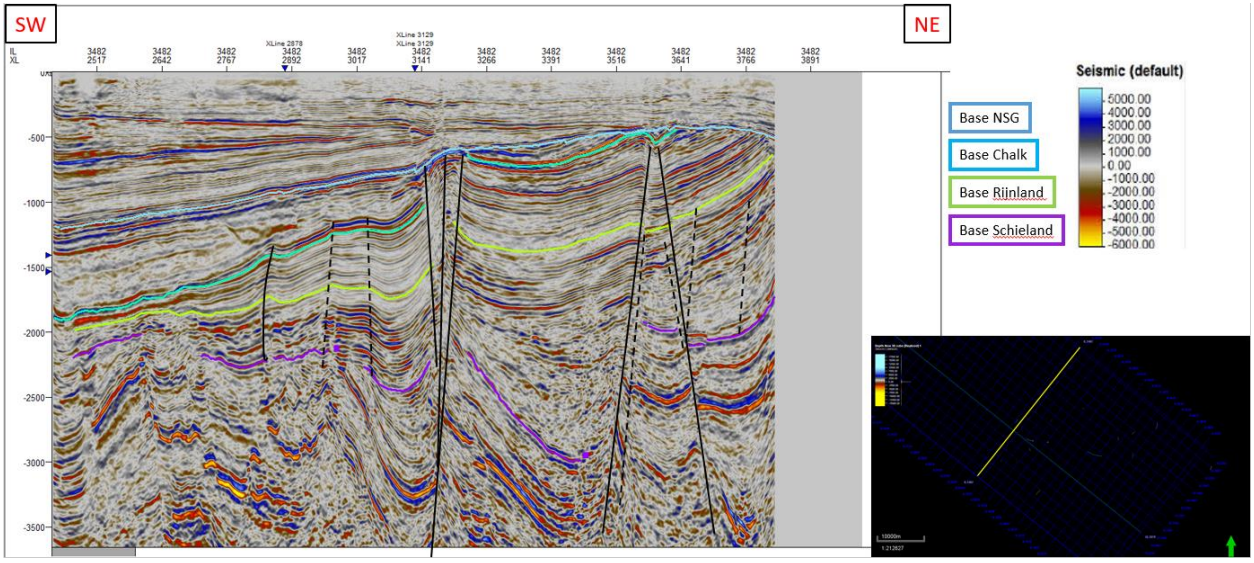

Figure 72 Horizons and Faults Interpretation in seismic cross-section at inline 3482

B.3.2 Seismic Cross-section at inline 3682

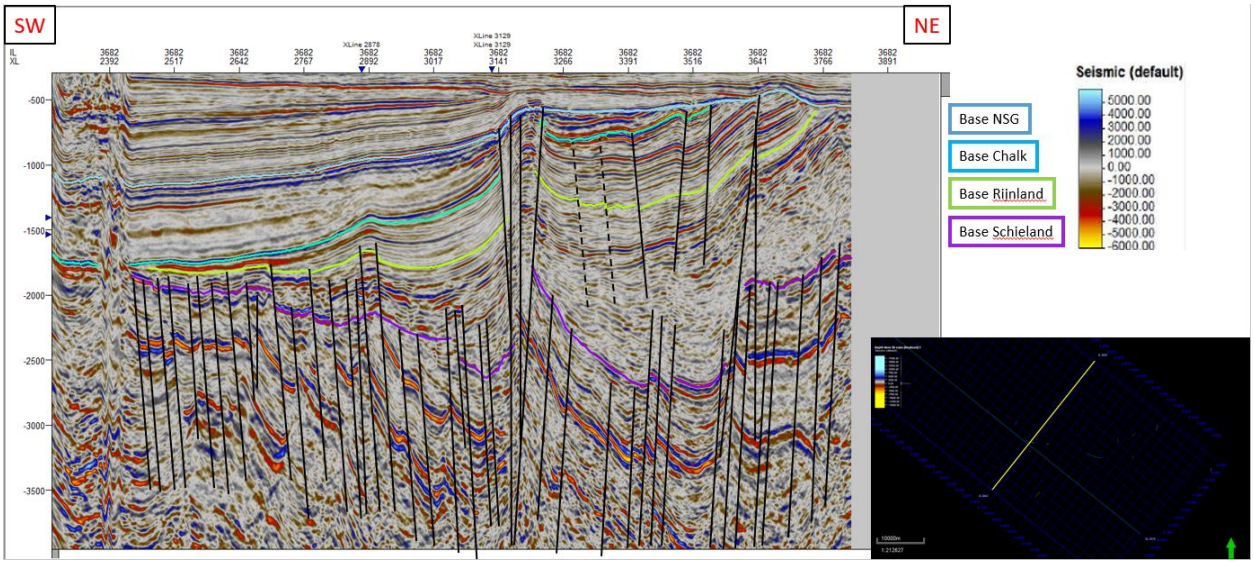

Figure 73 Horizons and Faults Interpretation in seismic cross-section at inline 3682

B.3.3 Seismic Cross-section at inline 3882

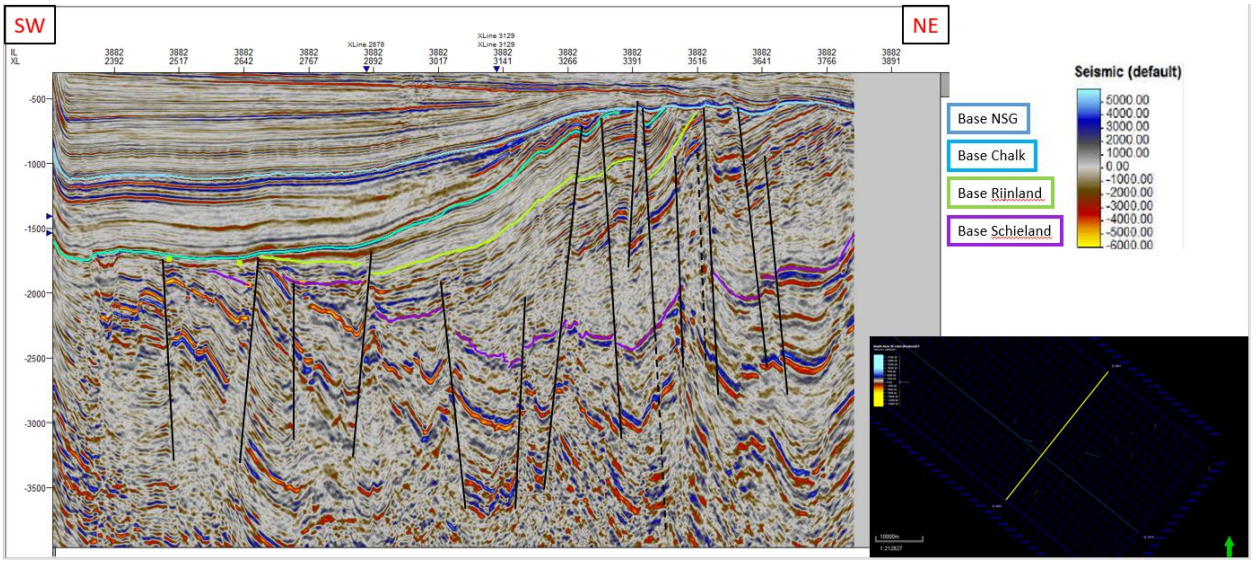

Figure 74 Horizons and Faults Interpretation in seismic cross-section at inline 3882

B.3.4 Seismic Cross-section at inline 4082

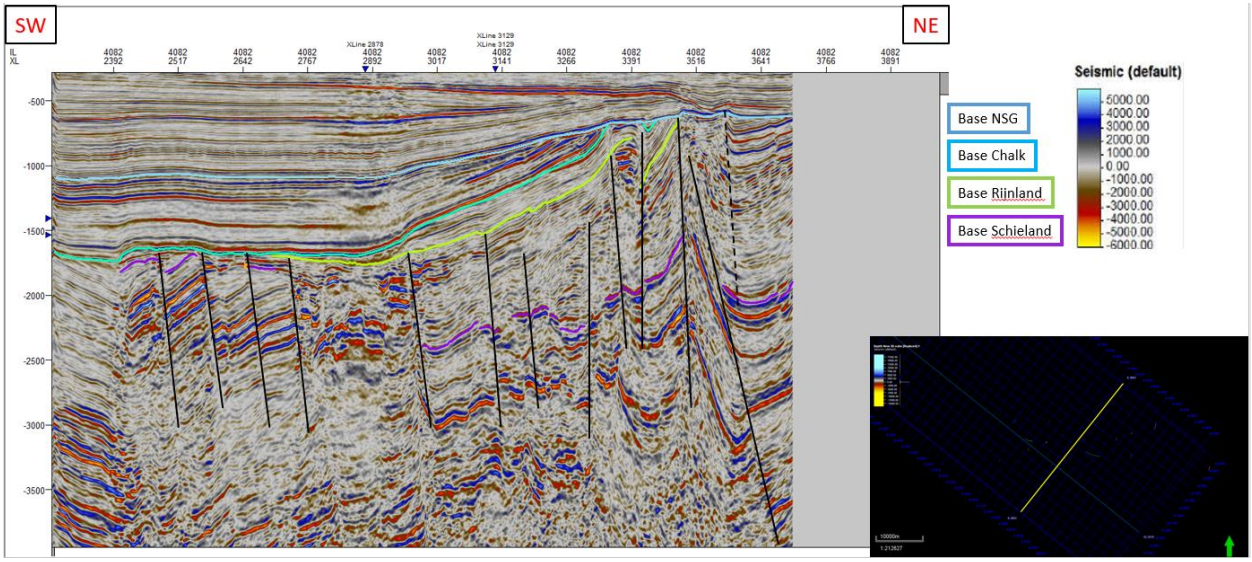

Figure 75 Horizons and Faults Interpretation in seismic cross-section at inline 4082

B.3.5 Seismic Cross-section at inline 4282

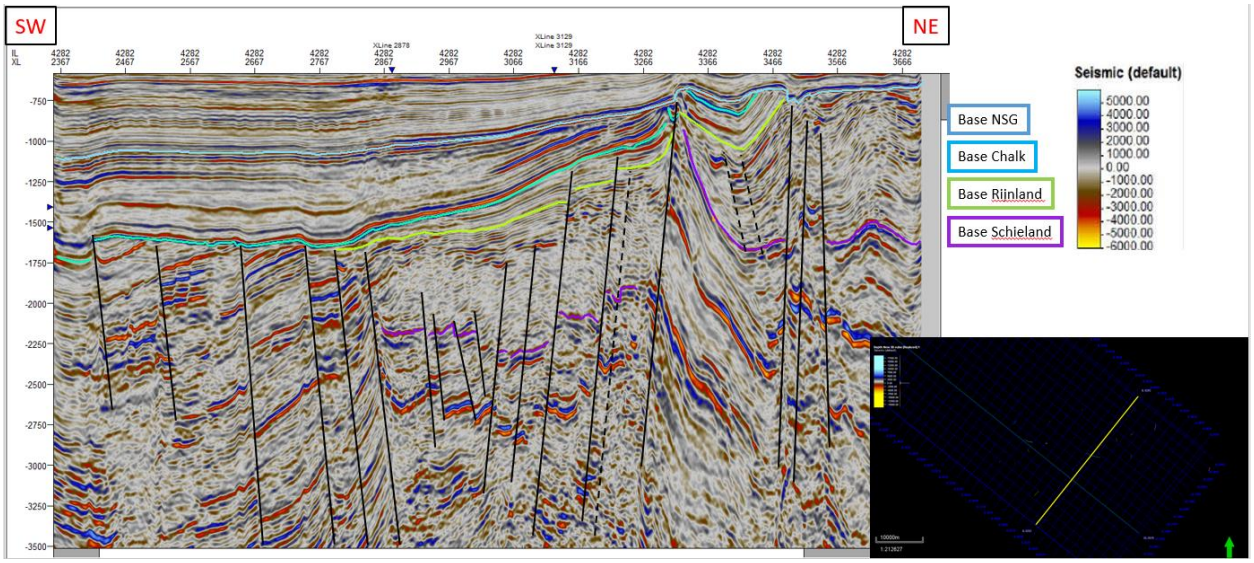

Figure 76 Horizons and Faults Interpretation in seismic cross-section at inline 4282

B.3.6 Seismic Cross-section at inline 4482

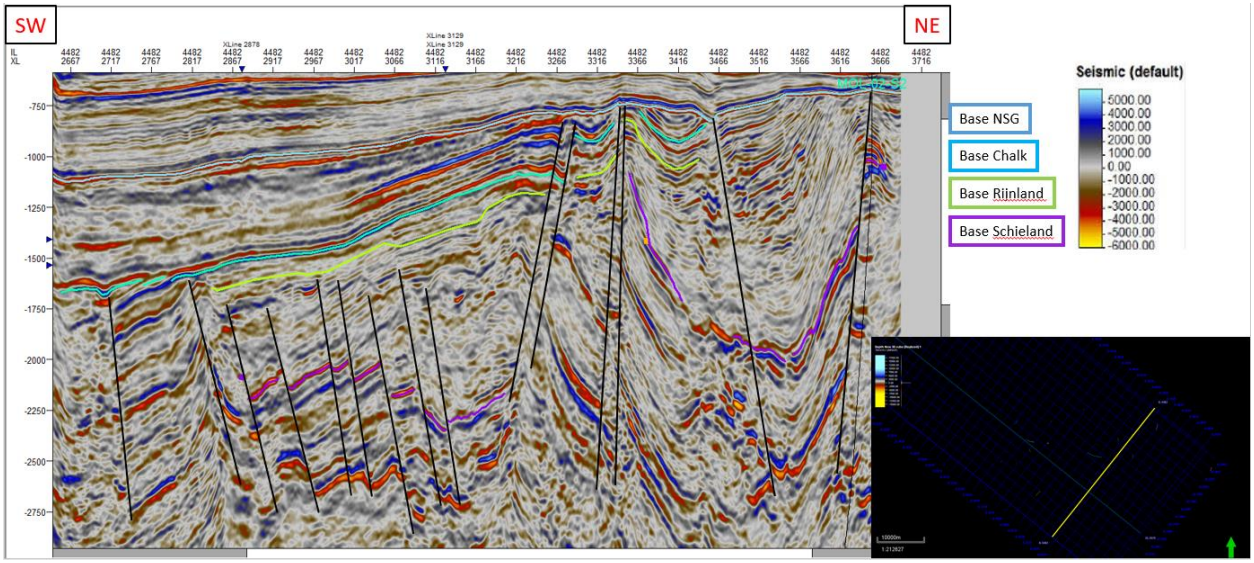

Figure 77 Horizons and Faults Interpretation in seismic cross-section at inline 4482

B.3.7 Seismic Cross-section at inline 4682

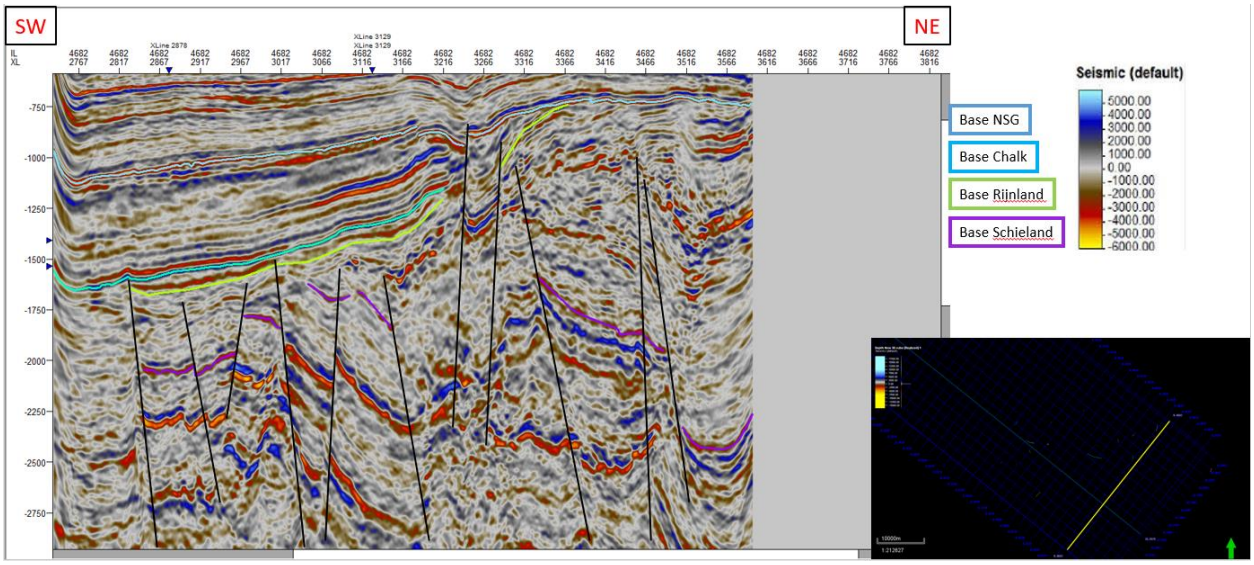

Figure 78 Horizons and Faults Interpretation in seismic cross-section at inline 4682

B.3.8 Seismic Cross-section at inline 4882

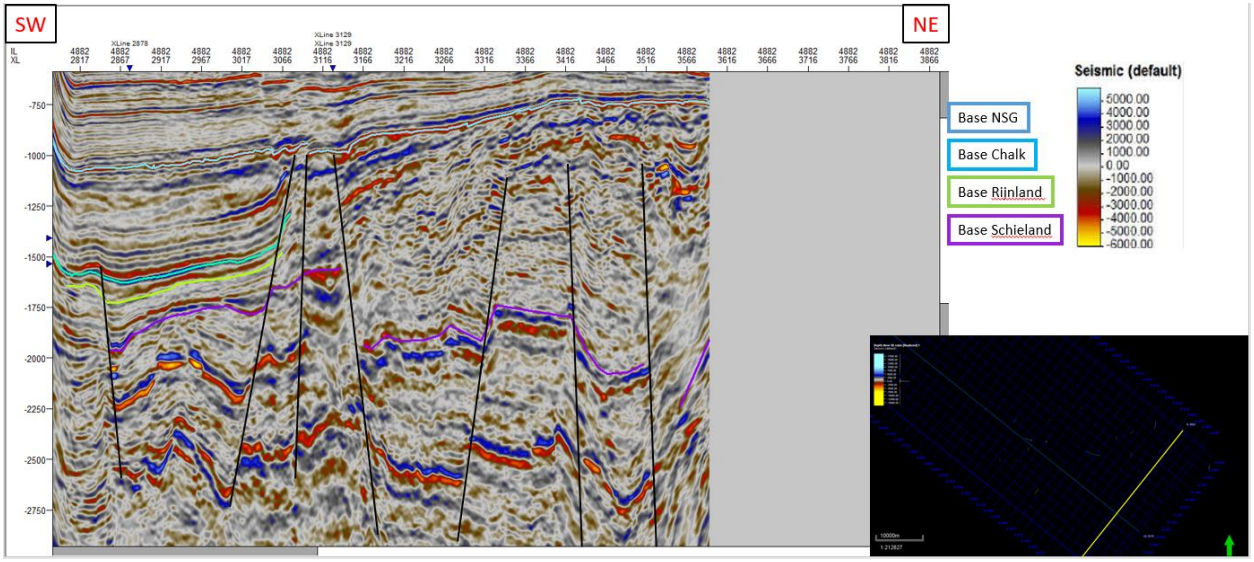

Figure 79 Horizons and Faults Interpretation in seismic cross-section at inline 4882

B.3.9 Seismic Cross-section at inline 5082

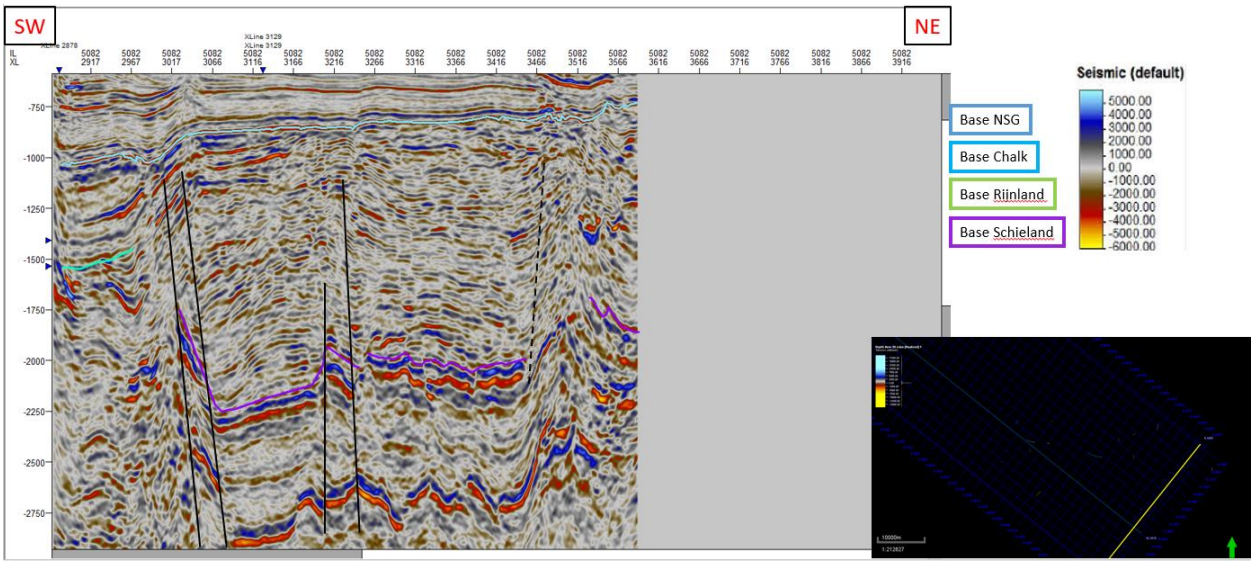

Figure 80 Horizons and Faults Interpretation in seismic cross-section at inline 5082

C. Petrophysical Evaluation

C.1 Petrophysical Evaluation in well RTD-01

Gamma-ray minimum : 45

Gamma-ray maximum : 110

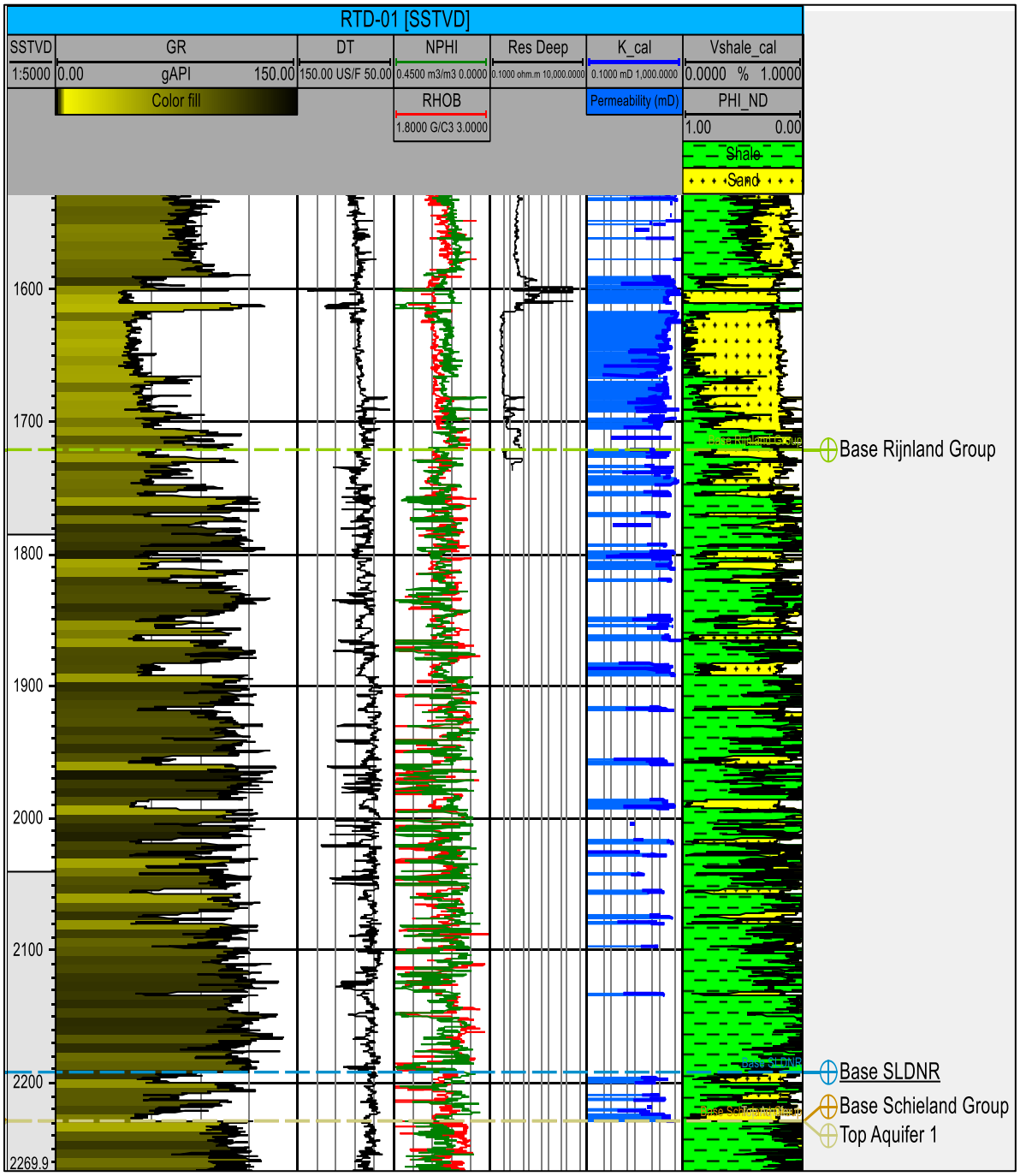

Figure 81 Result of petrophysical evaluation in well RTD-01

C.2 Petrophysical Evaluation in well CAP-01

Gamma-ray minimum : 20

Gamma-ray maximum : 70

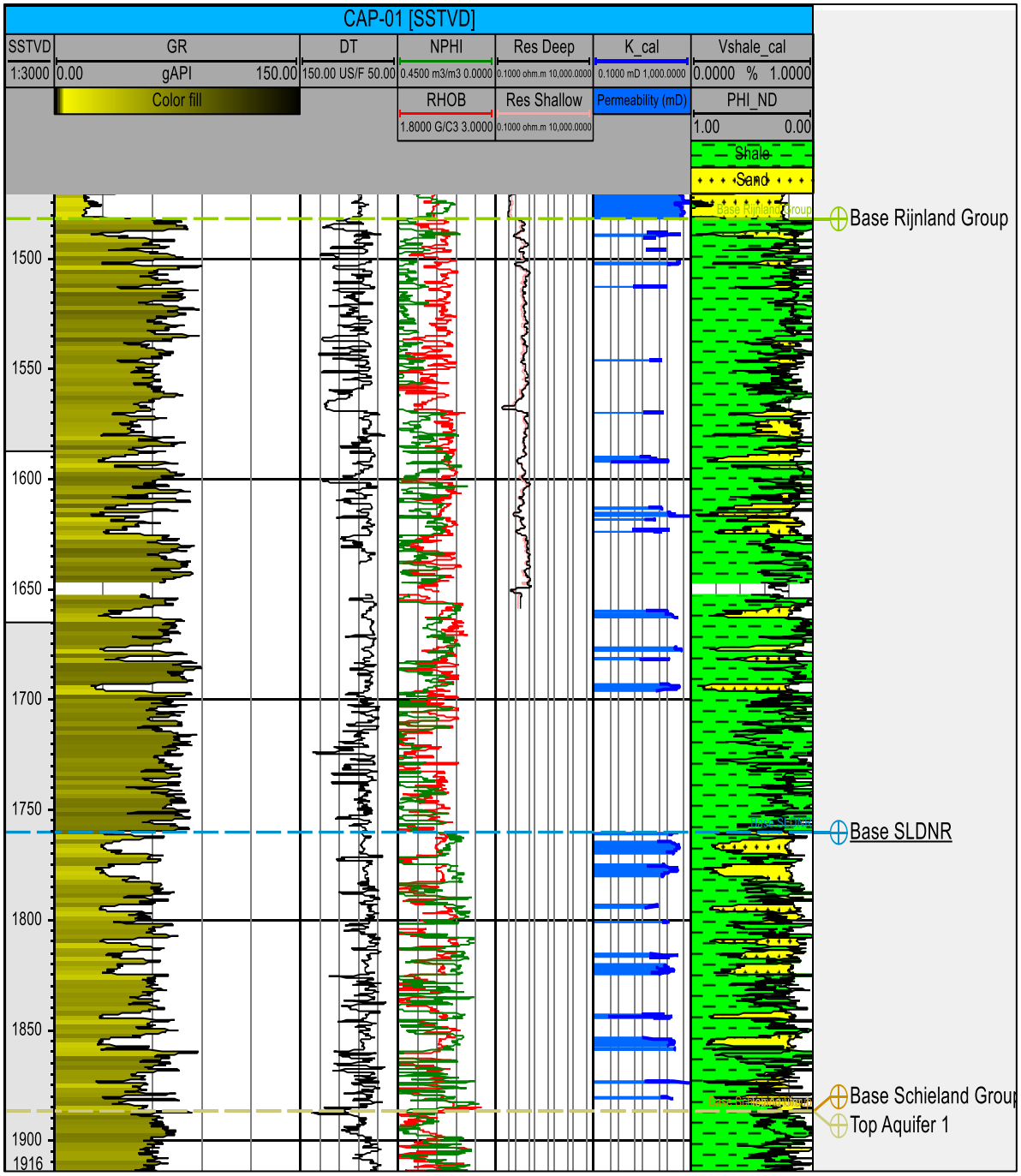

Figure 82 Result of petrophysical evaluation in well CAP-01

C.3 Petrophysical Evaluation in well RKK-32

Gamma-ray minimum : 25

Gamma-ray maximum : 110

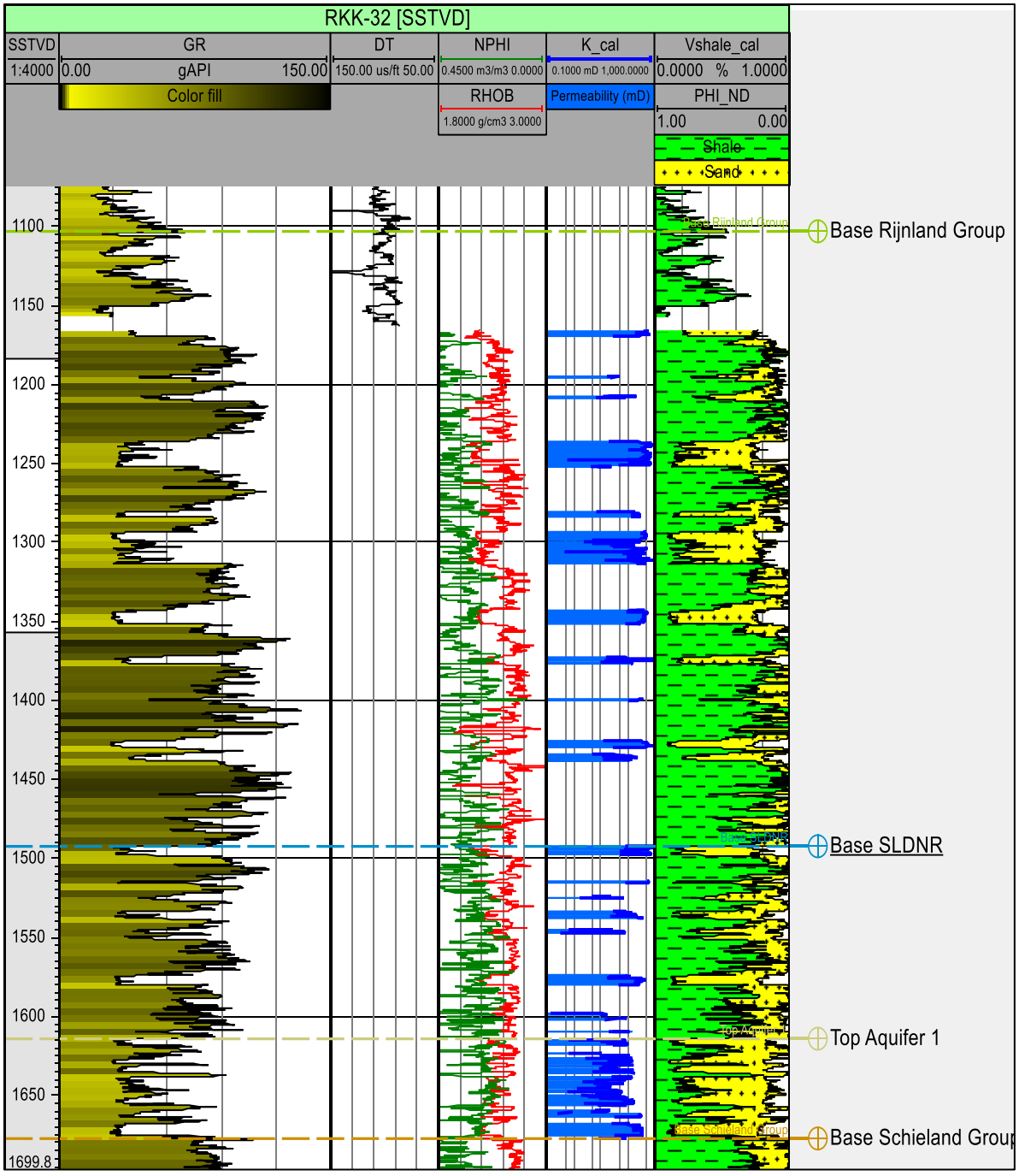

Figure 83 Result of petrophysical evaluation in well RKK-32

C.4 Petrophysical Evaluation in well IJS-43-S1

Gamma-ray minimum : 20

Gamma-ray maximum : 120

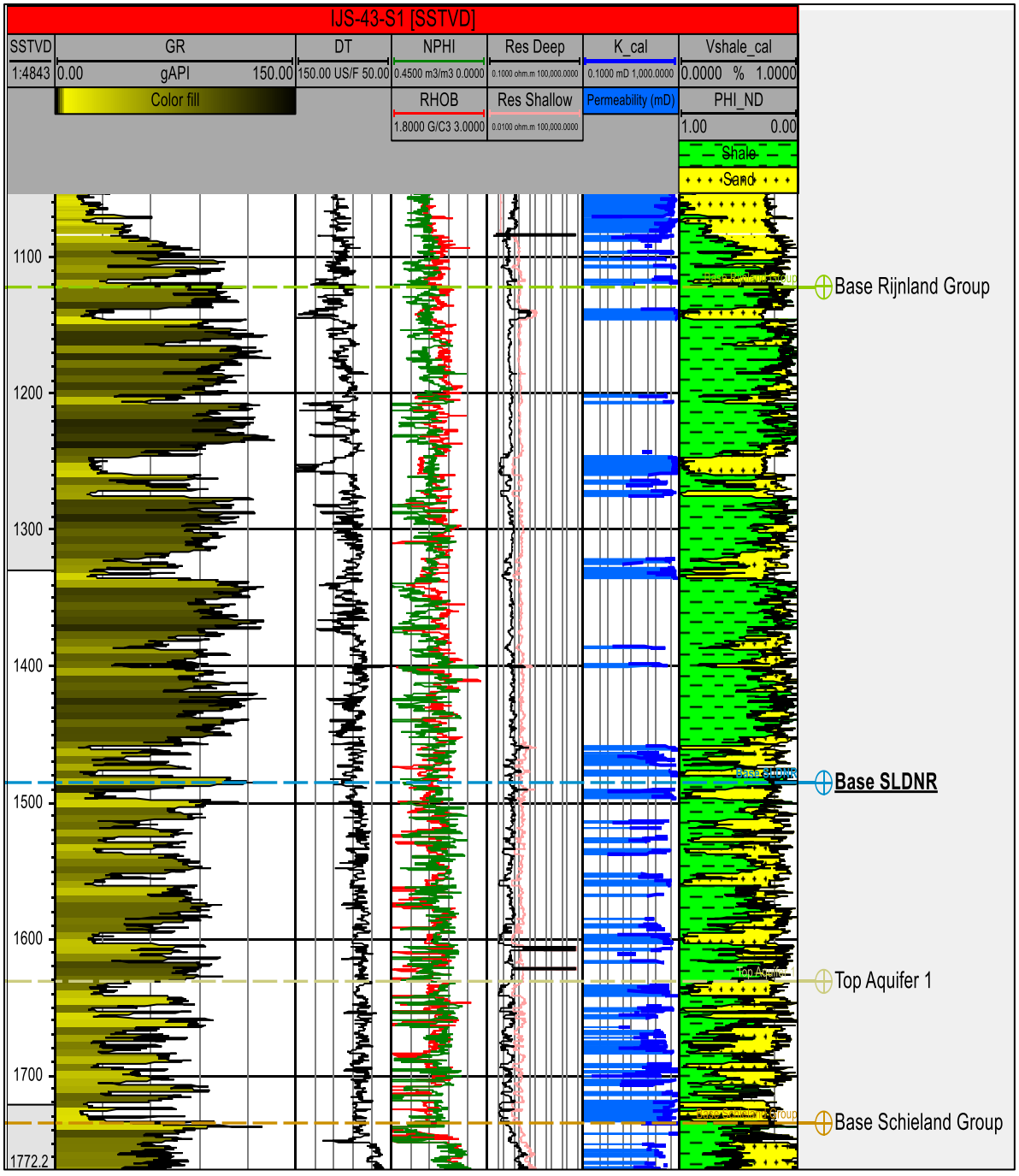

Figure 84 Result of petrophysical evaluation in well RKK-32

C.5 Petrophysical Evaluation in well GSD-01

Gamma-ray minimum : 20

Gamma-ray maximum : 90

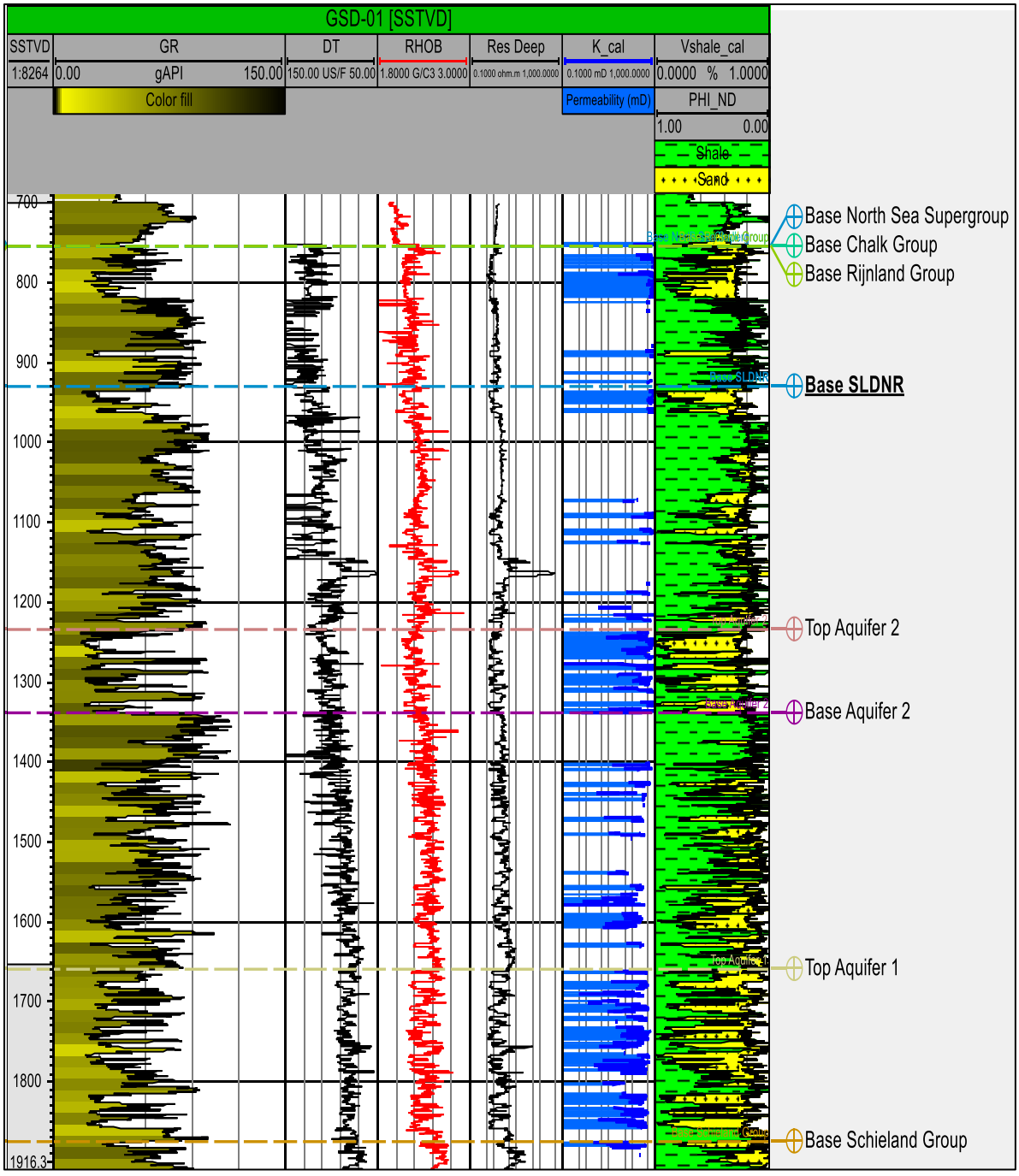

Figure 85 Result of petrophysical evaluation in well GSD-01

C.6 Petrophysical Evaluation in well WGD-01

Gamma-ray minimum : 60

Gamma-ray maximum : 135

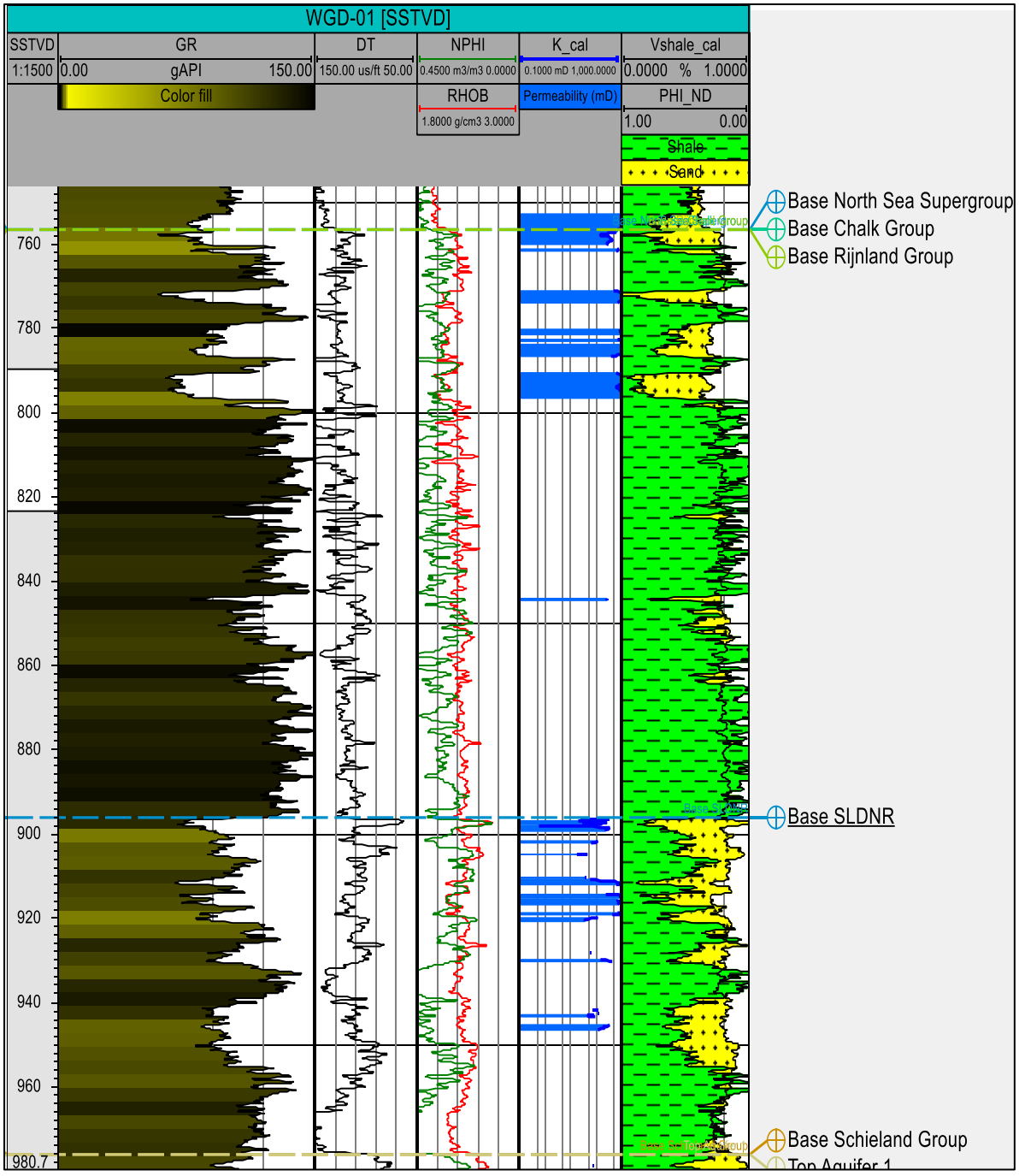

Figure 86 Result of petrophysical evaluation in well WGD-01

C.7 Petrophysical Evaluation in well WED-03

Gamma-ray minimum : 70

Gamma-ray maximum : 130

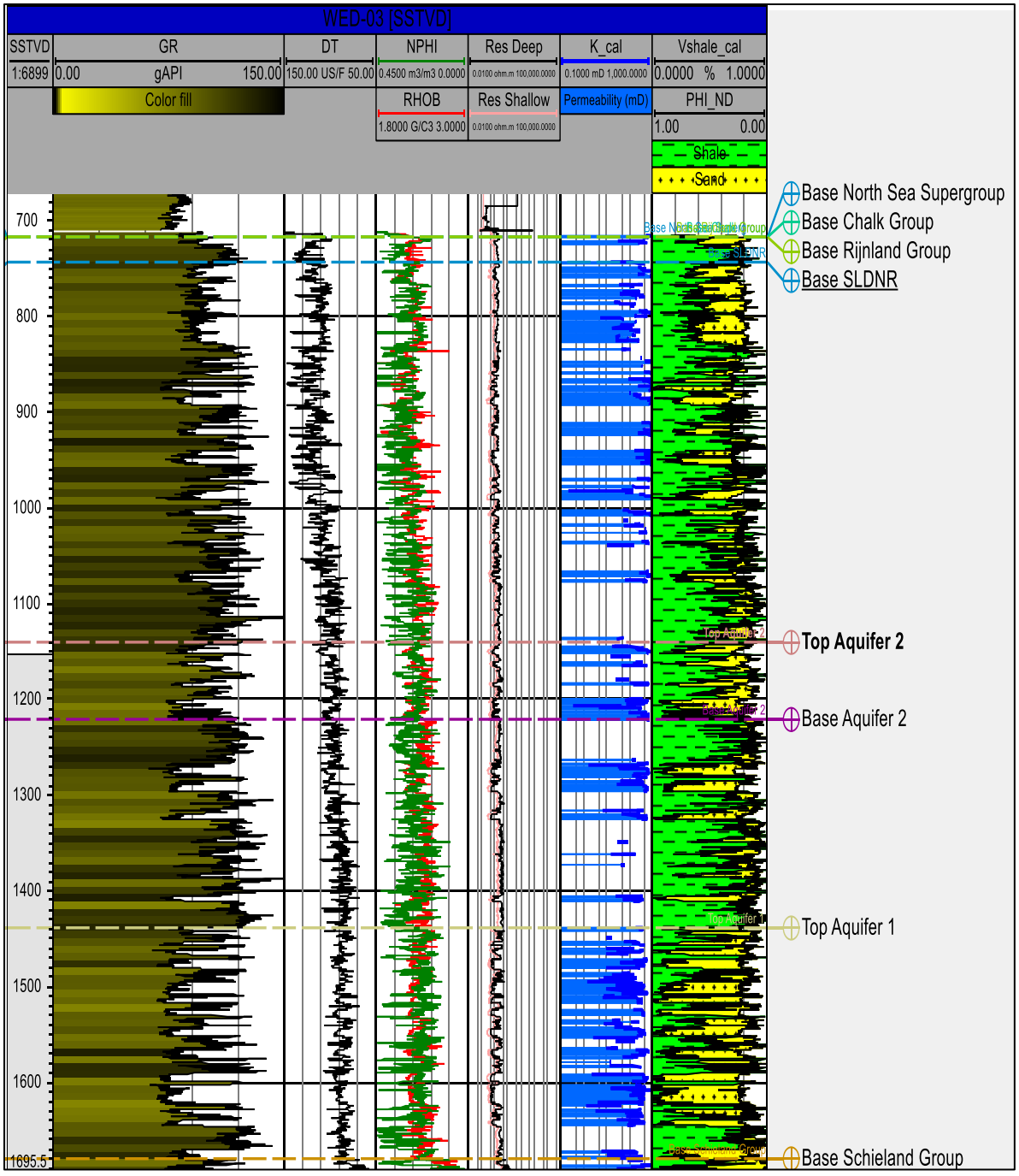

Figure 87 Result of petrophysical evaluation in well WED-03

D. Core Description

D.1 Core from well Bleskensgraaf-2 (BLG-02)

Well Bleskensgraaf – 02 is located on the NE side of the area study (Figure 10). It is a dry well and abandoned which was used to as an exploration hydrocarbon purpose well. The well was drilled at the higher part of an eroded anticline structure.

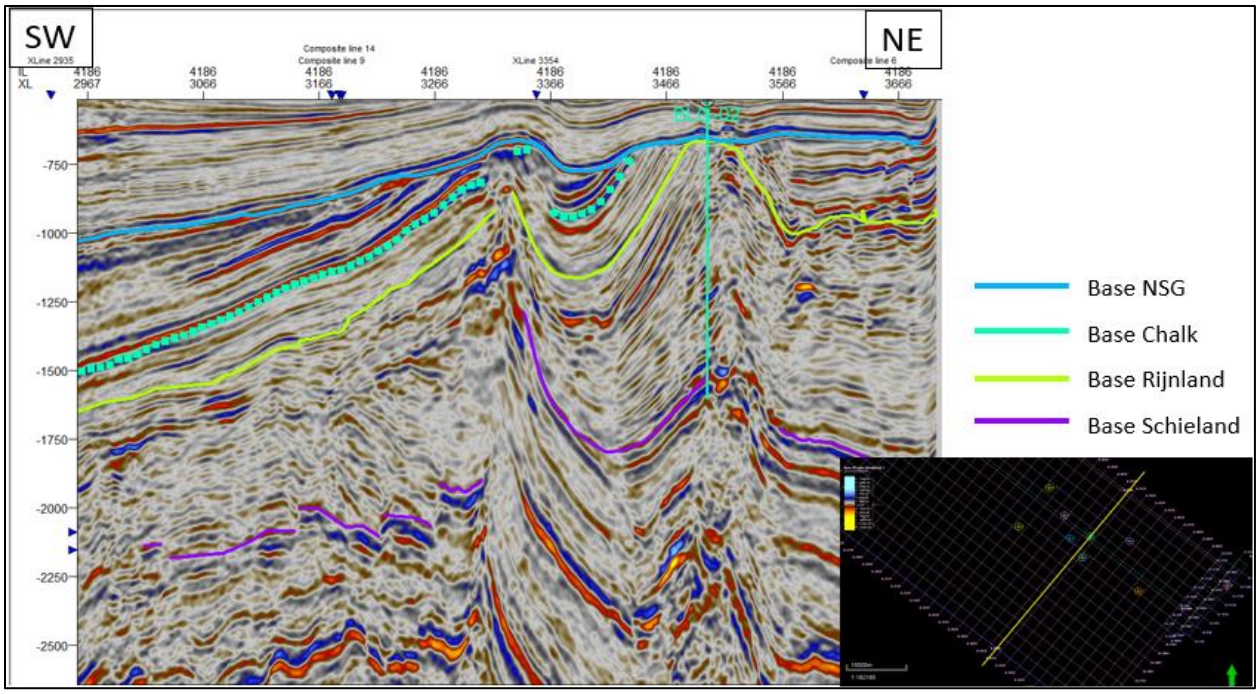

Figure 88 Well BLG-02 in seismic cross-section at inline 4186

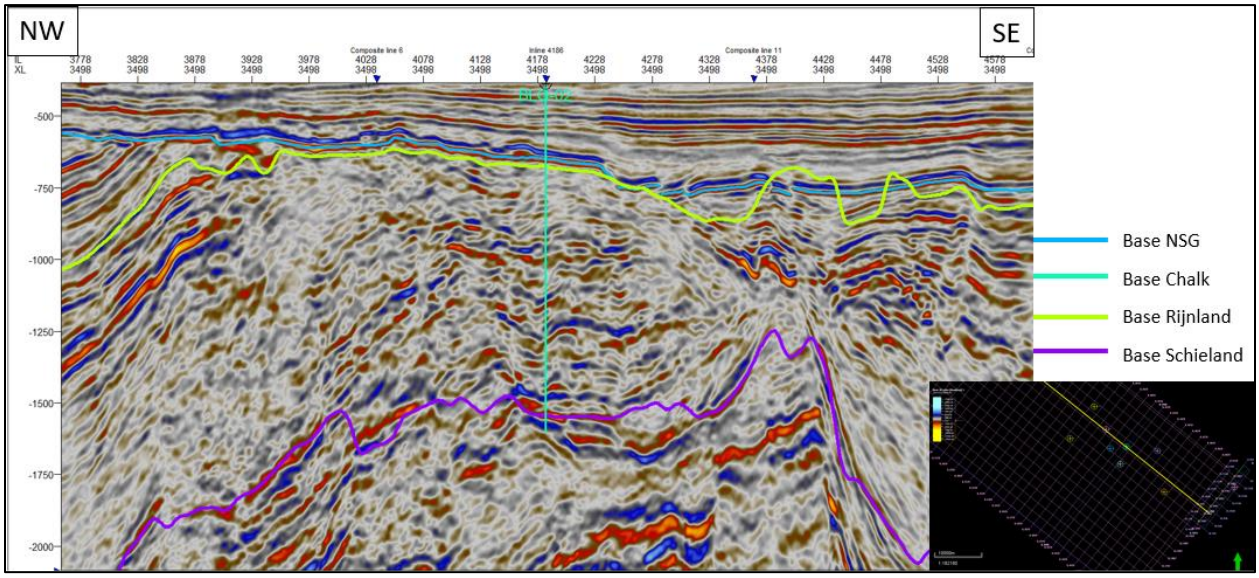

Figure 89 Well BLG-02 in seismic cross-section at xline 3498

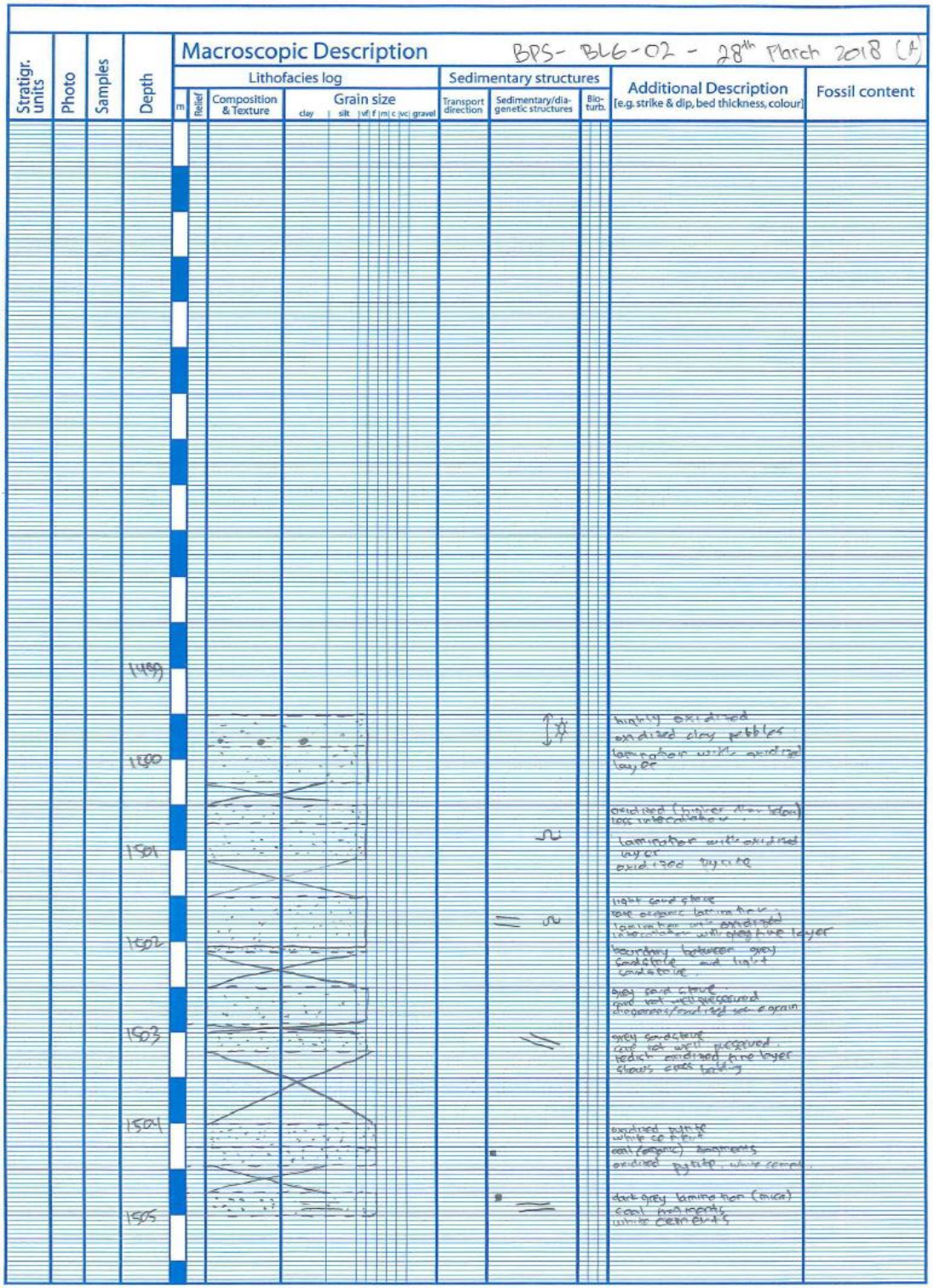

Figure 90 Core Description A (-1499.5 to -1505 m) of well BLG-02

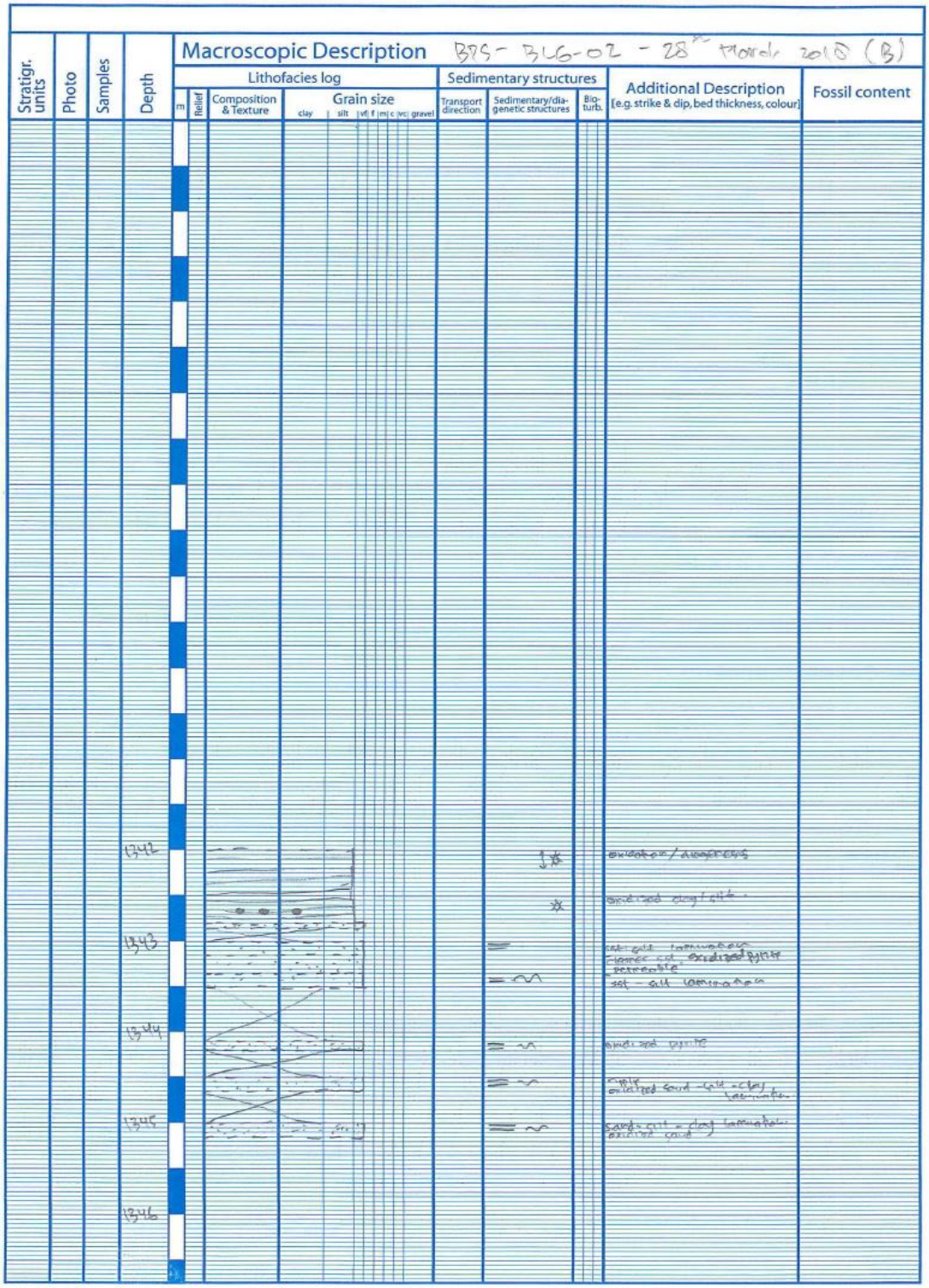

Figure 91 Core Description B (-1342 to – 1345.2 m) of well BLG-02

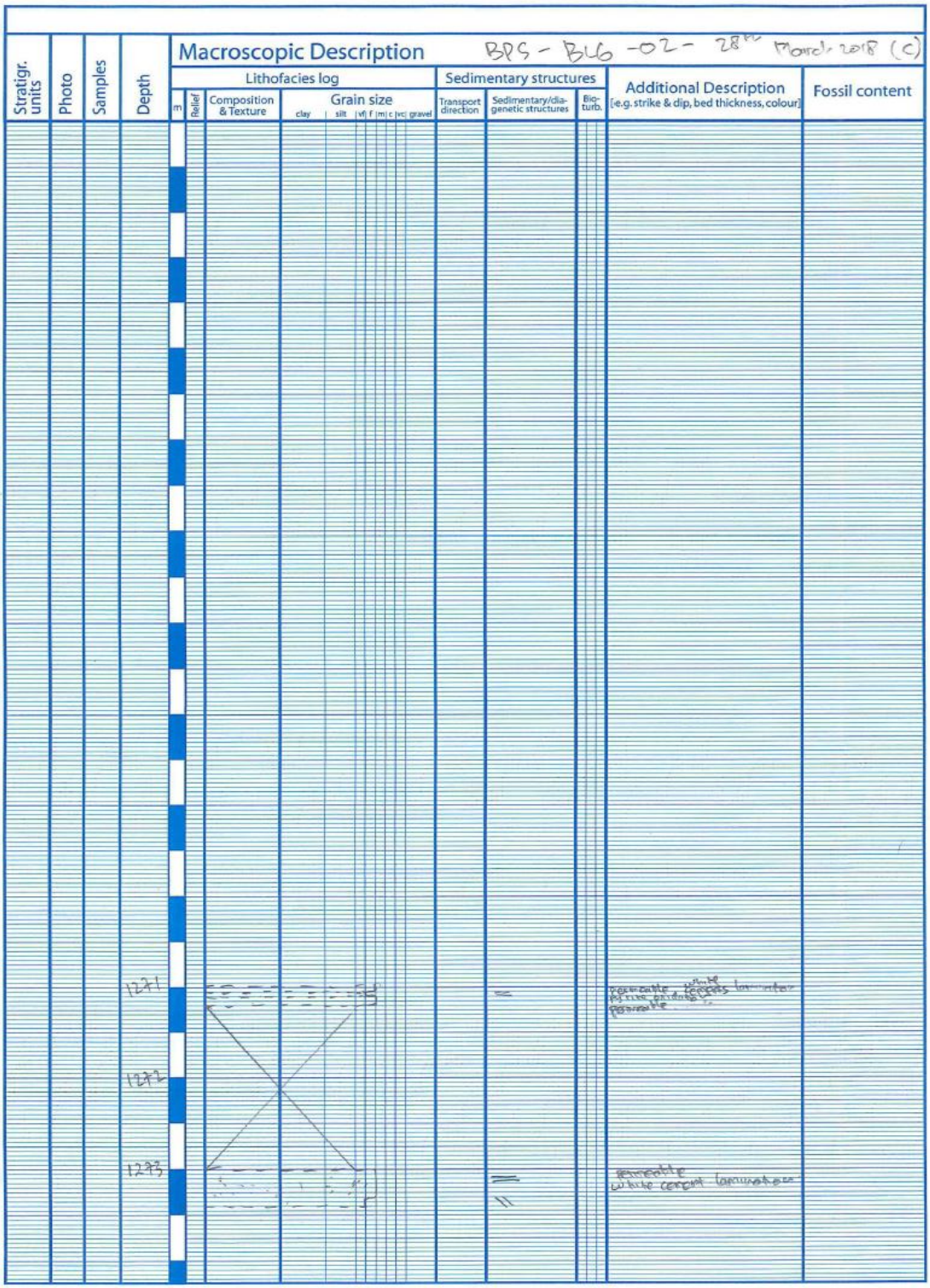

Figure 92 Core Description C (-1271 to -1273.4 m) of well BLG-02

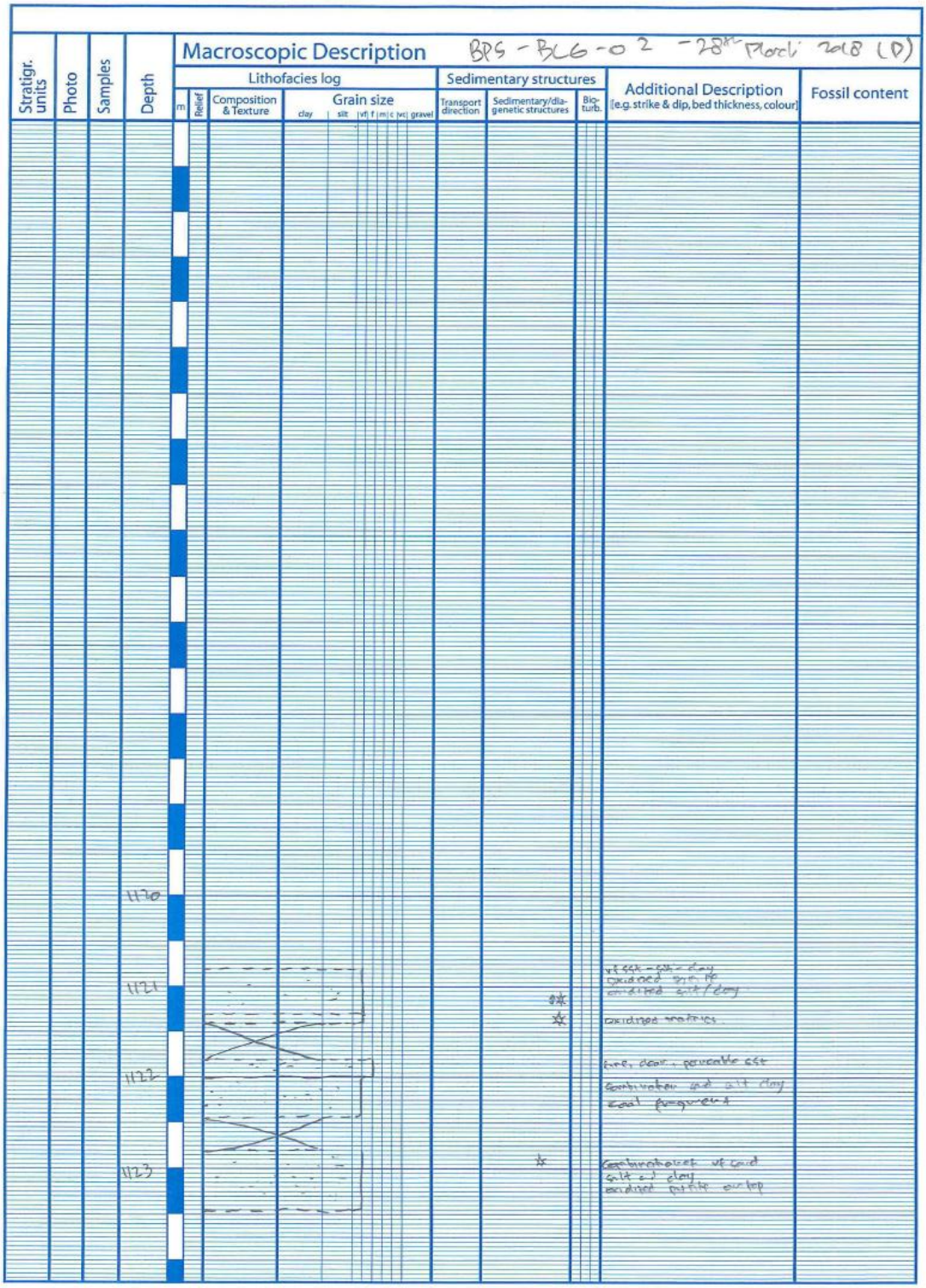

Figure 93 Core Description D (-1120.8 to -1123.5 m) of well BLG-02

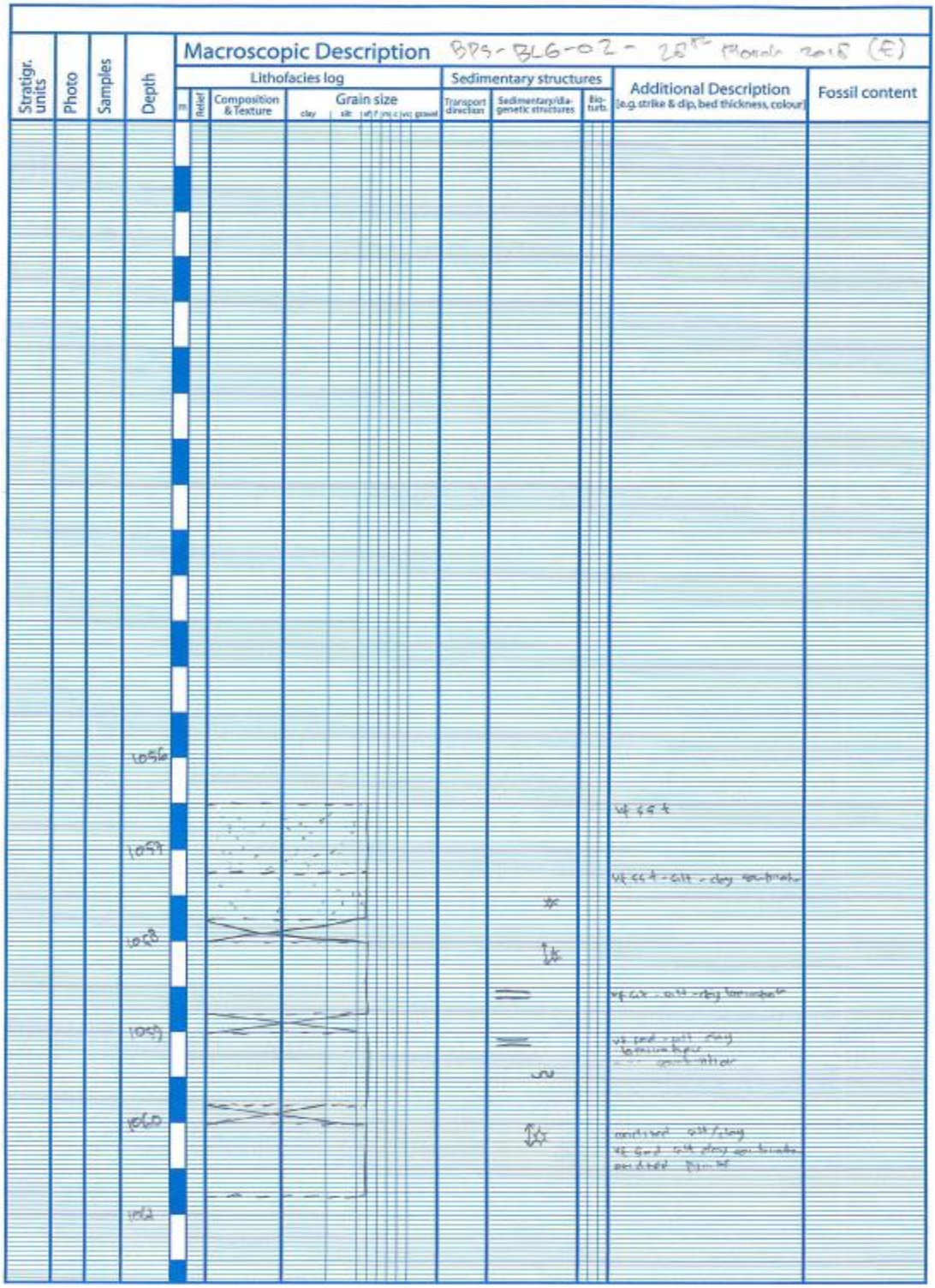

Figure 94 Core Description E (-1056.5 to -1060.8 m) of well BLG-02

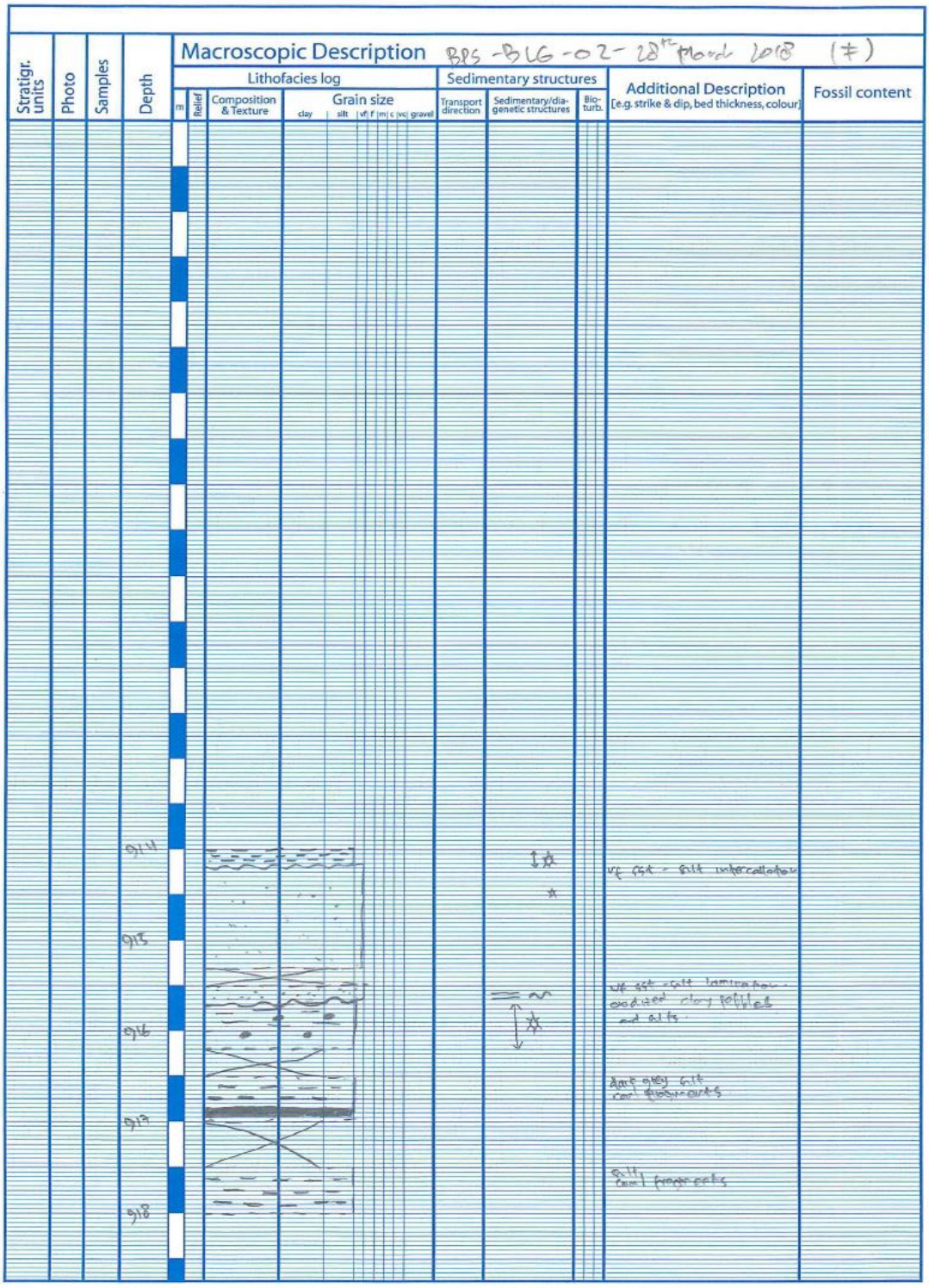

Figure 95 Core Description F (- 914 to -918 m) of well BLG-02

D.2 Core from well Lekkerkerk-1 (LEK-01)

Well Lekkerkerk – 01 is located in NE side of the Drechtsteden (Figure 10). It is an exploration hydrocarbons-well with oil as a result. Drilled at high compressional zone and erosion with absent of Chalk Group.

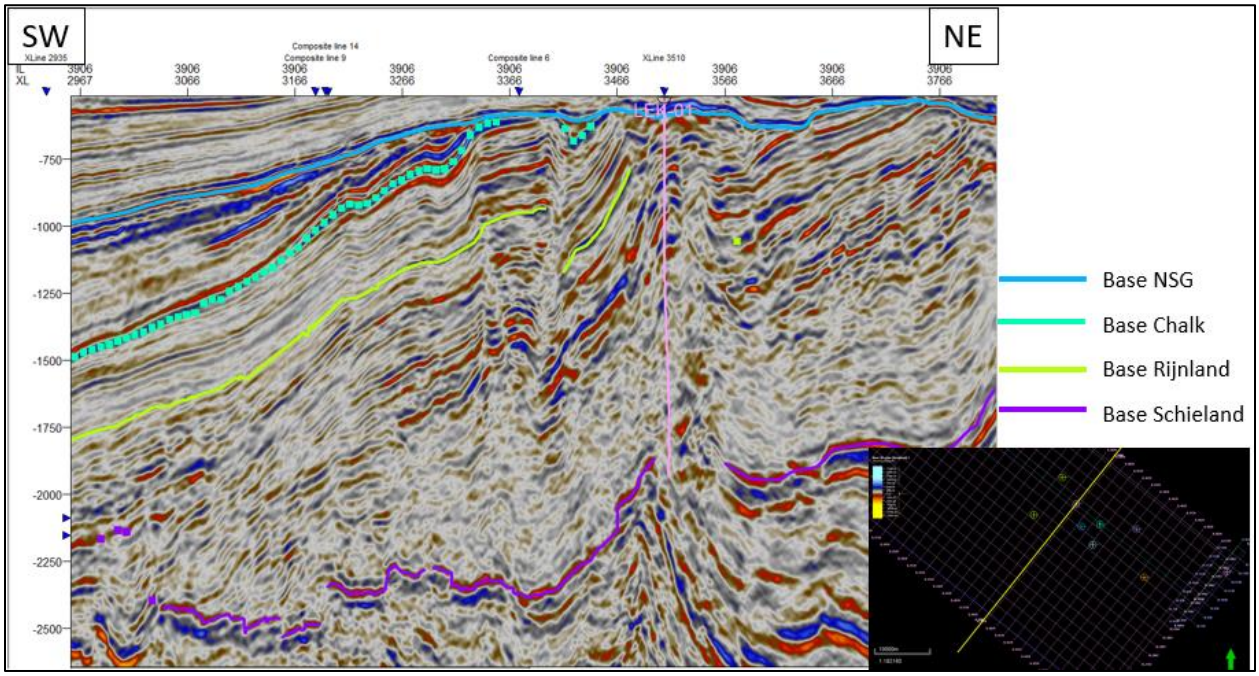

Figure 96 Well LEK-01 in seismic cross-section at inline 3906

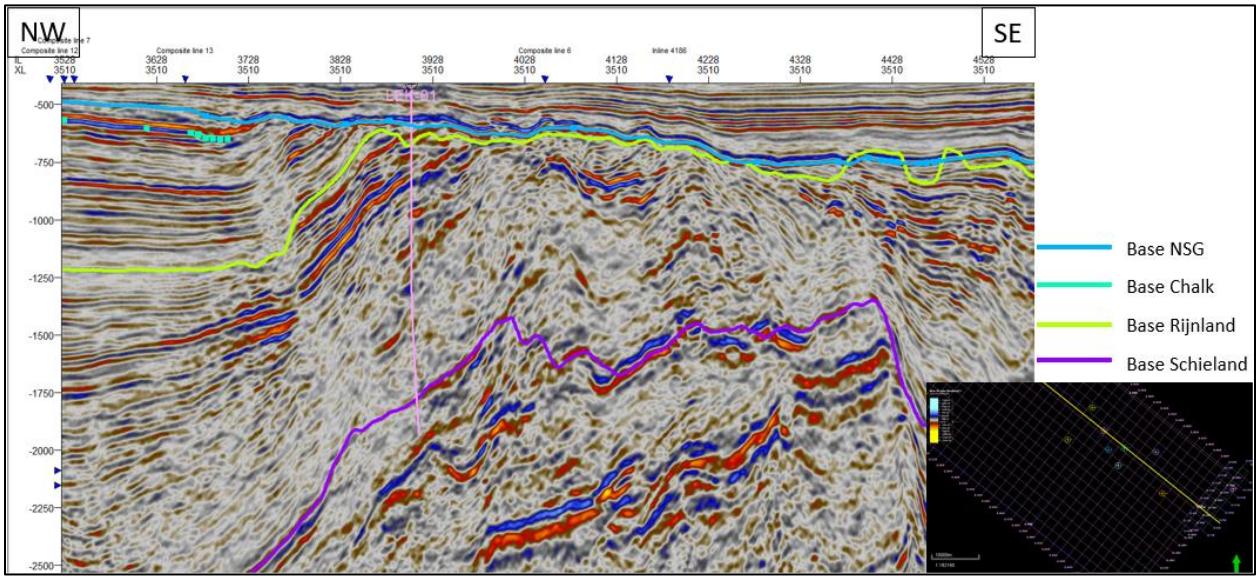

Figure 97 Well LEK-01 in seismic cross-section at xline 3510

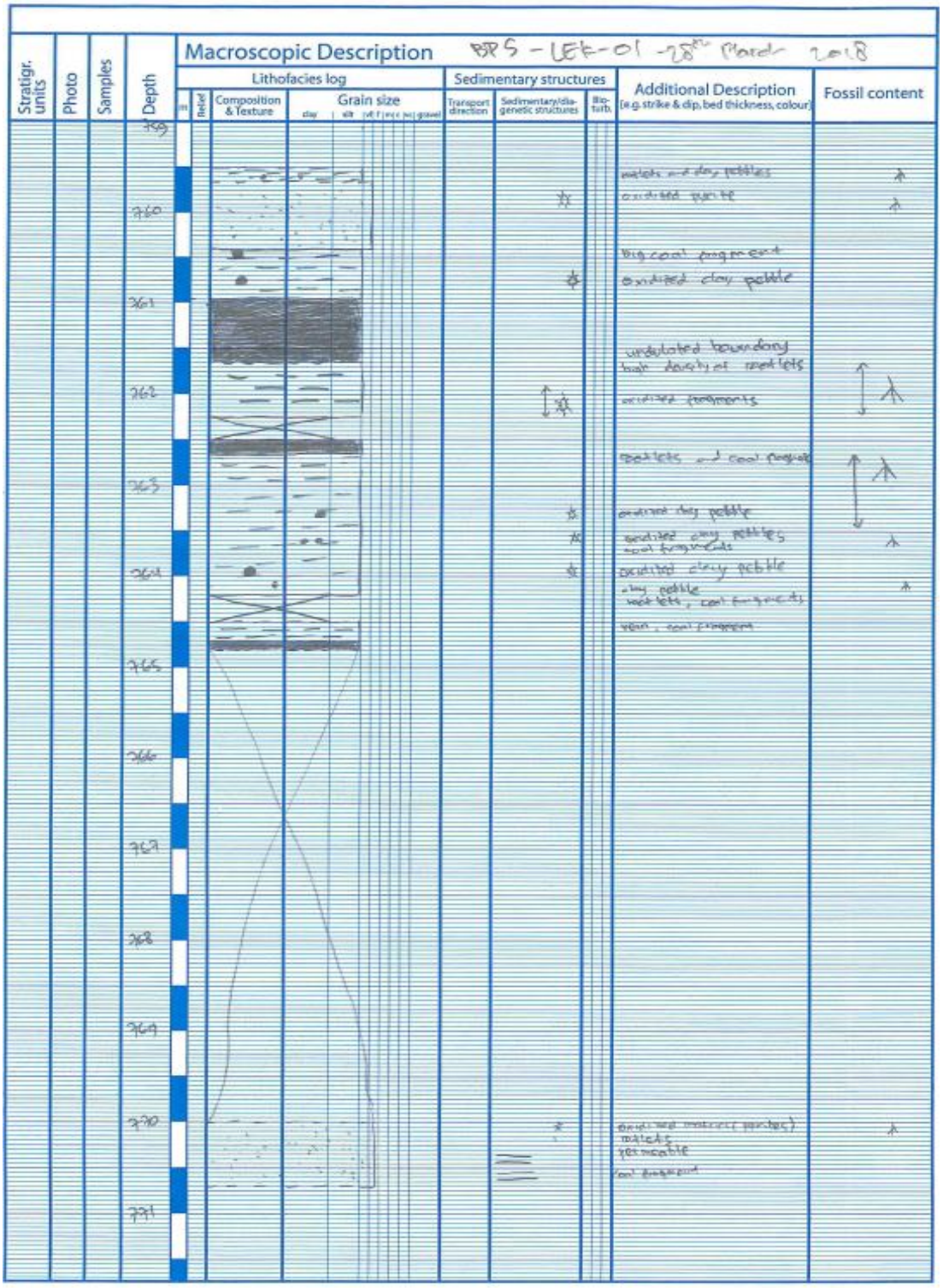

Figure 98 Core Description of well LEK-01

D.3 Core from well Nieuwerkerk – 01 (NKK-01)

Well Nieuwerkerk – 01 is located in NE side of the study area (Figure 10). It is the North-Western most well with an available core that penetrates the SLDNR and SLDNA. It used to be a hydrocarbons exploration well with gas as a result and drilled at about the hinge of a normal faulted anticline.

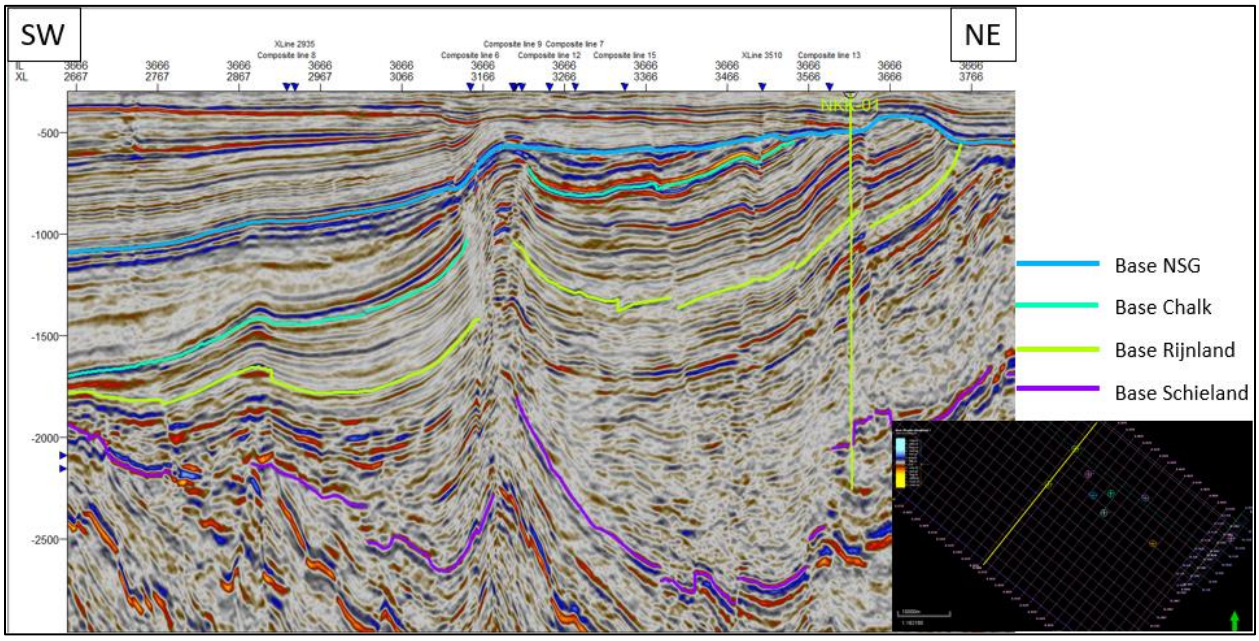

Figure 99 Well NKK-01 in seismic cross-section at inline 3666

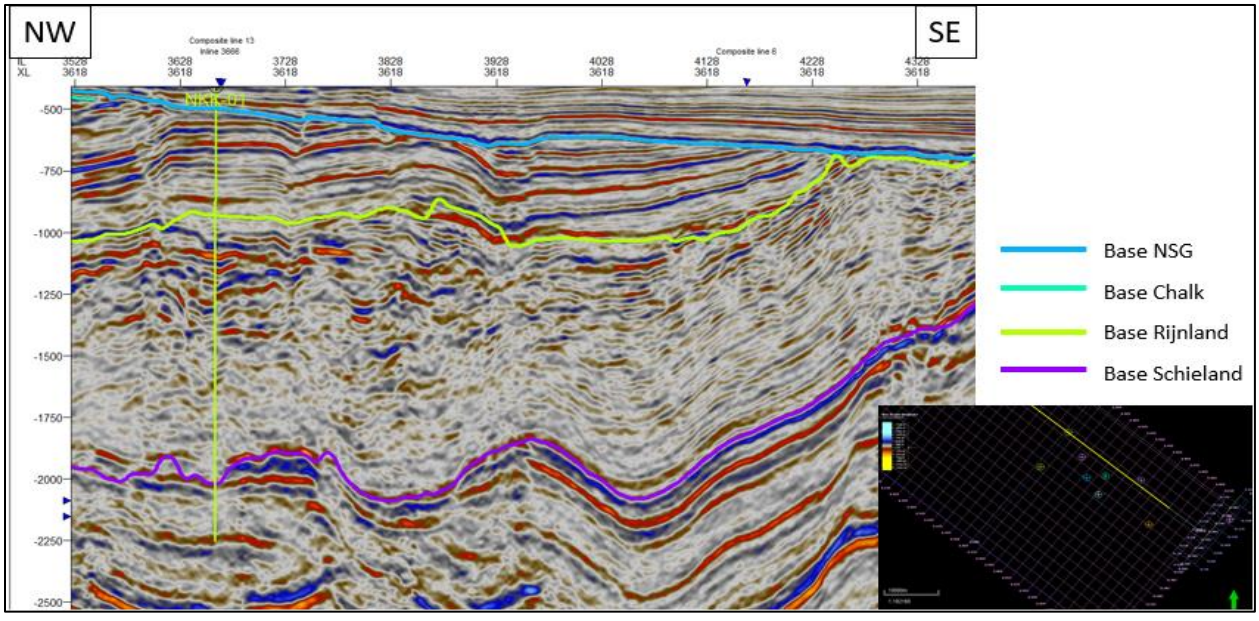

Figure 100 Well NKK-01 in seismic cross-section at xline 3618

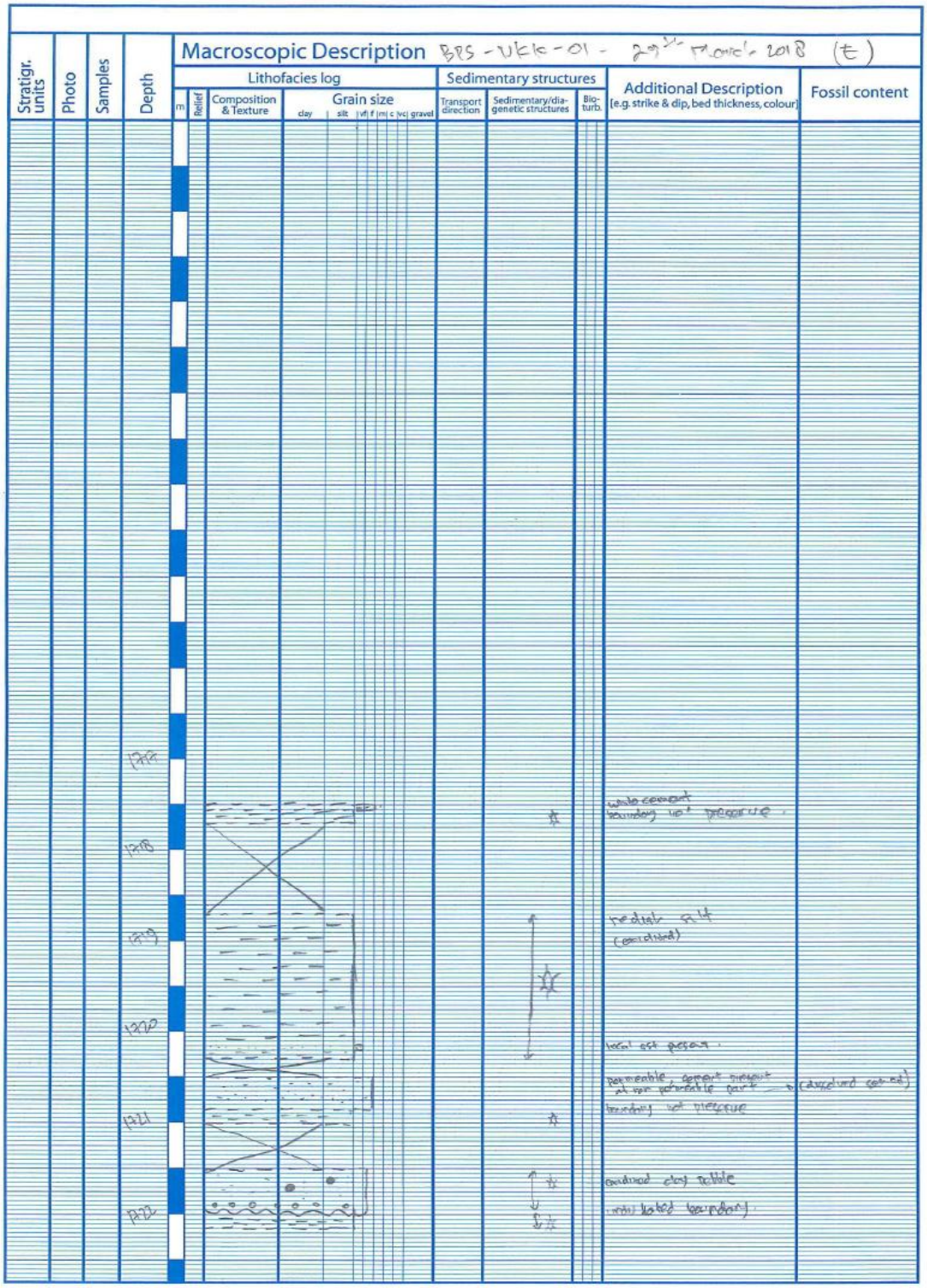

Figure 101 Core Description E (-1717.5 to -1722.2 m) of well NKK-01

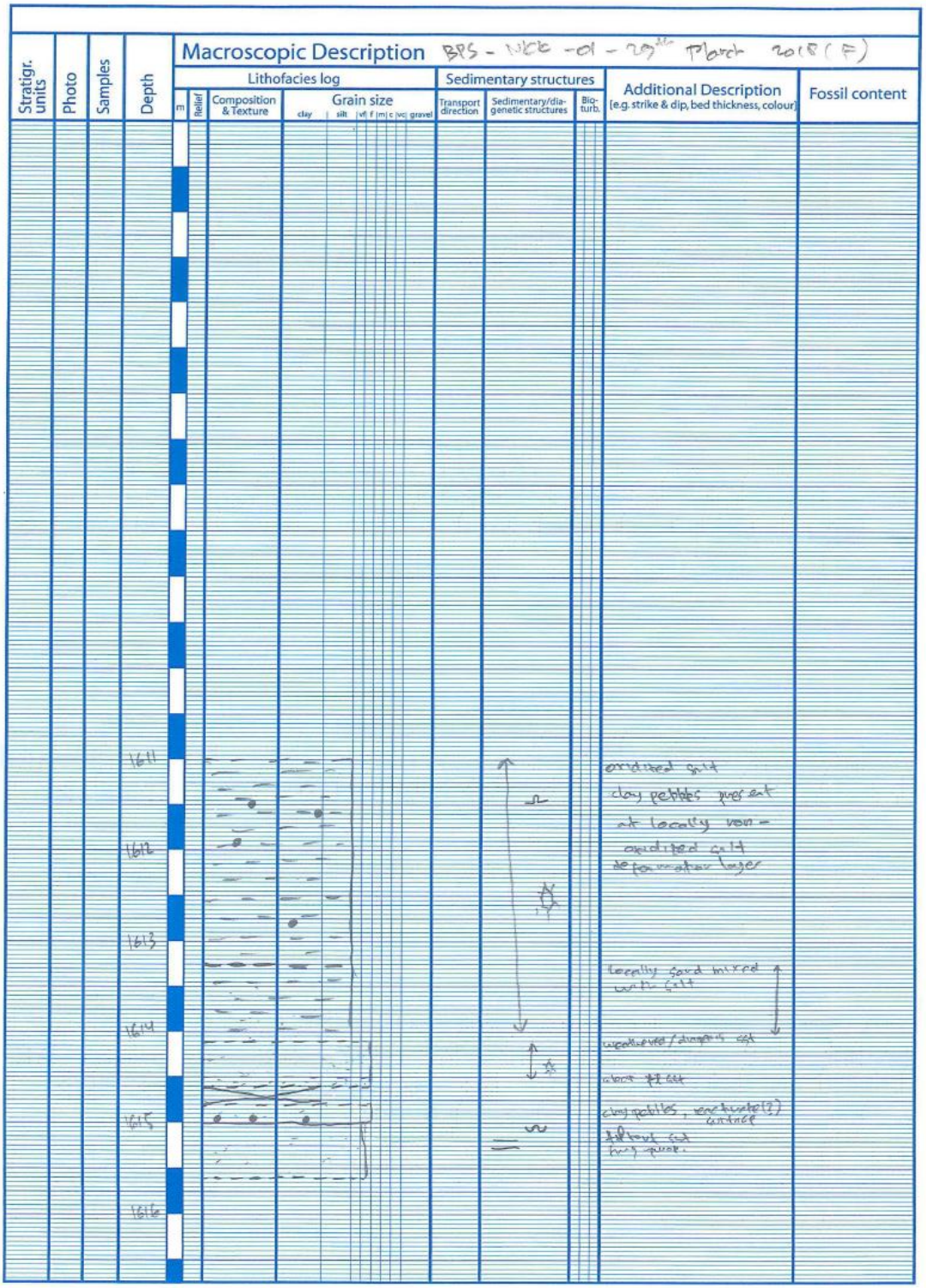

Figure 102 Core Description F (-1611 to -1615.6 m) of well NKK-01

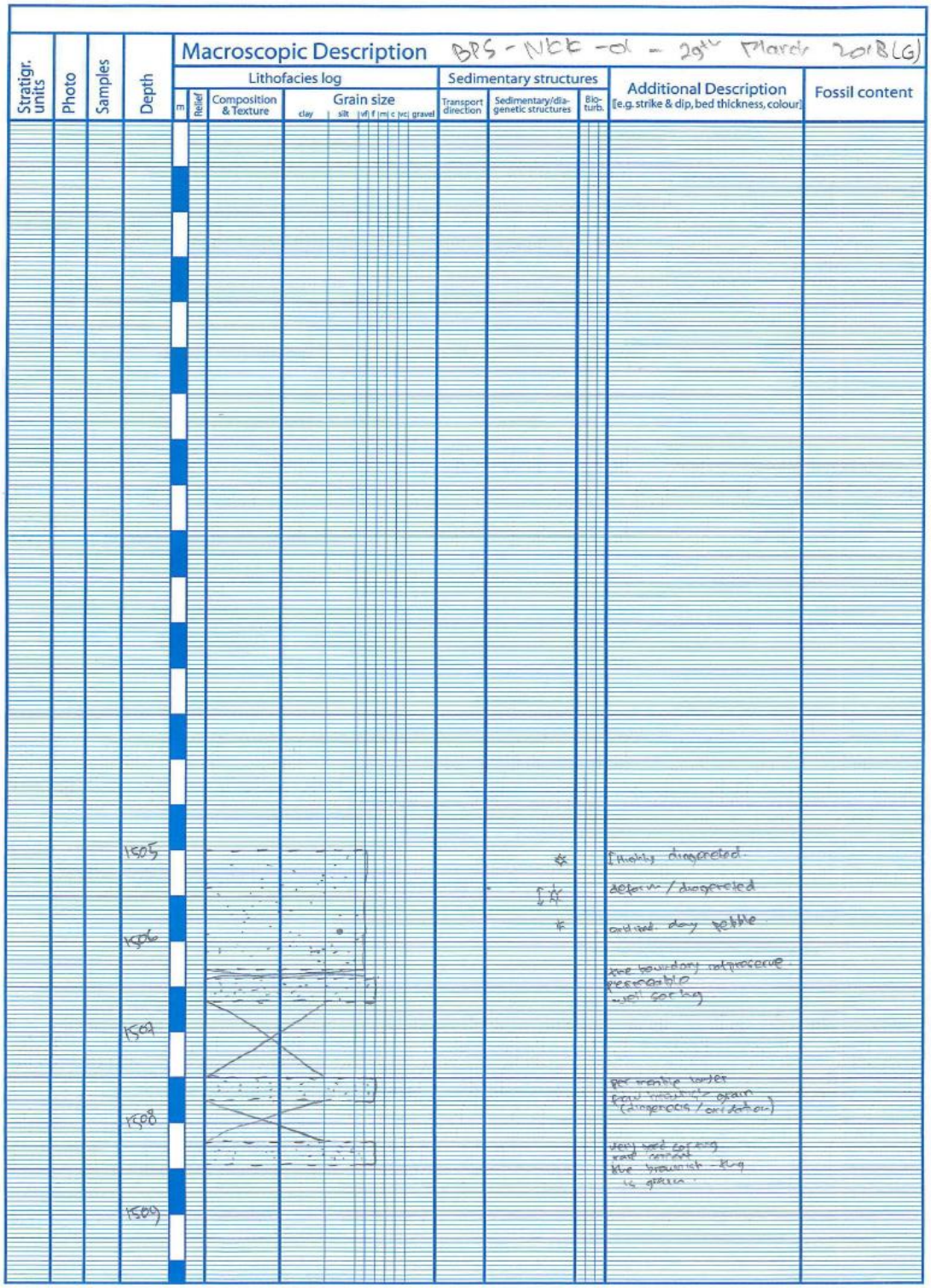

Figure 103 Core Description G (-1505 to -1508.5 m) of well NKK-01

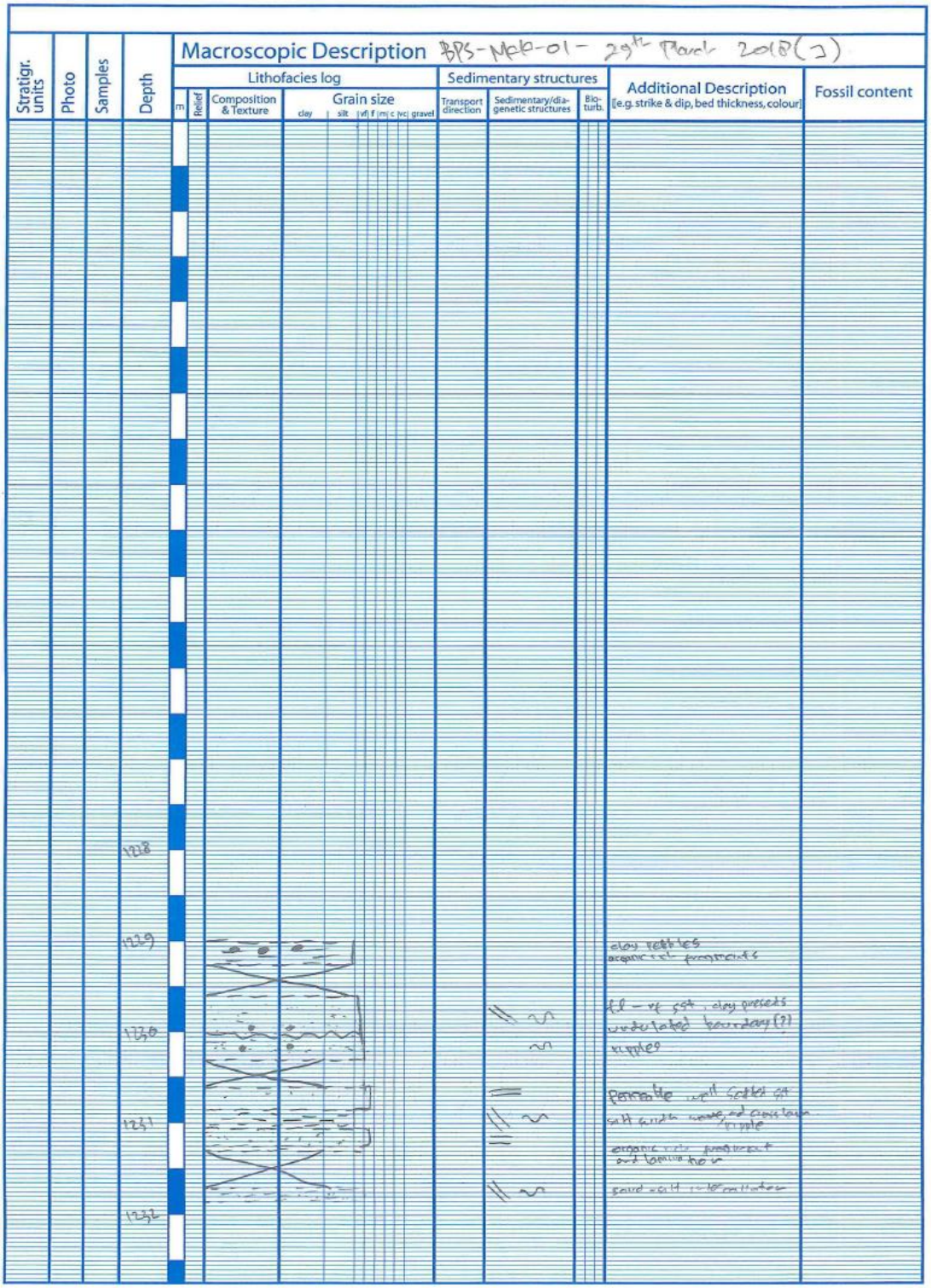

Figure 104 Core Description J (-1229 to -1231.9 m) of well NKK-01

D.4 Core from well Alblasserdam (ALD-01)

Well Alblasserdam – 01 is located in the central part of the study area (Figure 10). It is an appraisal hydrocarbons-well with oil as a result. Drilled at plateau zone in between a fragmented anticlinal structure.

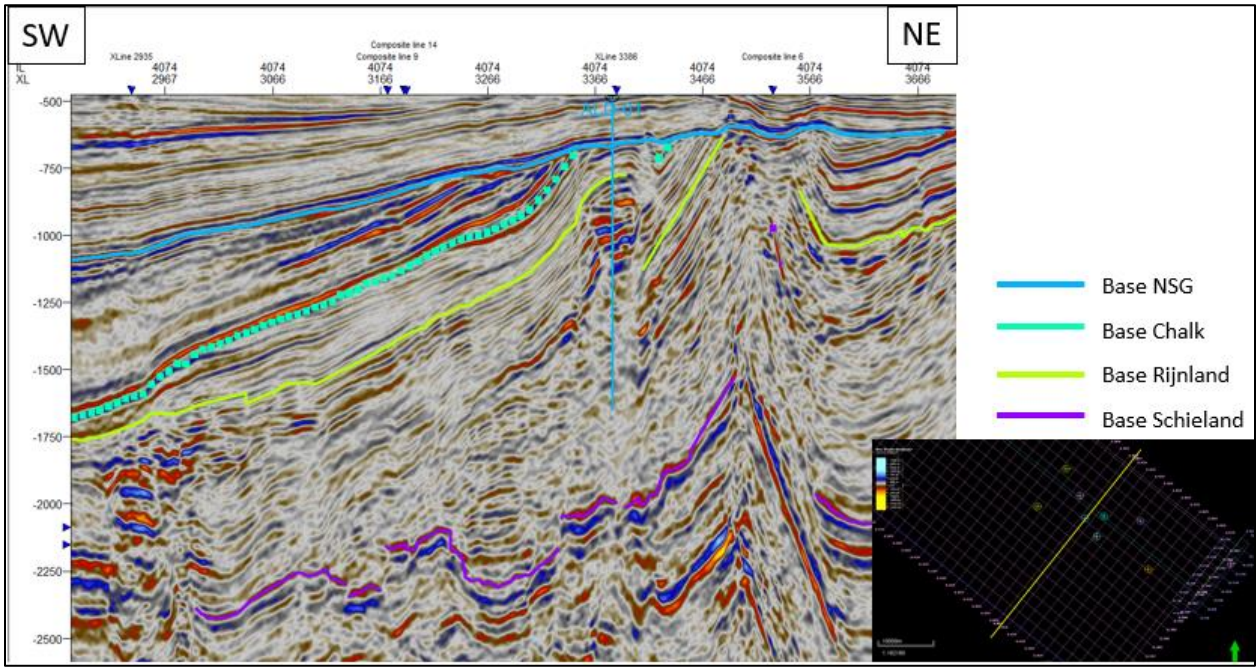

Figure 105 Well ALD-01 in seismic cross-section at inline 4074

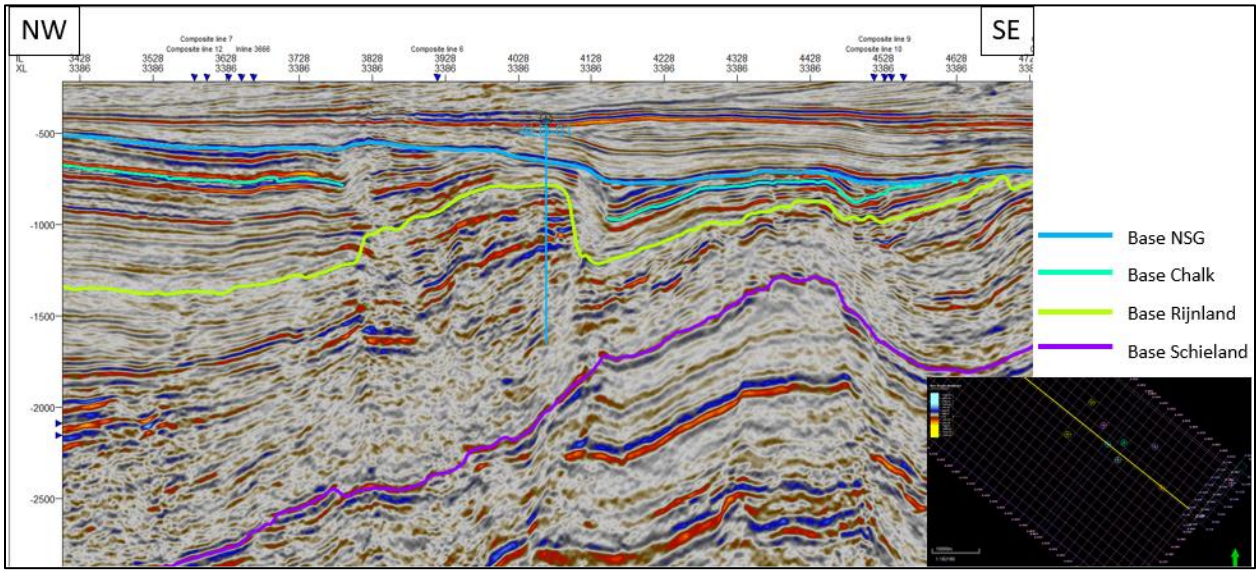

Figure 106 Well ALD-01 in seismic cross-section at xline 3386

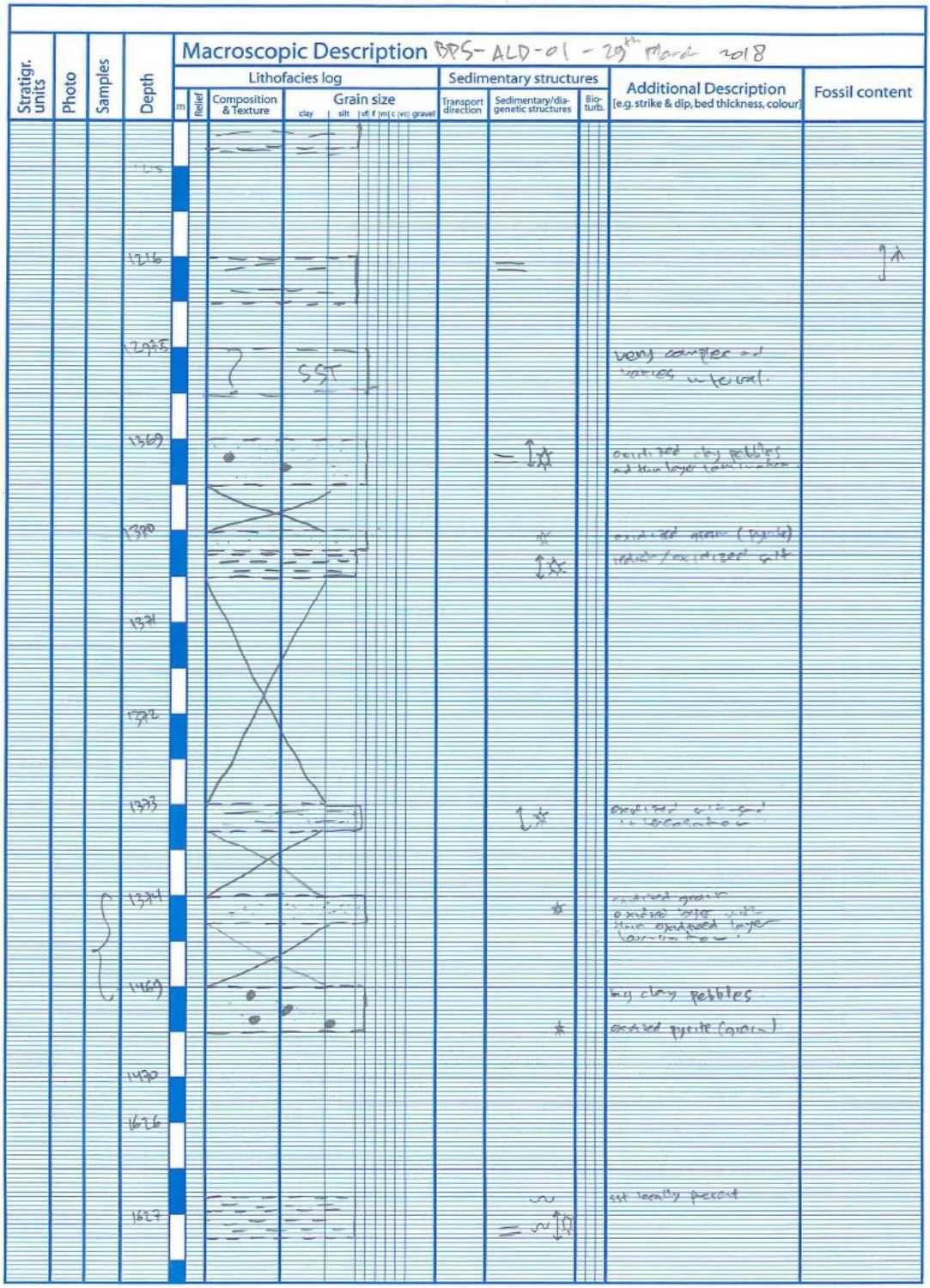

Figure 107 Core Description of well ALD-01